Distribution Agreement

In presenting this thesis of dissertation as a partial fulfillment of the requirements for an advanced degree from Emory University, I hereby grant to Emory University and its agents the non-exclusive license to archive, make accessible, and display my thesis or dissertation in whole or in part in all forms of media, now or hereafter known, including display on the world wide web. I understand that I may select some access restrictions as part of the online submission of this thesis or dissertation. I retain all ownership rights to the copyright of the thesis or dissertation. I also retain the right to use in future works (such as articles or books) all or part of this thesis or dissertation.

Signature:

_____ _____

Bing Bai Date

Comprehensive Proteome and Transcriptome Studies Reveal RNA Processing Dysfunction in Alzheimer's disease

By

Bing Bai

Doctor of Philosophy

Graduate Division of Biological and Biomedical Science
Molecular and Systems Pharmacology

_____
Junmin Peng, Ph.D.
Advisor

_____
Yue Feng, Ph.D.
Committee Member

_____
James Lah, M.D., Ph.D.
Committee Member

_____
Zixu Mao, Ph.D.
Committee Member

_____
David C. Pallas, Ph.D.
Committee Member

Accepted:

_____
Lisa A. Tedesco, Ph.D.
Dean of the James T. Laney School of Graduate Studies

_____
Date

Comprehensive Proteome and Transcriptome Studies Reveal RNA Processing Dysfunction in Alzheimer's disease

By

Bing Bai

B.A., M.S., Nanjing Medical University, China, 2003

Advisor: Junmin Peng, Ph.D.

An abstract of
A dissertation submitted to the Faculty of the
James T. Laney School of Graduate Studies of Emory University
in partial fulfillment of the requirements for the degree of
Doctor of Philosophy
in
Graduate Division of Biological and Biomedical Science
Molecular and Systems Pharmacology
2014

ABSTRACT

Comprehensive Proteome and Transcriptome Studies Reveal RNA Processing Dysfunction in Alzheimer's disease

By Bing Bai

Alzheimer's disease (AD) is an age-related neurodegenerative disorder, currently with no effective cure. The major hypothesis posits that AD is caused by two hallmark proteins, Aβ and Tau. However, patients with similar Aβ and Tau pathology can demonstrate completely different types of dementia.

In order to find more mechanistic proteins to better understand AD neurodegeneration, we comprehensively studied the insoluble proteome where Aβ and Tau were initially discovered. Proteins resistant to detergents were extracted from affected frontal cortex in postmortem brains of AD and non-demented controls, and then analyzed by liquid chromatography coupled to tandem mass spectrometry (LC-MS/MS).

Among the 4,216 proteins identified, 36 are significantly increased in AD. These include Aβ, Tau and other proteins in pathways known to be disrupted in AD. In addition to these known proteins, novel proteins from RNA splicing pathway such as U1-70K and U1A were found to be significantly enriched in AD patients.

Validation by western blotting showed specific, widespread and early-occurring accumulation of U1-70K and U1A insoluble in AD. Brain tissue immunohistochemical staining of U1-70K and U1A demonstrated cytoplasmic tangle-like structures in AD neurons, indicating possible aggregation and dysfunction. Aberrancy of these U1 spliceosomal proteins may lead to defective RNA splicing in AD.

Analysis of the mRNA transcriptome by RNA-seq revealed several splicing alterations in AD: 1) accumulated pre-mRNA, where the ratio of exon reads to intron reads is reduced; 2) altered exon junctions; 3) increased premature cleavage and polyadenylation in AD, where more polyA reads were mapped to the 5' terminus of coding regions rather than the 3' UTR region. All these point to deficient RNA splicing in AD.

In summary, two comprehensive analyses involving proteomics and transcriptomics both revealed RNA splicing disruption in AD, providing a novel mechanistic clue to AD neurodegeneration.

Comprehensive Proteome and Transcriptome Studies Reveal RNA Processing Dysfunction in Alzheimer's disease

By

Bing Bai

B.A., M.S., Nanjing Medical University, China, 2003

Advisor: Junmin Peng, Ph.D.

A dissertation submitted to the Faculty of the
James T. Laney School of Graduate Studies of Emory University
in partial fulfillment of the requirements for the degree of
Doctor of Philosophy
in Graduate Division of Biological and Biomedical Science
Molecular and Systems Pharmacology

2014

ACKNOWLEDGEMENT

In great appreciation of the support for my PhD training, I sincerely thank all those who have made substantial contributions to my achievements in these six years.

First and foremost, I especially thank my advisor, Dr. Junmin Peng. He is truly exceptional at mentoring students. He personally ran SDS-PAGE with me when I first joined his lab in order to show me the importance of paying attention to every detail of a project. He taught me how to design experiments thoroughly and work them out effectively. By his training, I learned critical thinking, improved my skills in seminar speaking and academic writing, and broadened my scientific vision. He fully prepared me for the next stage as an outstanding postdoctoral candidate. These six years with him will be one of the most important experiences in my life.

I am grateful to my dissertation committee members, Drs.Yue Feng, James Lah, Zixu Mao and David Pallas. Dr.Feng always raised critical questions for me to understand the project more thoroughly. Dr.Lah supervised the entire process of my project as a major collaborating investigator. Dr.Mao was never late in responding to my questions in emailing, and brought up many valuable comments on the strength of my experimental data. Dr.Pallas was my rotation mentor. He actively continued mentoring me for the entirety of my PhD research. All these members kept track of my progress, spent significant amount of time for meetings and communications, helped make me aware of my weaknesses and improve my presentation and writing skills. Although Dr.Allan Levey is not on my committee, he has provided many insightful comments on my work as a co-principle investigator of this U1 project.

I would thank the whole U1 team. Chadwick Hales, Ping-Chung Chen, Eric B. Dammer, Jason J. Fritz, Howard Rees, Craig Heilman, Yair Gozal, Qiangwei Xia, Duc M. Duong, Nicholas T. Seyfriedc, Thomas Wingo, Hao Wu, Peng Jin, Dongmei Cheng, Craig Street Xusheng Wang and Yuxin Li, are all involved this project and some of them made important contributions. It is all of their participation that has made the U1 study completed and published.

I would also like to express my gratitude to the members of the Peng laboratory and St.Jude proteomics facility core. The postdoc Ping Xu was my role model when I first came to this lab. Eric Dammer is one of my favorite postdocs. He has a passion in science and is always willing to help me with biological knowledge and experiments. He played critical role in my initial PhD stage. Duc Duong is the best proteomics software developer. I never saw any problems that he could not fix. He generously and patiently taught me many software basics. The postdoc Ping-Chung Chen provided substantial help with my experiments. He is the most qualified student mentor I have ever seen. I would

also thank Zhiping Wu, Chan-Hyun Na, Yanling Yang, Yuxin Li, Drew Jones, Joseph Mertz and Hong Wang for their technical assistance and helpful discussion. I would also extend my appreciation to Anthony High, Vishwajeeth Pagala, Xusheng Wang, Haiyan Tan, Kanisha Kavdia and Ashutosh Mishra for their critical help with my proteomics experiments.

I would like to thank members of the “molecular and systems pharmacology” program such as Drs. Edward Morgan, John Hepler, Randy Hall, David Weinshenker, Eric Ortlund, Roy Sutliff and my student counselor T. J. Murphy. I would also thank the academic coordinator- Tricia Satkowski and the chair of Structural Biology- Dr.Stephen White at St.Jude Children’s Research Hospital.

I am heartily thankful to my family. My wife Qian Zheng has supported me incredibly for all these years, taking almost full responsibility for o family. We have been together through this difficult financial situation. My mother, in order to save me time in preparing for the dissertation and defense, came here from China to take care of our newly born baby Liam. My father helped to relieve my financial burden. I would also thank my son Daniel who understands his daddy is in a school with no breaks and vacation but endless night homework. Without support from each of you, I would not have been able to go this far. The achievement of a PhD degree is attributed to the integrated effort from an entire family.

The pursuit of a PhD degree is a major experience in my life. All different kinds of supports that I have received are considered indispensable contributions to my achievement, and will never be forgotten.

Table of Contents

LIST OF FIGURES

Chapter 1

Chapter 2

(As published)

Chapter 3

(As published)

Chapter 4

ABBREVIATIONS

AD	Alzheimer's disease
MCI	Mild cognitive impairment
PD	Parkinson disease
FTDL-U	Ubiquitin-positive frontotemporal lobar degeneration
FTDL-Tau	Tau-positive frontotemporal lobar degeneration
ALS	Amyotrophic lateral sclerosis
LBD	Lewy body dementia
CBD	Corticobasal degeneration
GVD	Granulovacuolar degeneration
MTL	Medial temporal lobe
EC	Entorhinal cortex
CBF	Cerebral blood flow
NFT	Neurofibrillary tangles
MAPT	Microtubule associated protein Tau
MS	Mass spectrometry
LC- MS/MS	Liquid chromatography coupled to tandem mass spectrometry
ESI	Electrospray ionization
MALDI	Matrix-assisted laser desorption/ionization
SC	Spectral counts
SILAC	Stable isotope labeling by amino acids in cell culture
SILAM	Stable isotope labeling in mammals
TMT	Tandem mass tags
U1 snRNP	U1 small nuclear ribonucleoprotein complex
PCPA	Premature cleavage and polyadenylation
GWAS	Genome-wide association studies

NGS	Next-generation-sequencing
RIN	RNA integrity number
BAM	Binary Sequence Alignment/Map
BED	Browser Extensible Data
SAM	Significance Analysis of Microarrays
IHC	Immunohistochemical staining
PCNA	Proliferating cell nuclear antigen
CCE	Cell cycle reentry
GSK3β	Glycogen synthase kinase-3 beta
CDK5	Cyclin-dependent kinase 5
MARK	Microtubule-affinity-regulating kinase
ROS	Reactive oxygen species
ER	Endoplasmic reticulum
TLRs	Toll-like receptors
RAGE	Receptor for advanced glycation end products
8OHdG	8-hydroxy-2-deoxyguanosine
8OHG	8-hydroxyguanosine
ABAD	Alcohol dehydrogenase
NMDA	N-methyl-d-aspartate
UPR	Unfolded-protein response
NGF	Nerve growth factor
BDNF	Brain-derived neurotrophic factor
NT-3	Neurotrophin-3
NT-4	Neurotrophin-4
TrkB	Tropomyosin receptor kinase B
MRI	Magnetic Resonance Imaging
PET	Positron Emission Tomography

Chapter 1:
INTRODUCTION

1. Neurodegenerative disease and protein aggregation

Neurodegenerative diseases such as Alzheimer's disease (AD), Parkinson's disease (PD), Huntington's disease (HD), amyotrophic lateral sclerosis (ALS) and prion diseases are all hallmarked by aggregates of misfolded proteins that form beta-sheet conformation aberrantly (1).

AD is the most common form of dementia with manifestations of memory loss and cognitive deficit. It is age-related synaptic loss and neuronal loss in the brain. AD has two types of protein aggregates: extracellular amyloid plaques and intracellular neurofibrillary tangles. The plaques are mainly composed of the peptide Aβ generated by sequential proteolytic cleavage from protein APP, and the tangles mainly comprise hyperphosphorylated protein Tau. The plaques and tangles usually initiate in the medial temporal lobe and then spread into neocortex and other non-cortical regions.

PD mainly affects motor movements, exhibiting symptoms such as rigidity, bradykinesia, tremor, gait, and balance problems (2). It is caused by death of dopamine-generating cells in the substantia nigra of midbrain. The pathological feature of PD is the accumulation of protein alpha-synuclein in the Lewy bodies in neurons. The protein inclusions are often in the cytoplasm near the nucleus or in the neurites. The anatomical distribution of the Lewy bodies is directly correlated to the clinical symptoms of movement disorders.

Huntington's disease (HD) is a neurodegenerative genetic disorder that affects muscle coordination and also demonstrates cognitive decline and psychiatric problems (3). It is caused by expanded CAG repeat in the huntingtin gene, resulting in production of abnormal protein huntingtin with long repeat of polyglutamine that makes it aggregation-prone. This mutant protein huntingtin forms aggregates in both cytoplasm and nucleus in the striatum and other basal ganglia areas, and the cortex as well. The length of the polyglutamine correlates well with the density of the inclusions, but the existence of inclusion body may not completely overlap with degenerating neurons (4).

ALS is characterized by rapidly progressive motor weakness including muscle atrophy and spasticity, with the results of difficulty speaking, difficulty

swallowing, and difficulty breathing (5). It is the most common motor neuron diseases. In ALS, the ubiquitinated TDP-43 can form aggregates in neuronal cell bodies and axons in the spinal motor neurons and motor cortex (6). Its causal role in ALS has been supported by genetic evidence (7).

Prion diseases are a group of progressively neurodegenerative disorders. They are caused by non-viral proteins that can induce wide spread of both intracellular and extracellular protein aggregates in the nervous system (8). These aggregates appear to be similar to the plaques in AD.

There are several factors that contribute to protein aggregation. First, the aggregation can be accelerated by protein concentration. For example, Down's syndrome in which an extra copy of APP is present shows early deposition of Aβ plaques (9). PD patients with triplication of the α-synuclein locus have extensive Lewy bodies and earlier onset of parkinsonism (10). Secondly, protein aggregation is enhanced by covalent modifications. Examples include oxidation of α-synuclein (11), phosphorylation of Tau (12) and ubiquitination of TDP-43 (6). Last, Proteolytic cleavage can lead to protein aggregation too. The amyloid culprit Aβ is the fragment cleaved from the soluble protein precursor APP sequentially β- and γ-secretase. Besides, the N-terminal truncate of mutant huntingtin, which contains the expanded polyglutamine, has much more tendency to undergo conformational change and aggregate (13).

Overall, insoluble protein deposition is a hallmark of neurodegenerative diseases, and may involve common cellular and molecular mechanisms. The different protein aggregates have provided mechanistic clues to the pathogenesis of neurodegenerative disorders.

2. AD general facts

Alzheimer's disease (AD) is the most common dementia. It is caused by aging-related neurodegeneration in the brain (14, 15). AD patients usually experience memory loss, cognitive impairment, sociability reduction and personality change (16-18).

The AD situation is worsening in this society. There are currently about 5.2 million Americans estimated to have AD, comprising ~5.0 million people over 65

years old and ~0.2 million younger patients (19-22). AD is now becoming the sixth leading cause of death in the United States. The direct financial cost of AD in 2013 was more than 200 billion dollars. Because of no effective cure, the proportion of AD deaths has been continuously growing over the other major health problems such as cardiovascular disease, strokes and cancer.

In an attempt to address the effect AD has on society, the government is investing more on AD research. About 400 million dollars has been provided by National Human Genome Research Institute and the National Institute on Aging to support conducting whole-genome and whole-exome studies on AD patients, aiming to "prevent and effectively treat Alzheimer's disease by 2025".

3. AD pathology

AD pathology is hallmarked by: 1) brain atrophy; 2) massive neuronal and synaptic loss; 3) extracellular plaques and 4) intracellular tangles in cerebral cortex and the medial temporal lobes (MTL) including the amygdale, subiculum, hippocampal CA-1 region, entorhinal cortex, and transentorhinal regions (23-25), although early changes in the olfactory bulb can also be observed (26). AD brains usually look shrunk, about 10% smaller than age-matched non-demented controls, with widened sulci and narrowed gyri. The MTL is usually the earliest affected region (27), shrinking by about 15% per year (28) and by about 66% in the end (29). The atrophy is even more accelerated when the disease proceeds from the stage of mild cognitive impairment (MCI) to symptomatic AD (30). The cortical and MTL atrophy can now be easily monitored in live patients by CT and MRI (30, 31).

Neuronal loss is a remarkable characteristic in AD. It is considered the cause of dementia. Normally, the number of neurons in nondemented brains can be relatively stable for several decades after 60 years old. However, more than 50% of neurons are lost in AD brains in the superior temporal sulcus (32), and hippocampal neurons can even drop by 84% in the end stage (29). The entorhinal cortex (EC) is another most affected region in AD. It is part of the neural circuit with hippocampus responsible for memory consolidation and maintenance. In certain layers of this region, there are 32% fewer neurons in patients with mildest

dementia, 40%~60% loss in moderate cases and up to 90% loss in severe cases (33). It's notable that Layer II of this region demonstrates the most remarkable loss, suggesting its critical role in the development of AD. Moreover, the dead neurons in the neocortex and the hippocampus, regions exhibiting high Aβ and Tau pathology, are mostly cholinergic. Because of this, AD was proposed to be caused by the failure of the cholinergic system (34).

Synaptic loss occurs very early and even before plaque and tangle formation in AD pathogenesis. It is proposed to be the key event in AD (35). In the AD temporal cortex, about 25% of all synapses in layers II-III and nearly 36% in layer V are lost; and in the frontal cortex, synapse density is reduce by 27% in layer V. In average, about 14%~38% of synapses are lost on each neuron (36). The prominent feature of synaptic loss was further confirmed (37-40).

Deposition of aggregated proteins is intensively studied in AD pathology, which is hallmarked by extracellular plaques and intracellular tangles. The plaques mainly include two types: diffuse and neuritic. The diffuse plaques have no clear boundary and contain no dystrophic neurites or glial cells. They appear early in the cerebral cortex. In contrast, the neuritic plaques are more condensed and often mixed with neurites, activated glial cells and inflammatory components. They can eventually evolve into so-called "burned-out" plaques when other cells and proteins components are degraded. Plaques occur initially in the neocortex (24, 25), and might be more abundant in temporal and occipital lobes, while moderate plaque numbers are seen in the parietal lobe and fewest in limbic and frontal lobes (41). There is no significant correlation between plaque pathology and dementia severity in AD (42).

Neurofibrillary tangles (NFT) are made up of paired helical filaments from the Microtubule-associated Protein Tau (MAPT, or Tau) protein, each of which contains two axially opposed helical filaments (43-45). They are usually present in the cell body and neurites of neurons, and called "neuropil" when they appear in the bundles of axons. When neurons die and neurites disappear, they become the so-called "ghost tangles"(25). In addition, by age of 85, almost all people will develop tangles (46). The tangles in AD first appear in the transentorhinal region, then spread to the adjacent hippocampus, later to the temporal cortex and finally

to the parietal and frontal and cortex. According to the tangle progression and distribution, AD pathology can be characterized into six stages. In Braak I & II stages (early stage): tangles are confined to the transentorhinal region; in III & IV (intermediate stage): tangles spread into entorhinal and transentorhinal regions; in V and VI (late stage): tangles proceed into neocortex. The NFT stages correlates better with dementia progression than plaques. In Braak stages I & II, the cognitive deficit is mild, while it will become much worse in stages V and VI when the neocortex is widely affected (25).

4. AD molecular research

4.1. Toxic insults and disrupted pathways

4.1.1. Amyloid plaque and Aβ toxicity

The major component of the extracellular plaques are small protein fragment species called Aβ peptides (47). They are sequentially cleaved from the membrane protein APP (Amyloid Protein Precursor) by two proteases: β-secretase (48, 49) and γ-secretase (50).

APP is a cell surface receptor that is thought to regulate neurite growth, neuronal adhesion and axonogenesis in neurons. Normally, APP is directly cleaved by α-secretase (51) predominantly on the cell surface. However, it can also be cleaved intracellularly to generate Aβ (the culprit in AD) by β-secretase (48). In this pathway, APP is internalized into endosomes where it will either translocate back to the membrane again or merge with proteases-containing vesicles to become a lysosome to be degraded. A certain portion of APP in the endosome will be recycled to trans-Golgi network in which it will be cleaved by β-secretase (52). The β-secretase is also present at low level in endoplasmic reticulum, endosomes and on the cell surface.

Despite these promising advances in our understanding, the more specific details of APP trafficking and cleavage in neurons are not very clear in neurons (50). The fundamental question of why APP favors the β-secretase cleavage pathway in AD is not very clear. The proposed mechanisms include perturbed

APP processing, increased neuronal and synaptic activity (53), altered cell membrane composition (54-56), reduced level of neurotrophic factors and declined clearance of Aβ (57), etc.

Extracellular plaques are mostly composed of Aβ fragments that can have different peptide lengths. Aβ42 and Aβ40 (named based on the cleavage residue in the APP protein) are the two major forms, in which the Aβ42 is more toxic while Aβ40 shows potentially protective role. Their ratio in AD determines neuronal toxicity (58). Treating rat primary hippocampal neurons with Aβ can directly cause synaptic and neuronal degeneration. Transgenic mice that express Aβ and form plaques in the brain demonstrate certain extents of impaired cognition (59).

The Aβ fragment can be detected in three forms: soluble monomers and oligomers as well as the insoluble fibrils. These different forms are present in patients in dynamic equilibrium (60). The soluble monomers and oligomers are generally considered more toxic (61-63), causing synaptic and network dysfunction by binding to and interrupting certain receptors on neurons or glial cells (42, 64). In addition, intracellular Aβ can be present in mitochondria where it causes oxidative stress through ROS generation in neurons (65).

4.1.2. Tau hyperphosphorylation and aggregation

The intracellular tangles are mainly made of the microtubule associated protein Tau (MAPT) (66-68) which is highly phosphorylated (69). MAPT is an adaptor protein that connects neural plasma membrane and axonal microtubules to regulate microtubule assembly and structural stability. It is also likely involved in the establishment and maintenance of neuronal polarity. In AD, MAPT is heavily phosphorylated at multiple sites, which is thought to allow it to aggregate and form tangle-like structures. Because dozens of sites are phosphorylated on Tau, there are many kinases that are involved. The major ones are GSK3β (Glycogen synthase kinase-3 beta), CDK5 (Cyclin-dependent kinase 5) and MARK (microtubule-affinity-regulating kinase) (70). Involvement of these kinases links tau hyperphosphorylation to inflammation, oxidative stress,

dysregulated energy metabolism, trophic factor deprivation and possible cell cycle re-entry events.

Tau hyperphosphorylation and aggregation has both neurotoxic loss-of-function and gain-of-function roles. Normally, phosphorylation of Tau causes its dissociation from microtubules, preventing its ability to regulate antegrade axonal transportation. In this way, uncontrolled hyperphosphorylation of Tau certainly makes it lose this function. Besides this loss-of-function role, soluble hyperphosphorylated tau induces neuronal toxicity in both rat and mouse primary neurons (71). It also interferes with mitochondrial respiration (72, 73). Thus, intracellular Tau tangles usually represent a neuron in the process of dying.

More importantly, Tau mediates amyloid-β toxicity in both in vitro and in vitro experimental systems. For example, Aβ-induced neuronal death in cultured primary neurons is not seen when Tau is knocked out (74). A similar phenomenon is also confirmed in mouse models (75, 76). This ability of Tau to mediate Aβ toxicity is proposed to be the major mechanism of AD neurodegeneration.

4.1.3. Inflammation

Inflammation is widely present in AD brains (77). First, there are substantial amounts of complement components (C3, C1q, etc.) that colocalize with extracellular plaques (78). In the AD insoluble proteome, the amount of C3, C4a and C4b is comparable to the Aβ level (79). The final activation effector MAC (membrane attack complex, composed of C5b-9) can also be found on the neuron membrane and cytoplasm (80). In addition to the complement system, activated microglia and astrocytic cells also appear surrounding the plaques (81, 82). These surrounding cells highly express proinflammatory factors including MHC class II, Cox-2, MCP-1, TNF-a, IL-1b, and IL-6 (83, 84), some of which can activate or recruit other glial or immune cells to elicit inflammatory responses (85). Finally, additional chemokines and cytokines and their receptors such as IL-1a, CXCR2, CCR3, CCR5, and TGF-b, have been detected in post-mortem AD brains (86, 87).

In recent years, the whole-genome genotyping and genome-wide association studies have identified new risk genes and gene loci. Some of these include

TREM2(88), CLU, PICALM, CR1, BIN1(89), CD33, ABCA7, MS4A6A CD2AP(90), EPHA1, HLA-DRB5/DRB1, SORL1, PTK2B, SLC24A4, ZCWPW1, CELF1, FERMT2, CASS4, INPP5D and MEF2C(91). More than half of these belong to the immune and inflammatory pathways. Such strong genetic evidence clearly highlights the role of inflammation in AD, which is now a major direction of research in the field.

Aβ peptide is believed to be an initiator of the inflammation in AD (92). Aβ soluble oligomers or insoluble plaques activate the complement cascade by binding to the component C1 (93). They also bind to TLRs (Toll-like receptors) and RAGE (Receptor for Advanced Glycation End products) on microglia cells. This leads to activation of transcription factors such as NF-κB and AP-1 and production of reactive oxygen species (ROS) and inflammation factors (94), which can then act on cholinergic neurons and stimulate astrocytes to be involved in this inflammation process. Continuous insult by Aβ amplifies these immune responses to an uncontrollable extent. Besides, degenerating neurons release ATP which further activates microglia through the P2X7 receptor, making the whole process become a vicious cycle (95-97).

It is notable that inflammation is initially useful for clearance of Aβ (98, 99). The overall deleterious inflammation in AD is probably due to chronic accumulation of an unbalanced immune response caused by continuous insult of Aβ.

4.1.4. Endocytosis

The discovery of risk loci, *PICALM*, *BIN1*, *CD2AP* and *SORL1* by genome-wide association studies (GWAS) has highlighted the potential role of endocytosis in AD neurodegeneration(91). Endocytosis is a process of cellular internalization of extracellular material and subsequently a migration through a series of vesicular compartments. Abnormal endocytosis has been indicated in multiple human diseases(100).

In neurons, endocytosis is required for maintenance of synaptic transmission and regulation from extracellular environment. After firing, some neurotransmitters or other substance released into the synaptic cleft are

internalized and repacked with other substances to become a fully mature presynaptic vesicle for the next firing(101). Disruption of this process certainly affects the efficiency of constant transmission between neurons. Besides, endocytosis is the major approach for neurons to receive regulatory signaling by extracellular molecules, such as hormones and growth factors. For example, the nerve growth factor(NGF) binds to the neuronal surface receptor and then internalized into endosome, where it continue to signal in complex with other partners (TrkA, Ras-MAPK)(102). Defective endocytosis affects neuronal survival. Because of the synaptic transmission and the enormous distance between neurites and the cell body, neurons heavily rely on endocytosis which is extremely active in the dendrites(103). Subtle impairment of endocytosis might cause neurodegeneration.

Indeed, endosomal abnormality is observed in AD and might play a causal role. At early stage of the disease when soluble Aβ starts to increase, endosomes appears enlarged and overexpress Rab5 and Rab4, proteins that regulate endosome formation and trafficking(104), suggesting endosomal alteration is an early event in AD pathogenesis. In contrast, such change was not reported in the early stage of other neurodegenerative diseases.

This uniqueness of endosomal alteration in AD can be corroborated by Aβ generation. After APP is internalized, it is first cleaved by β-secretase in the endosome, and then cleaved again by γ-secretase in the late endosome or trans-Golgi complex for generation of Aβ fragments(105). These fragments are less soluble and tend to aggregate into amyloid. This is a highly specific process in AD. Therefore, the endosomal alteration and Aβ generation, the two closely related events and both unique to AD, might have inherently mechanistic connection, in which endosome pathology is not likely to be consequential(106).

The potential causal role of endosomal aberrancy can be further implied by a disease with mutations that cause lysosomal storage disorder. Lysosome is a fusion of late endosome with membrane vesicles that contains proteases. Formation of lysosomes is part of the endocytic process. In *Neimann-Pick type C disease* (NPC), mutation in either gene NPC1 or NPC2 leads to disrupted trafficking of cholesterol into trans-Golgi for esterification. The resultant over-

accumulation of immature cholesterol imposes tremendous stress on the late endosomes. The NPC patients demonstrate neurodegeneration-related manifestations including cognitive decline, a typical symptom in AD. More importantly, what most attractive is that the NPC brains present with robust neurofibrillary tangles, another AD hallmark, strongly suggesting endosomal dysfunction has a causative effect in AD.

PICALM, *BIN1*, *CD2AP* and *SORL1* are genes mainly involved in endocytosis. Their genetic evidence directly from AD patients by GWAS, together with the existence of endosomal abnormality, might provide new mechanistic clues. More studies are required for our better understanding of their roles in AD pathogenesis.

4.1.5. Oxidative stress

Oxidative stress is clearly evident in AD brains at different molecular targets including protein, lipid, DNA/RNA and sugars (107). Carbonyls and nitration are significantly elevated in AD on tyrosine residues, the marker of oxidized proteins (108, 109). Increased levels of thiobarbituric acid reactive molecules, malondialdehyde, isoprostanes and 4-hydroxy-2-trans-nonenal, are found in AD brain extract, indicating excess lipid peroxidation (110, 111). The DNA and RNA oxidation markers, 8-hydroxy-2-deoxyguanosine (8OHdG) and 8-hydroxyguanosine (8OHG) products, are highly expressed in both nuclear and mitochondrial DNA (112-118). The demonstration of increased amounts of glycation and glycoxidation shows that sugars are also likely to be over-oxidized in AD (119).

The major contributor of oxidative stress in AD is proposed to be age-related mitochondrial dysfunction, which is caused by accumulation of mutation in its DNA over decades of years (117, 120-123). As neurons do not divide, it is reasonable to assume that any unrepairable modification or damage on the mitochondrial DNA by spontaneously leaking ROS (Reactive Oxygen Species) products will be accumulated over time. This accumulation will be accelerated in neurons at senior age when uncontrolled ROS leaking happen more frequently and the DNA repairing system is less effective. Mitochondrial DNA encodes 13

proteins that are critically involved in the oxidative respiratory chain, a process that has to be tightly controlled for proper control of ROS generation. Mutations on the DNA can result in aberrant function of these proteins, leading to disastrous production of ROS. Then, the vicious cycle begins.

Aβ is the second insult in AD that can disrupt mitochondrial function. Aβ, especially the more toxic form Aβ42, can be detected in mitochondria (65, 124, 125) In mice, Aβ directly binds to the protein alcohol dehydrogenase to interrupt its redox function, leading to dysfunctional mitochondria and impaired memory (126). In addition, altered metabolism of the Aβ precursor protein APP is thought to be associated with mitochondrial Dysfunction in Down's syndrome, an AD-like disease that is caused by a trippled APP-containing chromosome (127).

Altered levels of oxidized metals are another important source contributing to oxidative stress in AD. The Aβ plaques in AD brains contain remarkably high concentrations of Cu (400μM), Zn (1 mM) and Fe (1 mM) ions which can bind to Aβ in vitro directly (128, 129). Thus, the plaques can be considered as localized source of oxidative stress (130).

4.1.6. Excitotoxicity

From the studies presented above, it appears that oxidative stress from excessive free-radical generation plays an important role in AD mechanism (131-133).

Excitotoxicity in the context of AD is caused by overactivation of NMDA (N-methyl-d-aspartate) receptors on neurons (134). Almost every neuron in the brain has this type of ionotropic L-glutamate receptor to mediate postsynaptic Ca^{2+} influx. Although normal levels of NMDA receptor signaling are essential for proper post-synaptic Ca^{2+} homeostasis, high levels can be detrimental. For example, high levels of L-glutamate in the growth medium causes extended period of elevated intracellular Ca^{2+} for up to one hour, and neuronal death in 24 hours (135, 136).

The excessive activation by NMDA receptors can be caused by Aβ. Synthetic Aβ peptides can potentiate glutamate neurotoxicity in human cortical cultures (137). Besides, an increased level of Aβ42 makes mouse hippocampal neurons

more vulnerable to excitotoxic necrosis (138), possibly by inhibiting glutamate reuptake or enhanced release (139, 140). More interestingly, NMDA receptor overactivation can increase Tau expression, phosphorylation and toxicity in cultured neurons (141-144). Thus, Aβ and Tau can be linked again through NDMA receptors.

4.1.7. ER (endoplasmic reticulum) stress

ER is the subcellular organelle responsible for a number of functions such as protein synthesis and folding, calcium storage, and metabolism of lipid and carbonate. ER stress is a common feature in many neurodegenerative diseases including AD, Huntington's disease, ALS (amyotrophic lateral sclerosis) and Parkinson's disease (145).

Several studies showed that the unfolded-protein response (UPR) and other multiple ER-stress associated proteins are altered in AD (146-152). It is reported that UPR can even be seen in pretangle neurons (153), implying ER stress can be an early event in AD neurodegeneration.

Abnormal intracellular concentration and distribution of calcium ions is another indicator of dysfunction of ER in which Ca^{2+} is mainly stored. In AD, neurons bearing tangles demonstrate more dysregulated Ca^{2+} than those without tangles (154). This, again, indicates ER stress is present in AD degenerating neurons.

As all these lines of evidence point to the ER dysfunction, we might expect AD brains should have considerable misfolded proteins because protein folding is mainly performed in ER. However, in a large scale study of potentially misfolding proteome using mass spectrometry in this thesis, only 43 proteins showed remarkable accumulation in AD while the other 4000~ proteins show similar levels in AD and non-demented controls (79). This suggests that the consideration of ER dysfunction as a causal event in AD pathogenesis needs be cautious.

4.1.8. Calcium dyshomeostasis

As mentioned previously, intracellular calcium is altered in AD brain neurons (146, 155, 156). Although it is technically difficult to measure calcium in situ in AD postmortem brains, calcium dyshomeostasis is supported by several lines of evidence.

First, both protein-bound and -free calcium in tangle-bearing neurons are higher than tangle-free neurons. The increased level of calcium can occur even at the early stage of neurons with hyperphosphorylated Tau. Moreover, elevated calcium is observed in spines of neurons surrounding plaques in APP transgenic mice (157). Secondly, the calcium-dependent protease “Calpain” is widely activated in AD brains (158, 159). It is notable that calcium dyshomeostasis is not restricted to neurons, but also appears in other tissues and cells in AD, such as fibroblasts.

The disrupted calcium can be attributed to ER stress and calcium-binding proteins. In addition to the dysfunctional ER mentioned before, the calcium-buffering protein calbindin also plays a role in maintaining calcium balance. Calbindin levels decrease during aging and much more significantly in AD as compared to nondemented controls. Furthermore, calbindin knockout mice have elevated basal calcium in dendritic spines (160) and develop abnormal spine morphologies (161).

Finally, Aβ oligomers can bind to NMDA receptors to induce calcium influx (162), linking calcium dyshomeostasis to the Aβ cascade in AD neurodegeneration.

4.1.9. Neurotrophic factor deprivation

There are mainly four types of neurotrophic factors in the human brain. These are NGF (Nerve growth factor), BDNF (Brain-derived neurotrophic factor), NT-3 (Neurotrophin-3) and NT-4 (Neurotrophin-3). The best studied one in AD is BDNF.

BDNF is largely reduced in AD brain neurons in the cortex and hippocampus at both the mRNA and protein levels (163), and even in MCI (Mild Cognitive Impairment) patients (164), the early dementia stage of AD. The reduction is often in the most affected brain regions such as the hippocampus, entorhinal,

temporal, parietal and frontal cortices. Interestingly, BDNF is largely reduced in neurons bearing neurofibrillary tangles, but is more abundant in tangle-free neurons, implying a possible link between BDNF and Tau. However, BDNF is also reported to be increased not only in AD brains in hippocampal neurons (165, 166), but also in glial cells surrounding Aβ plaques in APP transgenic mice (167), suggesting the complicated role of BDNF in AD pathology.

The potential role of BDNF in AD was studied recently. Knockout of BDNF or its receptor TrkB (tropomyosin receptor kinase B) in mice leads to defective learning and memory (168), but the same effect of BDNF could not repeated in other reports (169, 170). A recent study published in *Nature medicine* confirmed again the neuroprotective effects of BDNF in APP transgenic mice (171), in which BDNF gene expression after formation of plaques and neuronal loss successfully rescued mice from development of learning and memory impairment. Nevertheless, the role of BDNF deprivation in AD pathogenesis requires more evidence to be established (172).

4.1.10. Energy metabolism alteration

GSK3B (Glycogen synthase kinase-3 beta) is one of the major kinases responsible for the phosphorylation of aggregated Tau. Because one of its major functions is regulating glucose homeostasis, energy metabolism in AD has gained even more attention in the field. Research found patients with type 2 diabetes or obesity/dyslipidemic disorders have higher risk factor for mild cognitive impairment (MCI) and AD, which is confirmed in animal studies (173-175). Moreover, brain insulin resistance and insulin deficiency correlate with the progression of AD (176-179). Insulin treatment can actually improve cognitive performance in both humans and animal models (180). Indeed, type 2 diabetes and AD do share common molecular alterations (181).

Altered energy metabolism is also evident in living AD patients using functional MRI (Magnetic Resonance Imaging) or PET (Positron Emission Tomography) technology. Brain regions often affected early by plaques, such as posterior cingulate, retrosplenial, and lateral parietal cortex, are very active in energy metabolism in young adults, while significantly reduced in AD patients

during memory retrieval (182). This regionally specific default activity might predispose these regions to plaque formation as more Aβ can be generated in neurons with increased activity (183, 184).

Neuronal energy crisis has also been suggested by reduced cerebral blood flow (CBF) in most affected brain regions in AD (185-191). Although conclusions from these reports are confounded by their difference in technological sensitivity and case selection, it is plausible that stoke and myocardial infarction reduce blood supply to the brain and thus certainly exacerbate the neuronal stress in AD.

4.1.11. Neuronal cell cycle reentry

Cell cycle re-entry in AD has been observed by several groups for more than a decade (192-197). Because one of the major kinases that phosphorylates Tau for its aggregation is CDK5, a cyclin-dependent kinase involved in mitosis, it is reasonable to speculate that cell cycle might be activated in the dying neurons. This assumption is supported by elevated levels of several other cyclins and cell proliferation markers PCNA and Ki67 in AD brain neurons (198-205).

Interestingly, Tau is phosphorylated during mitosis (206, 207), probably for reassembly of the tubulins required for cell division. Thus, it is possible that Tau hyperphosphorylation in AD is just a reflection of neuronal cell cycle reentry as a secondary effect to aberrant activation of other pathways in neurons. It is notable that mice overexpressing human Tau also display activated cell cycle event in brain neurons (194).

Interestingly, neuronal cell cycle reentry can be convincingly observed in APP transgenic mice (192). They appear much earlier, at about ~6 months of age, before visible plaques, indicating that it is soluble Aβ that plays the critical role to induce them. Again, the toxicity-initiating effect of Aβ is confirmed. What is more interesting is that the earliest regions to show cell cycle reentry are locus ceruleus and dorsal raphe. Although these two regions usually bear few plaques in AD, they start to demonstrate phosphorylated Tau in young adults as early as under 30 years old (208), a stage even before the initial formation of Tau tangles in the transentorhinal region (209). These findings highlight that the neuronal cell cycle reentry fits well into the hypothesis of the Aβ-Tau axis.

In this thesis study, I also observed the nuclear protein U1-70K, a RNA spliceosomal component, redistributes into the cytoplasm surrounding the nuclei. It is known that U1-70K moves out of nuclei during mitosis, which happens even before Tau phosphorylation. Therefore, neuronal cell cycle reentry is probably true in AD neurons as an early event in neuronal degeneration.

4.1.12. Neuronal death in AD

There are three important types of cell death in neurodegenerative diseases: apoptosis, necrosis and autophagy (210). Determination of the specific type of cell death can certainly focus the research on the particular triggers and dysregulated components in the upstream pathway.

Neuronal death in AD brains is not typical apoptosis. Substantial DNA fragmentation is observed in AD brains in the subiculum, the hippocampus and the entorhinal cortex with 50-fold increase in neurons those closely AD-associated regions (211). Although increased expression of both pro- and antiapoptotic proteins and other cell death-related factors has been evidenced in AD brains, only 0.02-0.05% hippocampal neurons show apoptotic morphology and express activated caspase-3. This suggests apoptosis is not the major type of cell death for neurodegeneration.

Necrosis is possibly involved in AD neuronal death. Although thorough examination of the morphology and biochemical characteristics is yet to be done in large number of sporadic AD cases, a ultrastructural study of dying neurons in neuronal familial Alzheimer's disease brains with E280A mutation on presenilin-1 has shown typical features of necrosis in the majority of TUNEL-positive neurons (212). Necrosis as a more prominent feature in AD neurons is also suggested in many other reports (213).

It’s notable that only about 28% degenerating neurons are nearby the plaques and about 41% degenerating neurons bear NFTs, suggesting both the Aβ plaques and neurofibrillary tangles are not likely the direct initiating death triggers. It’s reported that soluble form of Aβ can induce neuronal necrosis but not apoptosis(214). Moreover, activated caspase 3 can be detected in over 50% neurons showing signs of granulovacuolar degeneration (GVD); it was restricted

to the granules that have a “pre-tangle” stage but no nuclear alterations of apoptosis. These findings suggest that soluble Aβ might be able to induce neuronal death, but not Tau.

Autophagy could be the main type of neuronal death according to a study in which it was extensively present in AD neocortex as demonstrated by immuno-electron microscopy(215).

Considering the long duration of AD disease progression and complicated cellular context, we might expect that neuronal death can be an integrated type of apoptosis, necrosis and autophagy, which may even differ among individual neurons(216).

4.2. The genetics of Alzheimer disease

So far, through whole-genome genotyping and genome-wide association studies (GWAS), three genes are identified to have causative mutations in AD: APP, PSEN1 and PSEN2. In contrast, the other components in the paradigm Aβ-Tau pathway such as BACE1&2, PEN and APH (γ-secretase subunits) as well as Tau, have no mutations reported to be associated with AD so far. Mutations in APP either cause doubled APP protein expression or increased production of Aβ. Mutations in PSEN1&2 are loss-of-function, which changes their cleavage preference of APP at the C-terminus so as to increase the ratio of Aβ42/ Aβ40 although the total Aβ level is reduced. Because all these three mutated genes belong to the Aβ cascade pathway, their causal role in AD pathogenesis is greatly confirmed.

APOE and TREM2 (Triggering Receptor Expressed on Myeloid cells 2) are two risk genes for AD (91). APOE allele 4 and TREM2 mutation (R47H) are statistically associated with AD patients (88, 217, 218). APOE normally regulates cholesterol and lipid metabolism. It is also shown to be involved in Aβ aggregation and the allele 4 has greater ability to promote the formation of plaque than other alleles (219-221). TREM2 is a membrane protein that is involved in immune response and chronic inflammation.

Twenty one other variants are identified to be in loci close to genes including CLU, PICALM, CR1, BIN1, CD33, ABCA7, MS4A6A/MS4A4E, CD2AP, EPHA1, HLA-DRB5/DRB1, SORL1, PTK2B, SLC24A4, ZCWPW1, CELF1, FERMT2, CASS4, INPP5D, MEF2C, and NME8 respectively (91). Interestingly, they mainly belong to functions related to immune response and cholesterol metabolism. The comprehensive genetic evidence confirms APP metabolism and reinforce inflammation as am important contributor in the etiology of AD pathogenesis.

4.3. Animal Models of Alzheimer Disease

Many different animal models have been used in AD, including C. elegans, fly, zebra fish, monkey, etc. The most common one is mouse. Current mouse models are mainly transgenic lines using the three AD-associated genes: APP, presenilin and Tau. The common ones are Tg2576 (APP695-K670N/M671L), 5X FAD (APP695-K670N/M671L, I716V, V717I, PSEN1-M146L, L286V) and 3xTg (APP695-K670N/M671L, PSEN1-M146V, Tau- P301L) (222). These mouse models show plaques and/or tangles depending on the gene they express.

The mouse models described above have been used as a tool to study particular insult(s) in the brain and provided valuable information. However, there are certain limitations with these models. First, the APP transgenic mice usually do not develop tangles and Tau mice do not have plaques. Moreover, the AD hallmarked synaptic and neuronal loss are not always seen and never massively present like in AD, even in the triple transgenic mice (3xTg). Last, learning and memory impairment can be seen even before the formation of plaques or tangle, although this can be interpreted as neuronal toxicity caused by soluble Aβ rather than the insoluble plaque (223, 224). Because of the substantial difference of these mouse brains from human brains, we should be cautious when we consider them as “Alzheimer’s mice”.

4.4. Summarized AD model and the opening question

The major hypothesis in the field posits AD is initiated by Aβ and mediated by Tau **(Figure 1.1)**. The initiating role of Aβ is supported by genetic evidence.

Three AD associated genes that have been identified so far are APP, PSEN 1 and 2, all of which are involved in Aβ generation (225). Besides, a mutation in APP that leads to reduced production of Aβ prevents individuals from developing AD (226), supporting the requirement of Aβ in AD pathogenesis. However, the brain load of Aβ plaques does not correlate with the severity of dementia, in which patients with heavy Aβ amyloid may present no memory loss at all, indicating Aβ plaque alone cannot cause AD neurodegeneration. Therefore, disruption of other pathways is required to induce neuronal degeneration.

As mentioned previously, inflammation, oxidative stress, ER stress, neurotrophic factor deprivation and other toxic insults or aberrant cellular events are present in the brain either as a secondary effect to Aβ soluble oligomers and insoluble plaques or present as co-criminals. They should be the executors of neuronal death. However, it is not clear which one plays the major role in order for us to develop drugs to target it specifically. Tau hyperphosphorylation and aggregation can be one of the contributors, just like those disrupted pathways in the black box, but it could be just a consequence of those disrupted pathways, because the dying neurons outnumbers the tangle-bearing neurons and dysregulation of many pathways has already been observed prior to presence of the tangle.

Overall, Aβ aggregation is certainly the initiating event as it induces inflammation and causes disruption of multiple pathways, corroborated by the fact that neuritic plaques (the Aβ plaque merged with activated microglia and astrocytes, degenerating neurons and neurites with aggregated Tau) correlates much better than diffusive plaque (mainly Aβ aggregates only) with dementia stages. However, the remaining question in the current AD model is that we still have no clue how exactly the neurons are killed. Therefore, in this study, we try to find a widespread, AD-specific and early-occurring disruption of a protein or a pathway in order for better understanding the mechanism of AD neuronal death.

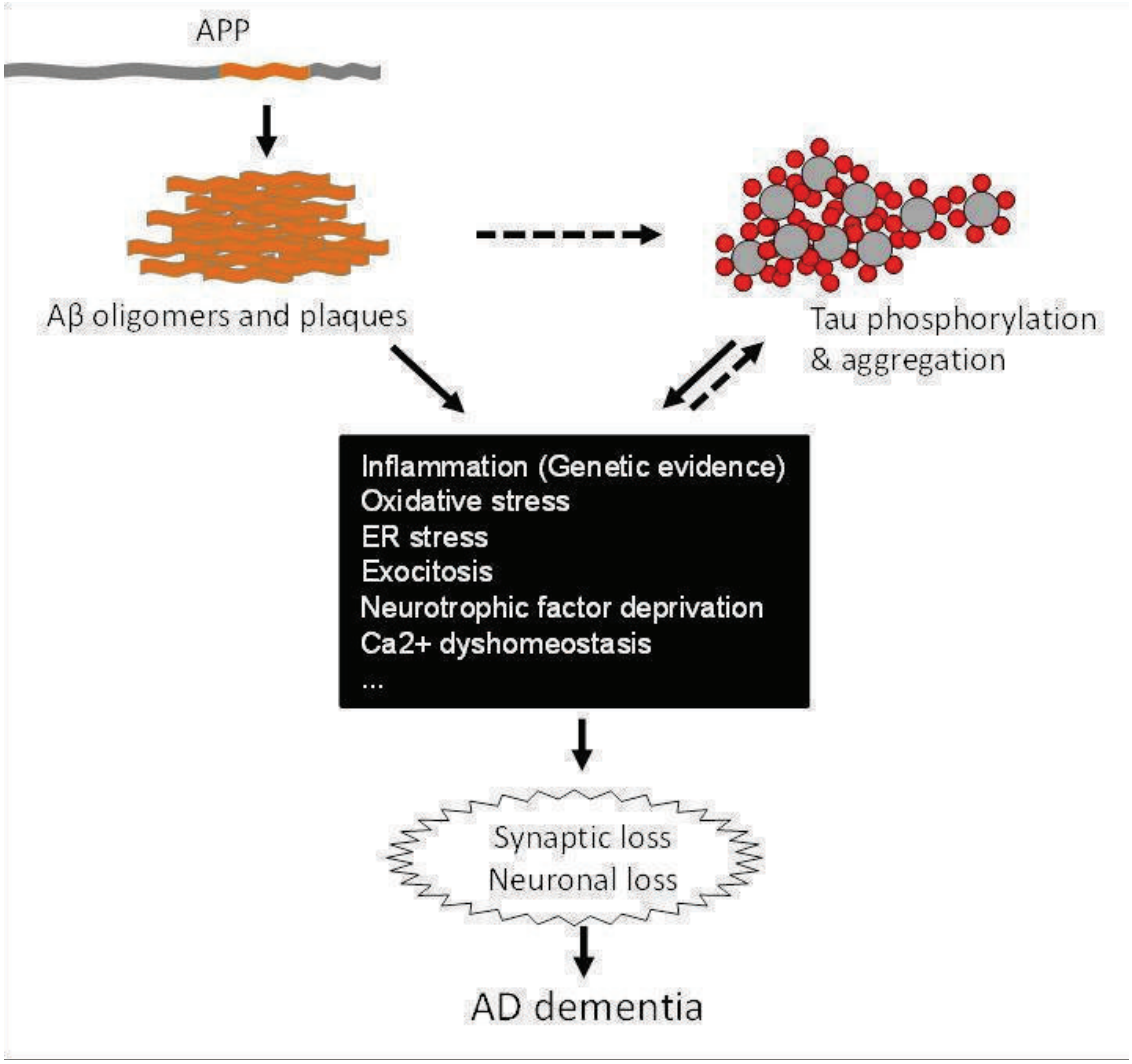

Figure 1.1 AD mechanism model. Aβ initiates the AD pathogenesis, but requires involvement of other pathway disruption to induce neuronal degeneration. Tau might be just one of the disrupted pathways in the black box. Which pathway plays the major role and how it causes the synaptic and neuronal loss is still an opening question in AD field. The aim of the thesis is to find potential molecules that can fit in this model for better understanding of AD mechanism.

5. Introduction of Proteomics by LC-MS/MS

5.1. Working principle of LC-MS/MS

Mass spectrometry (MS) measures the mass-to-charge ratio (m/z) of an analyte. The mass and charges of an analyte determine its moving track in a defined electromagnetic field, which can be captured and recorded by a specific detector (227, 228). A protein or a peptide is composed of amino acids with known molecular mass each. Thus, when it brings charges, its overall mass can be measured by MS.

Currently, there are two common methods for this purpose: Electrospray ionization (ESI) and matrix-assisted laser desorption/ionization (MALDI) (229, 230). ESI ionizes the analytes out of a solution and it is often used for detection of peptides with large complexity, while MALDI ionizes the samples out of a dry and crystalline matrix by laser pulses and it is suitable for detection of relatively larger and purer peptides or proteins. Therefore, ESI is applied in the LC-MS/MS pipeline.

LC-MS/MS (Liquid chromatography coupled with tandem mass spectrometry) is now the most prevalent method to analyze the proteins in highly complex samples like whole tissues or cell lysates. In this method **(Figure 1.2)**, whole lysate samples are first digested by a protease (usually trypsin) into peptides in a solution or in a gel band after SDS-PAGE. These peptides are then loaded to a capitulary column filled with hydrophobic micron beads for reverse phase liquid chromatography. Peptides with different hydrophobicity are sequentially eluted by the flowing buffer with increasing gradient of organic solvent like acetonitrile. Eluted peptides flow to the end tip of the column where high voltage (1.8~2.5kV) is applied. At such high voltage, peptides in the acid liquid mist full of hydrogens (H^+) are sprayed into the entry part of MS machine where high temperature suddenly evaporates the liquid droplets into gas phase. This makes the H^+ ions attach to the peptides, a process called peptide ionization or ESI. Ionized peptides keep moving toward traps with different well-defined electromagnetic field and scanned by the detector to measure their m/z ratio.

This first scan is commonly called MS1. Because many different peptides can have the same overall mass, mere m/z ratio is not sufficient to differentiate them. The MS machine then selects one peptide at a time to fragment it and measure the product ions. This generates the spectra which is MS2. The whole process only takes about 0.1 second. Thus, 18,000 sequencing events can be attempted in 30 min. Each peptide should have a particular spectrum of fragments and thus generate a unique MS2 spectra that can different it from others. The MS1 and MS2 can be mapped to a database that has theoretically standard spectra for each peptide. The best matched standard is considered as the peptide candidate.

Major limitations of protein detection by LC-MS/MS include: 1) Proteins have no suitable cleavage sites to generate MS compatible peptides with appropriate length and hydrophobicity; 2) Proteins have heavy modifications. Modified amino acids might not be cleavable by proteases for digestion. The additional mass is unpredictable if the modifications are largely unknown.

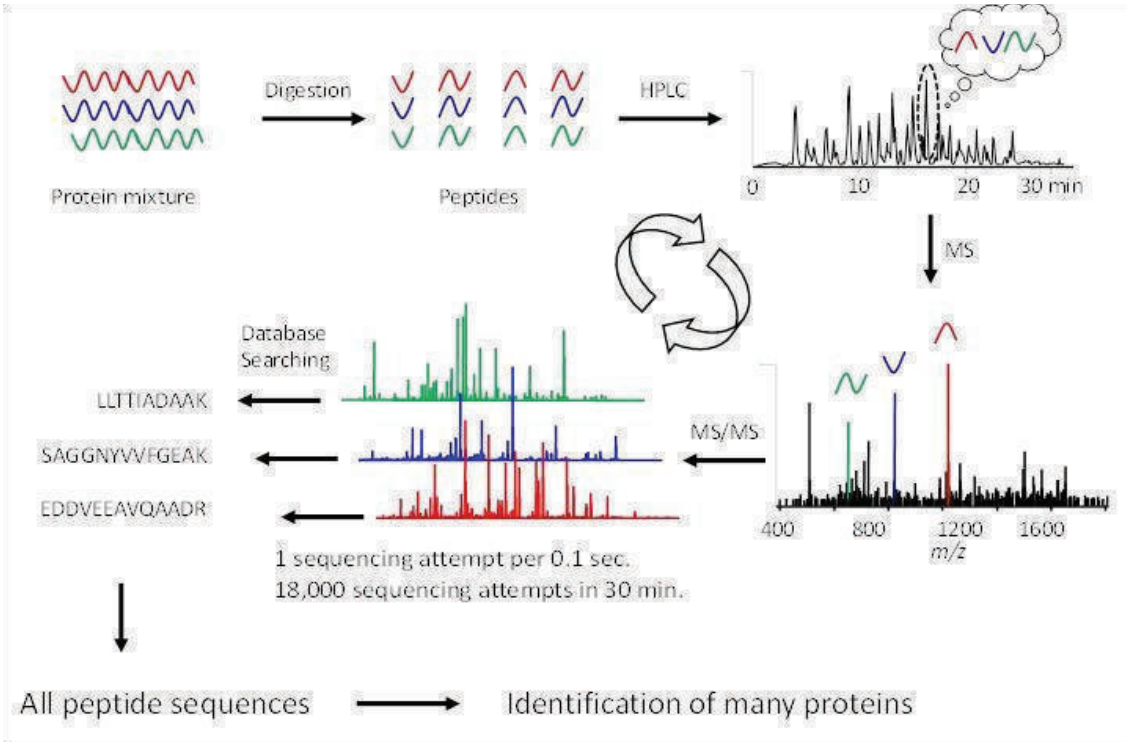

Figure 1.2 Working principle of liquid chromatography coupled with tandem mass spectrometry (LC-MS/MS).

5.2. LC-MS/MS application in neurodegenerative diseases

Mass spectrometry-based proteomic analysis has been widely used to study neurodegenerative diseases not only for large scale proteome profiling (231-236) but also for protein modifications such as phosphorylation (237), ubiquitination (238, 239), nitration (240, 241) and others in both human postmortem and mouse tissues. These proteomic studies have provided useful information for better understanding of the disease mechanism (242), and also discovered several candidates for disease-specific markers (243-245). Our discovery of U1 pathology in this study can be a great example for the first time that proteomic analysis can reveal proteins dysregulated in a critical pathway.

Despite the unique merit of MS technology, it also has some limitations in studying neurodegenerative diseases (235, 246). One major problem arises from the use of clinical tissue samples. These samples from different cases have large variations, including tissue complexity, disease stage, sample preservation, etc. Besides, each sample is composed of highly heterogeneous cells with different number, type, cycle stage, activation status and others. For example, if a subset of neurons has a protein change at about 10-fold, it could demonstrate no change at all in the whole tissue homogenate when this subset only occupy less than 10% of total cells. Selection of the sample at reasonable disease stage and from the pertinent brain regions is essential to guarantee the results will represent the disease status precisely.

The other problem comes from the current capability of LC-MS/MS. Because the brain is a highly complicated organ, the proteins in it are highly complex. It can be estimated that the number of proteins is about 20,000. This requires much higher performance of LC-MS/MS that has more efficient fractionation of peptides, higher resolution of the reverse phase liquid chromatography and enhanced sequencing speed and accuracy of MS machine.

These technical challenges are now under intensive study and progresses have been continuously made.

6. Transcriptome analysis by RNA-seq

6.1. Working principle of RNA-seq

RNA-seq is a revolutionary technique that was recently developed for comprehensive analysis of the transcriptome (247-249). In this technique, total RNA is first extracted from cell or tissue samples. Then the subset of RNA (e.g., mRNA, microRNA, etc.) is purified using specific methods. The highly enriched RNA is fragmented into RNA pieces and reverse transcribed into cDNA using random primers. (Sometimes, the fragmentation can also be performed after the reverse transcription.) After the second strand cDNA is synthesized by DNA polymerase I, the termini of the double strand DNA are end-repaired and adenylated in order to be ligated with adaptors next.

After purification, the cDNA template with about 200bp is chosen and amplified by PCR. Sequencing is done usually on a next-generation-sequencing (NGS) machine. The machine has a flow cell that is densely coated with two adaptors. The denatured DNA sample is loaded onto the flow cell. When the concentration is low enough, DNA stands are far from each other and bind to either of the adaptors. After the amplification process, each strand forms a cluster of amplified products on a micro-spot. After removing one of the strands, the other adaptor-specific primer and fluorescent nucleotide are added to start the sequencing. Nowadays, the transcriptome analysis can be done in just two weeks. It is now becoming widely used in studying human diseases by analyzing transcriptome of clinical tissues (250).

6.2. RNA-seq application in neurodegenerative diseases

RNA-seq has been recently used in neurodegenerative diseases (251). In the field of amyotrophic lateral sclerosis and frontotemporal degeneration, TDP-43 was discovered to be the major component of the protein aggregates in the patient brain. RNA-seq analysis revealed long pre-mRNA depletion and RNA missplicing in mice when TDP-43 was knocked down, providing evidence that

TDP-43 dysfunction in neurons can result in RNA disruption and neuronal vulnerability to death (252, 253).

RNA-seq was also utilized to study the mRNA transcriptome in brains of Alzheimer's disease, and revealed RNA expression level changes and certain splicing alterations in different brain regions (254, 255). It is also utilized to analyze total mRNA from AD mice brain tissues which has provided some useful information (256). However, most of the studies on clinical brain tissues were compromised by sample heterogeneity and case variation (257).

Chapter 2:
U1 SMALL NUCLEAR RIBONUCLEOPROTEIN COMPLEX AND RNA SPLICING ALTERATIONS IN ALZHEIMER'S DISEASE

U1 small nuclear ribonucleoprotein complex and RNA splicing alterations in Alzheimer's disease

Bing Bai[a,1], Chadwick M. Hales[b,c,1], Ping-Chung Chen[a,1], Yair Gozal[b,c,1], Eric B. Dammer[c], Jason J. Fritz[b,c], Xusheng Wang[d], Qiangwei Xia[c], Duc M. Duong[c], Craig Street[e], Gloria Cantero[f,g], Dongmei Cheng[c], Drew R. Jones[a], Zhiping Wu[a], Yuxin Li[a], Ian Diner[c], Craig J. Heilman[b,c], Howard D. Rees[b,c], Hao Wu[h], Li Lin[e], Keith E. Szulwach[e], Marla Gearing[c,i], Elliott J. Mufson[j], David A. Bennett[j], Thomas J. Montine[k], Nicholas T. Seyfried[c,l], Thomas S. Wingo[b,c], Yi E. Sun[f], Peng Jin[c,e], John Hanfelt[c,h], Donna M. Willcock[m], Allan Levey[b,c,2], James J. Lah[b,c,2], and Junmin Peng[a,d,2]

[a]Departments of Structural Biology and Developmental Neurobiology and [d]St. Jude Proteomics Facility, St. Jude Children's Research Hospital, Memphis, TN 38105; Departments of [b]Neurology, [e]Human Genetics, [h]Biostatistics and Bioinformatics, [i]Pathology, and [l]Biochemistry and [c]Center for Neurodegenerative Diseases, Emory University, Atlanta, GA 30322; [f]Departments of Molecular and Medical Pharmacology and Psychiatry and Behavioral Sciences, University of California, Los Angeles, CA 91301; [g]Departmento de Fisiología Médica y Biofísica and Centro de Investigación Biomédica en Red sobre Enfermedades Neurodegenerativas, Instituto de Biomedicina de Sevilla, University Hospital Virgen del Rocío, University of Sevilla, 41013 Seville, Spain; [j]Department of Neurological Sciences, Rush University Medical Center, Chicago, IL 60612; [k]Department of Pathology, University of Washington, Seattle, WA 98104; and [m]Department of Physiology and Sanders–Brown Center on Aging, University of Kentucky, Lexington, KY 40536

Edited by Gideon Dreyfuss, University of Pennsylvania, Philadelphia, PA, and approved August 12, 2013 (received for review May 30, 2013)

Deposition of insoluble protein aggregates is a hallmark of neurodegenerative diseases. The universal presence of β-amyloid and tau in Alzheimer's disease (AD) has facilitated advancement of the amyloid cascade and tau hypotheses that have dominated AD pathogenesis research and therapeutic development. However, the underlying etiology of the disease remains to be fully elucidated. Here we report a comprehensive study of the human brain-insoluble proteome in AD by mass spectrometry. We identify 4,216 proteins, among which 36 proteins accumulate in the disease, including U1-70K and other U1 small nuclear ribonucleoprotein (U1 snRNP) spliceosome components. Similar accumulations in mild cognitive impairment cases indicate that spliceosome changes occur in early stages of AD. Multiple U1 snRNP subunits form cytoplasmic tangle-like structures in AD but not in other examined neurodegenerative disorders, including Parkinson disease and frontotemporal lobar degeneration. Comparison of RNA from AD and control brains reveals dysregulated RNA processing with accumulation of unspliced RNA species in AD, including myc box-dependent-interacting protein 1, clusterin, and presenilin-1. U1-70K knockdown or antisense oligonucleotide inhibition of U1 snRNP increases the protein level of amyloid precursor protein. Thus, our results demonstrate unique U1 snRNP pathology and implicate abnormal RNA splicing in AD pathogenesis.

proteomics | liquid chromatography-tandem mass spectrometry | U1A | RNA-seq | premature cleavage and polyadenylation

Deposition of insoluble protein aggregates is a prominent feature of neurodegenerative diseases. Identification of the aggregated proteins provides crucial insights into molecular pathogenesis, such as β-amyloid (Aβ) and tau in Alzheimer's disease (AD) (1–3), α-synuclein in Parkinson disease (PD) (4, 5), and TDP-43 in ubiquitin-positive frontotemporal lobar degeneration (FTLD-U) and amyotrophic lateral sclerosis (ALS) (6). In AD, studies of amyloid (7) and tau (8) have provided extensive knowledge concerning pathogenic mechanisms; however, the underlying etiology of the disease remains incompletely understood (9).

Unbiased approaches have great potential to shed new light on AD pathogenesis. For example, genome-wide association studies have identified a growing list of more than 10 genes linked to AD risk. Advances in proteomics technologies (10, 11) allow unparalleled opportunities to directly examine protein level differences in neurodegenerative diseases. These differences can be used to develop biomarkers of disease and provide insights into disease pathogenesis. Feasibility of a proteomics approach as well as disease-relevant changes have been described in both plasma (12–14) and cerebrospinal fluid (15–17), highlighting the utility of proteomics in biomarker development. We, and others, have also demonstrated the potential for this approach in identifying neurodegenerative-specific changes in postmortem brain tissues. Using subproteome studies, constituents of isolated amyloid plaques (18), AD hippocampus (19), cortical Lewy bodies (20), AD membrane fraction (21), and specific phosphorylation sites in neurofibrillary tangles (22) were identified. Using broader discovery proteomics, we demonstrated unique candidate proteins in both AD (23, 24) and FTLD-U (25).

To achieve more detailed characterization of abnormally aggregated proteins in AD, we undertook a comprehensive study of the human brain-insoluble proteome in AD and other neurodegenerative diseases by liquid chromatography-tandem mass spectrometry (LC-MS/MS). Among the proteins that accumulate in the AD-insoluble proteome, we identified several components of the U1 small nuclear ribonucleoprotein (U1 snRNP), which is a constituent of the spliceosome complex responsible for RNA processing. Pathological examination demonstrated striking and widespread accumulation of extranuclear aggregated U1 snRNP components in neuronal cell bodies. Functional consequences of these observations were reflected in widespread alterations in RNA processing in human AD brains. Our findings demonstrate a unique pathological association and suggest that disruption of neuronal RNA processing may play a key role in AD pathogenesis.

Results and Discussion

LC-MS/MS Analysis Reveals an Enrichment of U1 snRNP in the AD Proteome Compared with Other Neurodegenerative Proteinopathies. We designed a pooling strategy with replicates (26) to simplify the analysis of protein aggregates in cortical tissue harvested from 10 AD and 10 age-matched, nondemented cases (Fig. 1*A*; Fig. S1, and Dataset S1). Aggregated proteins typically show low

Author contributions: B.B., C.M.H., Y.G., E.B.D., A.L., J.J.L., and J.P. designed research; B.B., C.M.H., P.-C.C., Y.G., E.B.D., J.J.F., X.W., Q.X., D.M.D., C.S., G.C., D.C., Z.W., Y.L., I.D., C.J.H., H.D.R., L.L., and N.T.S. performed research; M.G., E.J.M., D.A.B., T.J.M., D.M.W., and J.P. contributed new reagents/analytic tools; B.B., C.M.H., P.-C.C., E.B.D., J.J.F., X.W., Q.X., D.M.D., C.S., D.R.J., Z.W., Y.L., H.W., L.L., K.E.S., N.T.S., T.S.W., Y.E.S., P.J., J.H., A.L., J.J.L., and J.P. analyzed data; and B.B., C.M.H., P.-C.C., A.L., J.J.L., and J.P. wrote the paper.

The authors declare no conflict of interest.

This article is a PNAS Direct Submission.

Data deposition: The sequences reported in this paper has been deposited in the ProteomeXchange database, www.proteomexchange.org (identifier PXD000067); and raw RNA-seq files have been deposited in the National Center for Biotechnology Information Sequence Read Archive database, www.ncbi.nlm.nih.gov/sra (accession no. SRA060572).

[1]B.B., C.M.H., P.-C.C., and Y.G. contributed equally to this work.

[2]To whom correspondence may be addressed. E-mail: junmin.peng@stjude.org, jlah@emory.edu, or alevey@emory.edu.

This article contains supporting information online at www.pnas.org/lookup/suppl/doi:10.1073/pnas.1310249110/-/DCSupplemental.

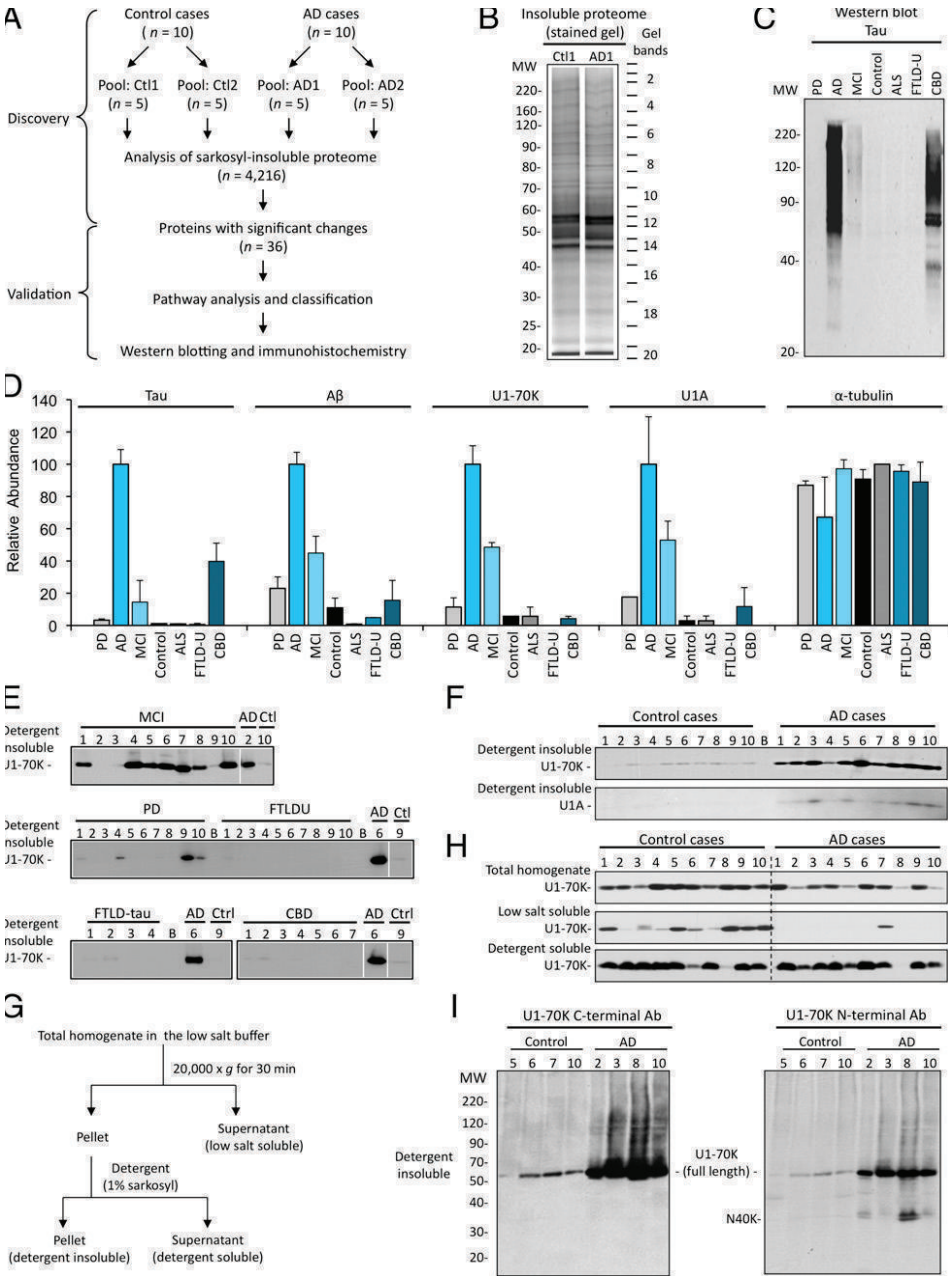

Fig. 1. Proteomic comparison reveals that U1-70K and U1A are enriched in the sarkosyl-insoluble proteome of AD. (*A*) Scheme for profiling the aggregated proteins in AD postmortem brains, with nondemented cases as controls (Ctl). (*B*) A stained SDS gel showing detergent-insoluble proteins in one set of pooled control and AD cases. (*C*) Similar proteomics analysis of seven groups of neurodegenerative disease samples. One set of sarkosyl-insoluble fractions was immunoblotted by phosphorylated tau antibodies to confirm tauopathies. (*D*) Relative level of representative sarkosyl-insoluble proteins across different diseases. The level was estimated by spectral counts of these identified proteins, and normalized to set the maximum to 100. Two replicates were analyzed, and the bars indicate the values of mean ± SEM. (*E–I*) Western blotting analysis of U1-70K or U1A in biochemical brain extracts from control and neurodegenerative cases, and the strategy for protein sequential extraction. The case numbers are shown. B, blank. The exposure time was longer in *I Left* than in others. At least one AD sample and one control sample were loaded on every gel for comparison.

solubility and differential extraction with the anionic detergent sarkosyl has been commonly used to enrich for aggregated tau (27), α-synuclein (28), and TDP-43 (6). We thus prepared and analyzed sarkosyl-insoluble fractions by gel electrophoresis (Fig. 1*B*) and LC-MS/MS. A total of 4,216 proteins were identified (<1% false discovery rate; raw data has been deposited at www.proteomexchange.org, identifier PXD000067), and 36 proteins accumulated in AD (<5% false discovery rate by two statistical approaches; Table 1). As expected, Aβ and tau were abundantly enriched in AD, together with other known proteins regulating Aβ metabolism (29). Consistent with the notion that inflammation (30), phosphorylation networks (8), synaptic plasticity (31), and mitochondrial regulation (32) are altered in AD, we found that numerous proteins involved in these pathways are preferentially enriched in the disease tissues. Interestingly, we observed that two subunits (U1-70K and U1A) of the U1 snRNP and the associated RNA helicase Prp5 (33) were highly elevated in the AD-insoluble proteome, indicating possible deposition of the U1 snRNP.

We used the same proteomics strategy to analyze cases of PD, FTLD-U, ALS, and corticobasal degeneration (CBD; Dataset S1), and determined whether the U1 snRNP changes are specific to AD or common in other diseases with protein aggregates. We also studied cases of mild cognitive impairment (MCI), which is often a prodromal stage of AD, to determine if proteomic changes occur early in the disease. As anticipated, the level of detergent insoluble tau was high in AD and CBD (a prototypical tauopathy), lower in MCI, and barely detectable in PD, FTLD-U, and ALS (Fig. 1 *C* and *D*); Aβ also showed a marked increase in AD, a moderate increase in MCI, but no accumulation in the other diseases. Importantly, the levels of insoluble U1-70K and U1A were highly correlated with that of Aβ rather than tau, supporting the conclusion that U1 snRNP accumulation is specific to AD and occurs early during the disease development.

To confirm the proteomic changes and further analyze the aggregation of U1 snRNP proteins in individual cases, we used specific antibodies (Fig. S2) to probe for U1-70K and U1A in brain extracts (Fig. 1 *E* and *F*). The detergent insoluble U1-70K

Table 1. Identified proteins that are accumulated in AD vs. control cases

Accession no.	Protein names	Spectral counts* Ctl1	Ctl2	AD1	AD2
Aβ peptide metabolism					
NP_000475.1	Aβ peptide	9	31	169	196
NP_000032.1	Apolipoprotein E	1	1	49	92
NP_115907.2	Collagen, type XXV, alpha 1 isoform 2	1	0	23	24
NP_004369.1	Cellular retinoic acid binding protein 1	0	0	9	7
Cytoskeleton maintenance					
NP_058519.2	Microtubule-associated protein tau	10	11	824	989
NP_116757.2	Dystrobrevin alpha	0	11	23	24
Inflammation					
NP_009224.2	Complement component 4a preproprotein	7	7	77	128
NP_001002029.3	Complement component 4b preproprotein	7	7	81	163
NP_000055.2	Complement component 3	1	2	57	93
Protein phosphorylation					
NP_005246.2	Cyclin G-associated kinase	0	1	7	11
NP_002842.2	Protein tyrosine phosphatase, zeta1	2	0	9	10
NP_644812.1	T-cell activation protein phosphatase 2C	0	0	6	7
Synaptic plasticity					
NP_982271.1	Synaptojanin 1	17	9	59	56
NP_001626.1	Amphiphysin	16	14	44	35
NP_640337.3	Syntaxin binding protein 5	2	9	24	22
NP_055804.2	Regulating synaptic membrane exocytosis 1	0	2	12	11
NP_056993.2	Neuroblastoma-amplified protein (with a Sec39 domain)	0	0	4	10
NP_066973.1	Glutamate receptor interacting protein 1	0	0	7	7
Mitochondrial regulation					
NP_892022.2	Mitochondrial nicotinamide nucleotide transhydrogenase	46	46	133	95
NP_066923.3	Mitochondrial NFS1 nitrogen fixation 1	11	17	45	40
NP_000134.2	Mitochondrial fumarate hydratase	5	12	34	33
NP_570847.1	Optic atrophy 1	1	2	15	15
NP_004270.2	Mitochondrial processing peptidase	1	1	13	8
RNA splicing					
NP_003080.2	U1 small nuclear ribonucleoprotein 70 kDa	2	2	31	39
NP_004587.1	U1 small nuclear ribonucleoprotein A	0	1	12	22
NP_055644.2	ATP-dependent RNA helicase DDX46, Prp5	0	0	9	17
Metabolic reactions					
NP_001120920.1	4-Aminobutyrate aminotransferase	20	25	56	60
NP_036322.2	10-Formyltetrahydrofolate dehydrogenase	10	16	40	33
NP_001094346.1	Phytanoyl-CoA dioxygenase domain containing protein 1	0	0	9	7
NP_835471.1	Nicotinamide nucleotide adenylyltransferase 3	0	0	7	4
NP_149078.1	Asparagine-linked glycosylation 2	0	0	5	4
Others					
NP_056450.2	GTPase activating protein and VPS9 domains 1	1	2	13	13
NP_065871.2	Phosphatidylinositol-dependent Rac exchanger 1 (P-REX1)	0	0	5	6
NP_006086.1	Aminophospholipid transporter	9	6	24	29
NP_055839.3	RAN binding protein 16 (exportin 7)	3	8	24	24
NP_055806.2	ALFY, involved in macroautophagy	0	0	5	4

Results of two control case pools (Ctl1 and Ctl2) and two AD case pools (AD1 and AD2). These proteins elevated in AD were analyzed by two statistical approaches (false discovery rate <5%) with accession no. in National Center for Biotechnology Information Reference Sequence Database. Aβ, ApoE, tau, and RNA splicing factors are shaded.
*Spectral counts are used as a quantitative index.

was increased in all 10 AD cases as well as in 7 of 10 MCI cases; U1A accumulated in 8 of 10 AD cases. In contrast, U1-70K was not aggregated in any other cases of PD, FTLD-U, FTLD-tau, and CBD, except in three PD samples. Reexamination of these three PD cases with additional histochemical staining identified coexisting AD plaque and tangle pathology. These data strongly validate the uniqueness of U1 snRNP accumulation to AD.

Biochemical Confirmation of U1 snRNP Alterations in AD. We next sought to examine the total protein level of U1-70K and to characterize U1-70K biochemically in the AD brain. Samples were homogenized and extracted using three buffers with increasing stringency: a low-salt buffer, a sarkosyl-containing solution, and 8 M urea (Fig. 1*G*). In a comparison of AD and control cases (Fig. 1*H*), U1-70K displayed no obvious difference

in either the total homogenate or the sarkosyl soluble fraction. Intriguingly, the low salt-extracted U1-70K was decreased in AD cases (~threefold difference; $P < 0.01$; Fig. S3). This result, together with the enrichment of U1-70K in the sarkosyl-insoluble (i.e., urea) samples, indicates that the biophysical characteristics of U1-70K are altered in AD, resulting in its aggregation and depletion from the low salt-soluble pool. These findings suggest a possible loss of U1-70K function in AD.

Aggregation of protein fragments is common in neurodegeneration (34, 35). We found that in the AD samples, U1-70K was identified by mass spectrometry in two regions of the SDS gels (~70 kDa and ~40 kDa; Fig. 1*B*), and the 40-kDa region contained only N-terminal peptides of U1-70K. The heterogeneous N-terminal fragments were confirmed by immunoblotting using antibodies specific to either N terminus or C terminus of U1-70K (Fig. 1*I*). Thus, U1-70K is internally cleaved and the resulting N-terminal fragments are detected in the detergent-insoluble proteome. We examined U1-70K for characteristics of prion-like domains (PrLDs) that were recently identified in heterogeneous nuclear ribonucleoproteins (hnRNP) in multisystem proteinopathy and ALS (36). Though structural analysis (37) indicates that the first 100-residue region in U1-70K is intrinsically disordered and may contribute to the aggregation process, no PrLDs were identified.

U1 snRNP Forms Tangle-Like Inclusions in AD Brain. Immunohistochemical analysis was performed to examine the localization and accumulation of U1 snRNP components in AD. These studies revealed that U1-70K and U1A form cytoplasmic tangle-like aggregates in 17/20 and 9/10 AD cases, respectively, but not in controls (Fig. 2 *A–D*; Dataset S1). These pathological changes were not present in FTLD-U and FTLD-tau cases (Fig. 2 *E–H*) despite the presence of TDP-43 (Fig. 2*F*) and tau (Fig. 2*H*) pathology. PD and CBD cases also did not show abnormal accumulations of U1 snRNP protein components (Dataset S1). Antibodies against the 2,2,7-trimethylguanosine cap that is characteristic of spliceosomal RNAs also stained cytoplasmic tangle-like aggregates (Fig. S4 *M* and *N*), and quantitative RT-PCR showed enrichment of U1 snRNA in the AD-insoluble fraction (Fig. S5*A*). Other RNA splicing factors, such as hnRNP A/B, recently suggested as a dysfunctional splicing factor in AD (38), and serine/arginine repetitive matrix protein 2 (SRRM2), did not demonstrate tangle-like aggregates, suggesting that this may be a U1 snRNP-specific process (Fig. S4 *A–D*). Although pure tauopathies (e.g., FTLD-tau and CBD) do not show U1-70K aggregation, double staining of AD cases indicates that U1-70K inclusions are closely associated with tau-immunoreactive neurofibrillary tangles (NFTs; Fig. 2 *I–L*), implying possible relationship between the mechanisms of U1-70K and tau deposition in AD. To better define the relationship of U1-70K pathology to that of NFTs, we examined hippocampus and temporal, frontal, and occipital cortices of AD cases with progressively severe neurofibrillary pathology (Braak stages 0, III, and VI). The appearance of U1-70K spreads across the brain in a sequence similar to that seen for tau NFTs (Fig. S4*O*). Dramatic progression in U1-70K pathology between Braak stage III and VI leads to uniform accumulation in all brain regions (Fig. S4 *E–L*). These data are highly consistent with our biochemical analyses, strongly demonstrating specific U1 snRNP pathology in AD.

Deep RNA Sequencing Demonstrates Splicing Abnormalities in AD. The biochemical and pathological changes in U1 snRNP components in AD brains suggest a possible loss of nuclear spliceosome activity. Though alternative splicing of specific genes has been previously reported (39), global disruption of RNA processing has never been suggested in AD. To address this possibility, we performed deep RNA sequencing (40) of frontal cortex RNAs using two independent sample groups from the brain banks of Emory University (four control and five AD cases) and the University of Kentucky (UKY; three control and three AD cases). In both groups, a higher proportion of AD brain-derived reads mapped to intronic sequences of known genes ($P = 0.041$ in Emory cases, $P = 0.003$ in UKY cases; Fig. 3*A*). For individual genes, we further defined the ratio between length-normalized intronic and exonic reads as a splicing deficiency score. The distribution of the splicing deficiency scores of all mapped genes clearly indicated splicing defects in AD ($n = 10{,}490$ in Emory group, $n = 14{,}583$ in UKY group; $P < 2.2 \times 10^{-16}$ in both groups; Fig. 3*B*). A large number of genes were affected in AD (3,014 genes with high splicing deficiency scores in both Emory and UKY AD cases, 5% false discovery rate, by two statistical approaches; Fig. 3*B* and Dataset S2). To confirm these findings, we applied the NanoString approach (41) to analyze 12 selected transcripts implicated in AD pathogenesis using high-quality RNA samples (average RNA integrity number score = 8.0; 14 control and 15 AD cases; Dataset S1). For each gene, we quantified the ratio

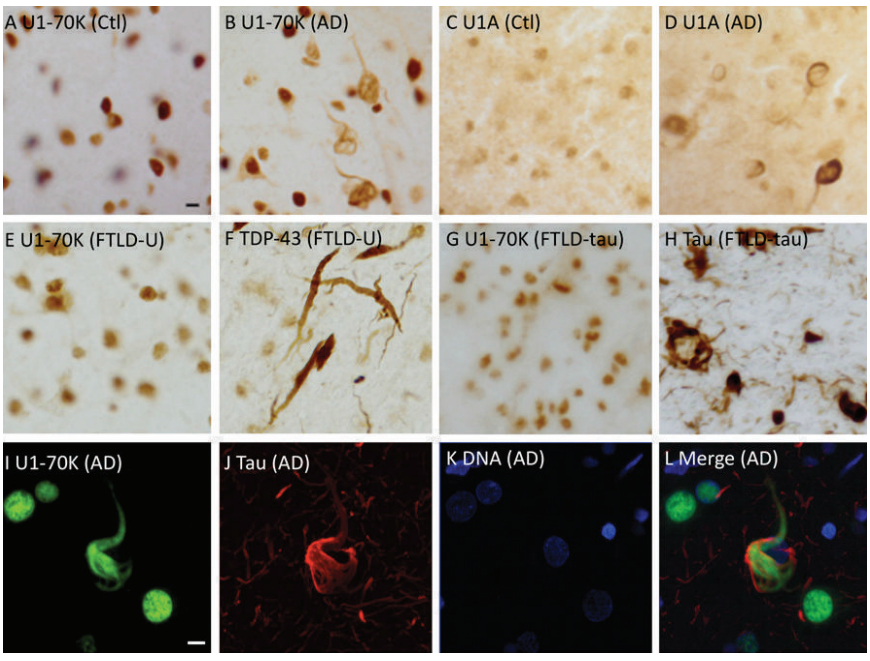

Fig. 2. U1-70K and U1A show neurofibrillary tangles in AD pathology. (*A–D*) Representative immunohistochemistry images with diaminobenzidine staining of selected control and AD brain slides (50-μm sections). (Scale bar, 5 μm.) (*E–H*) Representative adjacent sections of FTLD-U and FTLD-tau cases demonstrating normal U1-70K distribution despite the presence of TDP-43 and tau pathology, respectively. (*I–L*) Double-immunofluorescence staining indicates partial colocalization of U1-70K with tau in AD. (Scale bar, 5 μm.)

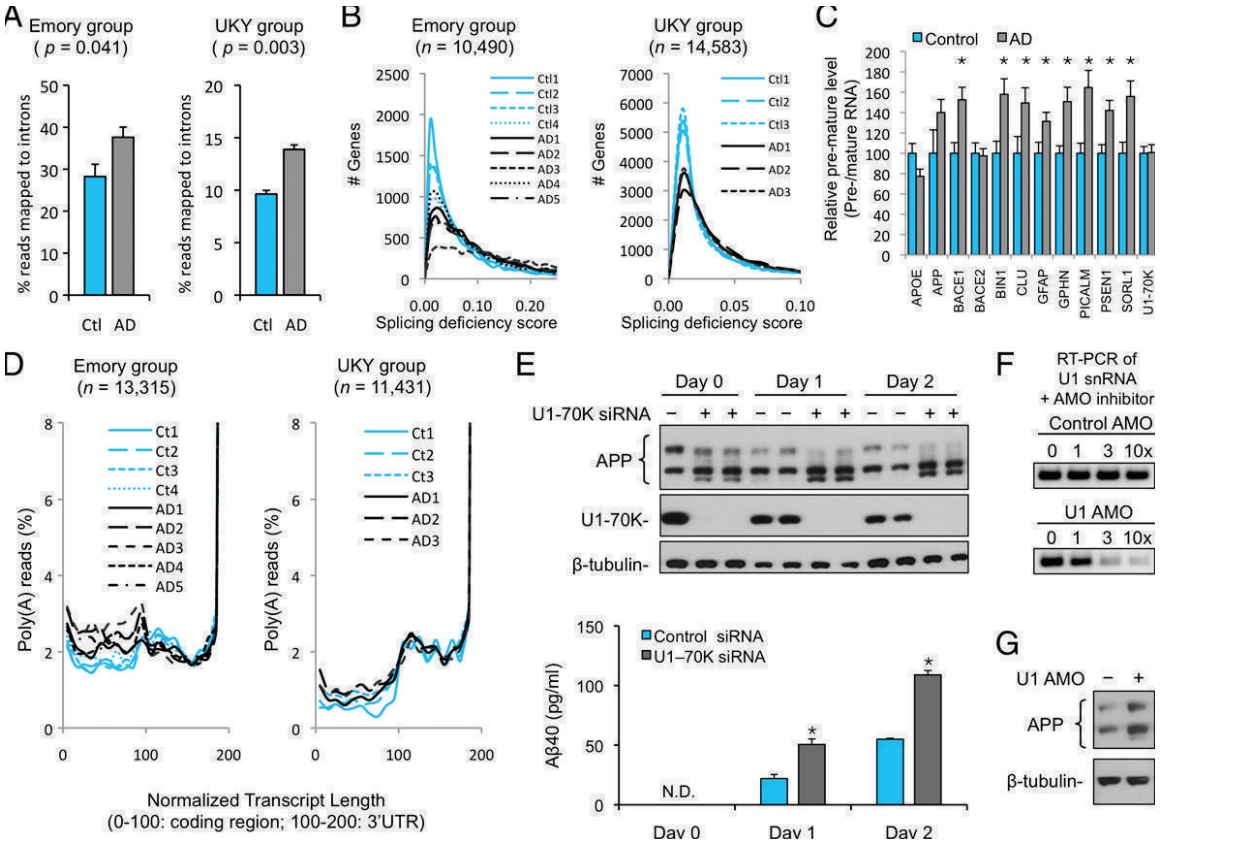

Fig. 3. RNA splicing impairment in AD, and APP up-regulation upon splicing inhibition. (*A*) The frequency of summed intron reads is higher in AD than in control. The bars indicate mean ± SEM (*P* value derived by Student *t* test). The Emory and UKY samples were processed independently. The batch discrepancy may be due to sample quality difference and experimental variations. (*B*) The histograms of splicing deficiency scores of all mapped genes show a statistically significant difference between AD and control in both Emory and UKY groups ($P < 2.2 \times 10^{-16}$ for both groups, Kolmogorov–Smirnov test). (*C*) Evaluation of RNA splicing efficiency by measuring mRNAs and pre-mRNAs of selected genes in control and AD cases. The bars indicate the values of mean ± SEM (AD: $n = 15$; control: $n = 14$; asterisks: $P < 0.05$, Student *t* test). (*D*) Poly(A)-containing reads from 5′ to 3′ of every gene were defined and normalized according to the total poly(A) reads of the gene. Every transcript was divided into coding region (0–100, from start to stop codon) and 3′ UTR region (100–200), then into 20 bins. The poly(A) read percentage in each bin was averaged for all genes in every case, and plotted to represent the frequency of PCPA. The PCPA frequency was markedly different between control and AD cases ($P < 2.2 \times 10^{-16}$ for Emory group, $P < 6.9 \times 10^{-15}$ for UKY group, Kolmogorov–Smirnov test). (*E*) U1-70K knockdown increases APP and Aβ40 levels in HEK293 cells. The cells were transfected for 2 d, then cultured in a low-serum medium and harvested at day 0, 1, and 2 for analysis (asterisks: $P < 0.05$, Student *t* test; N.D., not detected). APP and Aβ40 were analyzed by immunoblotting and ELISA, respectively. (*F*) PCR to examine the specificity of U1 AMO. The reaction was designed to amplify the U1 RNA 5′-end region with the addition of control AMO or U1 AMO as inhibitory competitor. (*G*) The APP level increases upon AMO inhibition of U1 snRNP.

between pre-mRNAs and mature mRNAs, comparing abundance of exon1–intron1 junction sequences to exon1–exon2 junction sequences, as a measure of splicing efficiency. The splicing efficiency for eight transcripts in the AD cases showed significant reduction (i.e., a relative increase in intron 1-containing RNAs; $P < 0.05$; Fig. 3*C* and Dataset S3). Finally, using traditional quantitative RT-PCR methods, we validated the results for three transcripts genetically linked to AD pathogenesis: myc box-dependent-interacting protein 1, clusterin, and presenilin-1 (Fig. S5*B*). Taken together, these results strongly support a profound alteration in RNA processing in AD.

In addition to a role in splicing, U1 snRNP is recruited to nascent transcripts to suppress premature cleavage and polyadenylation (PCPA) on cryptic poly(A) sites, and moderate inhibition of U1 snRNP by antisense morpholino oligonucleotide (AMO) leads to PCPA in a 5′–3′ direction (42). We did not perform high-throughput sequencing of differentially expressed transcripts (43) in our experiments and did not have sufficient data to fully assess potential changes in telescripting in AD; however, examination of RNA sequencing (RNA-seq) data revealed more poly(A)-containing reads in the 5′ end of transcripts among AD cases than controls in both Emory and UKY groups ($n = 13{,}315$ in Emory group, $n = 11{,}431$ in UKY group; $P < 1 \times 10^{-14}$ in both groups; Fig. 3*D*). These data suggest the intriguing possibility that partial loss of U1 snRNP function in AD might result in increased PCPA in addition to altered splicing.

U1 snRNP Deficiency Alters Amyloid Precursor Protein (APP) Expression and Aβ Levels. To assess U1 snRNP loss of function in an experimental system, we performed U1-70K knockdown in HEK293 cells and sought to determine possible effects on APP metabolism. U1-70K knockdown (<10% remaining) induced an increase in endogenous APP and Aβ40 compared with the scrambled siRNA control (Fig. 3*E* and Fig. S6*A*). Human APP has three isoforms (APP_{770}, APP_{751}, and APP_{695}) generated by alternative splicing (44). RT-PCR analysis indicated that U1-70K knockdown resulted in a decrease of APP_{770} transcript and an increase of APP_{751} and APP_{695} transcripts (Fig. S6*B*). This up-regulation of APP and Aβ40 was also observed in differentiated SH-SY5Y neuroblastoma cells (Fig. S6 *C–E*). In addition to U1-70K knockdown, U1 AMO inhibition of U1 snRNP function elevated APP level as well (Fig. 3 *F* and *G*). Though we did not observe an obvious isoform-switching phenomenon in human brain, NanoString experiments found an increase in RNA species containing contiguous exon1–intron1 sequences for APP in AD ($P = 0.068$; Fig. 3*C*).

These results indicate that disruption of RNA splicing function may result in mechanistically relevant changes in APP expression.

We have discovered U1 snRNP proteinopathy and global RNA processing defects in the AD brain, and a role for U1-70K in APP metabolism. The dysregulation of core RNA splicing machinery in AD was unexpected; remarkably, it is highly disease-specific, occurs early, and is widespread in AD cases. The malfunction of these core splicing factors provides important insight into molecular mechanisms outside of Aβ and tau that contribute to AD.

Methods

Case Materials. Human postmortem frozen and paraformaldehyde-fixed tissues from cortical areas were provided from clinically and pathologically well-characterized cases at the Alzheimer's Disease Research Center (ADRC) Brain Bank at Emory University, Rush Alzheimer's Disease Center's Religious Orders Study at Rush University Medical Center, the University of Washington ADRC, and the University of Kentucky ADRC, with signed informed consents for the studies (Dataset S1). Diagnoses were made in accordance with established criteria and guidelines of control and AD (45, 46), MCI (47, 48), PD (49), FTLD-tau (50, 51), FTLD-U (50, 51), ALS (52), and CBD (53, 54). Details of proteomic and RNA-seq analyses, Western blot, immunohistochemical staining, RT-PCR, U1-70K knockdown, and U1 snRNP inhibition procedures are described in SI Methods.

ACKNOWLEDGMENTS. The authors thank P. Xu, C. H. Na, W. Tang, and R. Qi for laboratory assistance; and X. Lin, Y. Feng, D. Pallas, Z. Mao, J. Glass, S. Li, and J. P. Taylor for helpful discussion. This work was partially supported by National Institutes of Health (NIH) Grants P50AG025688, P30NS055077, and P50AG005136; Consortium for Frontotemporal Dementia Research NIH Training Grants F30NS057902 (to Y.G.), F32AG038259 (to E.B.D.), and F32NS007480 (to N.T.S.); a American Academy of Neurology Foundation Clinical Research Training Fellowship (to C.M.H.); Sara Borrell Program Support (Spanish Instituto de Salud Carlos III) (G.C.); and Grants P01GM081621 and R01MH082068 (to Y.E.S.), P01AG14449 (to E.J.M.), and P30AG10161 (to D.A.B.). J.P. is supported by the American Lebanese Syrian Associated Charities.

1. Glenner GG, Wong CW (1984) Alzheimer's disease: Initial report of the purification and characterization of a novel cerebrovascular amyloid protein. *Biochem Biophys Res Commun* 120(3):885–890.
2. Masters CL, et al. (1985) Amyloid plaque core protein in Alzheimer disease and Down syndrome. *Proc Natl Acad Sci USA* 82(12):4245–4249.
3. Lee VM, Balin BJ, Otvos L, Jr., Trojanowski JQ (1991) A68: A major subunit of paired helical filaments and derivatized forms of normal Tau. *Science* 251(4994):675–678.
4. Spillantini MG, et al. (1997) Alpha-synuclein in Lewy bodies. *Nature* 388(6645): 839–840.
5. Polymeropoulos MH, et al. (1997) Mutation in the alpha-synuclein gene identified in families with Parkinson's disease. *Science* 276(5321):2045–2047.
6. Neumann M, et al. (2006) Ubiquitinated TDP-43 in frontotemporal lobar degeneration and amyotrophic lateral sclerosis. *Science* 314(5796):130–133.
7. Hardy J, Selkoe DJ (2002) The amyloid hypothesis of Alzheimer's disease: Progress and problems on the road to therapeutics. *Science* 297(5580):353–356.
8. Ballatore C, Lee VM, Trojanowski JQ (2007) Tau-mediated neurodegeneration in Alzheimer's disease and related disorders. *Nat Rev Neurosci* 8(9):663–672.
9. Pimplikar SW, Nixon RA, Robakis NK, Shen J, Tsai LH (2010) Amyloid-independent mechanisms in Alzheimer's disease pathogenesis. *J Neurosci* 30(45):14946–14954.
10. Gstaiger M, Aebersold R (2009) Applying mass spectrometry-based proteomics to genetics, genomics and network biology. *Nat Rev Genet* 10(9):617–627.
11. Choudhary C, Mann M (2010) Decoding signalling networks by mass spectrometry-based proteomics. *Nat Rev Mol Cell Biol* 11(6):427–439.
12. Hye A, et al. (2006) Proteome-based plasma biomarkers for Alzheimer's disease. *Brain* 129(Pt 11):3042–3050.
13. German DC, et al. (2007) Serum biomarkers for Alzheimer's disease: Proteomic discovery. *Biomed Pharmacother* 61(7):383–389.
14. Wada-Isoe K, et al. (2007) Serum proteomic profiling of dementia with Lewy bodies: Diagnostic potential of SELDI-TOF MS analysis. *J Neural Transm* 114(12):1579–1583.
15. Ryberg H, et al. (2010) Discovery and verification of amyotrophic lateral sclerosis biomarkers by proteomics. *Muscle Nerve* 42(1):104–111.
16. Wijte D, et al. (2012) A novel peptidomics approach to detect markers of Alzheimer's disease in cerebrospinal fluid. *Methods* 56(4):500–507.
17. Ringman JM, et al. (2012) Proteomic changes in cerebrospinal fluid of presymptomatic and affected persons carrying familial Alzheimer disease mutations. *Arch Neurol* 69(1):96–104.
18. Liao L, et al. (2004) Proteomic characterization of postmortem amyloid plaques isolated by laser capture microdissection. *J Biol Chem* 279(35):37061–37068.
19. Sultana R, et al. (2007) Proteomics analysis of the Alzheimer's disease hippocampal proteome. *J Alzheimers Dis* 11(2):153–164.
20. Xia Q, et al. (2008) Proteomic identification of novel proteins associated with Lewy bodies. *Front Biosci* 13:3850–3856.
21. Donovan LE, et al. (2012) Analysis of a membrane-enriched proteome from postmortem human brain tissue in Alzheimer's disease. *Proteomics Clin Appl* 6(3-4):201–211.
22. Rudrabhatla P, Jaffe H, Pant HC (2011) Direct evidence of phosphorylated neuronal intermediate filament proteins in neurofibrillary tangles (NFTs): Phosphoproteomics of Alzheimer's NFTs. *FASEB J* 25(11):3896–3905.
23. Xia Q, et al. (2008) Phosphoproteomic analysis of human brain by calcium phosphate precipitation and mass spectrometry. *J Proteome Res* 7(7):2845–2851.
24. Gozal YM, et al. (2009) Proteomics analysis reveals novel components in the detergent-insoluble subproteome in Alzheimer's disease. *J Proteome Res* 8(11):5069–5079.
25. Gozal YM, et al. (2011) Proteomic analysis of hippocampal dentate granule cells in frontotemporal lobar degeneration: Application of laser capture technology. *Front Neurol* 2:24.
26. Zhou JY, Hanfelt J, Peng J (2007) Clinical proteomics in neurodegenerative diseases. *Proteomics Clin Appl* 1(11):1342–1350.
27. Spillantini MG, et al. (1997) Familial multiple system tauopathy with presenile dementia: A disease with abundant neuronal and glial tau filaments. *Proc Natl Acad Sci USA* 94(8):4113–4118.
28. Fujiwara H, et al. (2002) Alpha-synuclein is phosphorylated in synucleinopathy lesions. *Nat Cell Biol* 4(2):160–164.
29. Weiner HL, Frenkel D (2006) Immunology and immunotherapy of Alzheimer's disease. *Nat Rev Immunol* 6(5):404–416.
30. Wyss-Coray T (2006) Inflammation in Alzheimer disease: Driving force, bystander or beneficial response? *Nat Med* 12(9):1005–1015.
31. Selkoe DJ (2002) Alzheimer's disease is a synaptic failure. *Science* 298(5594):789–791.
32. Lin MT, Beal MF (2006) Mitochondrial dysfunction and oxidative stress in neurodegenerative diseases. *Nature* 443(7113):787–795.
33. Staley JP, Guthrie C (1998) Mechanical devices of the spliceosome: Motors, clocks, springs, and things. *Cell* 92(3):315–326.
34. Taylor JP, Hardy J, Fischbeck KH (2002) Toxic proteins in neurodegenerative disease. *Science* 296(5575):1991–1995.
35. Ross CA, Poirier MA (2004) Protein aggregation and neurodegenerative disease. *Nat Med* 10(Suppl):S10–S17.
36. Kim HJ, et al. (2013) Mutations in prion-like domains in hnRNPA2B1 and hnRNPA1 cause multisystem proteinopathy and ALS. *Nature* 495(7442):467–473.
37. Pomeranz Krummel DA, Oubridge C, Leung AK, Li J, Nagai K (2009) Crystal structure of human spliceosomal U1 snRNP at 5.5 A resolution. *Nature* 458(7237):475–480.
38. Berson A, et al. (2012) Cholinergic-associated loss of hnRNP-A/B in Alzheimer's disease impairs cortical splicing and cognitive function in mice. *EMBO Mol Med* 4(8):730–742.
39. Mills JD, Janitz M (2012) Alternative splicing of mRNA in the molecular pathology of neurodegenerative diseases. *Neurobiol Aging* 33(5):1012.e1011–1024.
40. Mortazavi A, Williams BA, McCue K, Schaeffer L, Wold B (2008) Mapping and quantifying mammalian transcriptomes by RNA-Seq. *Nat Methods* 5(7):621–628.
41. Geiss GK, et al. (2008) Direct multiplexed measurement of gene expression with color-coded probe pairs. *Nat Biotechnol* 26(3):317–325.
42. Kaida D, et al. (2010) U1 snRNP protects pre-mRNAs from premature cleavage and polyadenylation. *Nature* 468(7324):664–668.
43. Berg MG, et al. (2012) U1 snRNP determines mRNA length and regulates isoform expression. *Cell* 150(1):53–64.
44. Rockenstein EM, et al. (1995) Levels and alternative splicing of amyloid β protein precursor (APP) transcripts in brains of APP transgenic mice and humans with Alzheimer's disease. *J Biol Chem* 270(47):28257–28267.
45. Mirra SS, et al. (1991) The Consortium to Establish a Registry for Alzheimer's Disease (CERAD). Part II. Standardization of the neuropathologic assessment of Alzheimer's disease. *Neurology* 41(4):479–486.
46. Hyman BT, Trojanowski JQ (1997) Consensus recommendations for the postmortem diagnosis of Alzheimer disease from the National Institute on Aging and the Reagan Institute Working Group on diagnostic criteria for the neuropathological assessment of Alzheimer disease. *J Neuropathol Exp Neurol* 56(10):1095–1097.
47. Petersen RC, et al. (1999) Mild cognitive impairment: Clinical characterization and outcome. *Arch Neurol* 56(3):303–308.
48. Ritchie K, Artero S, Touchon J (2001) Classification criteria for mild cognitive impairment: A population-based validation study. *Neurology* 56(1):37–42.
49. Gelb DJ, Oliver E, Gilman S (1999) Diagnostic criteria for Parkinson disease. *Arch Neurol* 56(1):33–39.
50. Trojanowski JQ, Dickson D (2001) Update on the neuropathological diagnosis of frontotemporal dementias. *J Neuropathol Exp Neurol* 60(12):1123–1126.
51. McKhann GM, et al.; Work Group on Frontotemporal Dementia and Pick's Disease (2001) Clinical and pathological diagnosis of frontotemporal dementia: Report of the Work Group on Frontotemporal Dementia and Pick's Disease. *Arch Neurol* 58(11): 1803–1809.
52. Ince PG, Lowe J, Shaw PJ (1998) Amyotrophic lateral sclerosis: Current issues in classification, pathogenesis and molecular pathology. *Neuropathol Appl Neurobiol* 24(2): 104–117.
53. Dickson DW, et al.; Office of Rare Diseases of the National Institutes of Health (2002) Office of Rare Diseases neuropathologic criteria for corticobasal degeneration. *J Neuropathol Exp Neurol* 61(11):935–946.
54. Dickson DW (2001) Neuropathology of Pick's disease. *Neurology* 56(11, Suppl 4): S16–S20.

Supporting Information

Bai et al. 10.1073/pnas.1310249110

SI Methods

Sample Pooling. To minimize the variations caused by the confounding biological and other uncontrollable factors (1), we employed the following strategies: (i) to use well-characterized brain specimens; (ii) to select brain tissues without large bias in race, age and gender; (iii) to enhance datasets by correlating protein changes with disease progression (e.g. MCI and AD); (iv) to adapt a pooling strategy (Fig. 1*A*) to average variations induced by the confounding factors (2, 3). Since samples of poor quality (e.g. degraded) may negatively influence the result of the entire pool, we tested the integrity of brain homogenates prior to pooling (Fig. S1). Finally, we implemented one biological replicate for each pool to facilitate statistical evaluation of differentially expressed proteins.

Sequential Biochemical Fractionation. The brain tissues were sequentially extracted similar to previously described methods (4, 5) with a low salt buffer (10 mM Tris, pH 7.5, 5 mM EDTA, 1 mM DTT, 10% (wt/vol) sucrose, Sigma protease inhibitor cocktail, ~10 ml buffer per gram tissue), a detergent buffer (the low salt buffer with the addition of 1% (wt/vol) sarkosyl, N-Lauroylsarcosine), and finally 8 M urea with 2% (wt/vol) SDS. Generally, the protein yield in final urea samples (detergent insoluble fractions) during sequential extraction was approximately 2% of the starting material.

Protein Identification by Shotgun Mass Spectrometry (MS). MS analysis of detergent insoluble fractions was processed based on our optimized LC-MS/MS protocol (6, 7). 50 μg of protein per sample were resolved on an SDS gel (9%, wt/vol) and stained with Coomassie blue. Each gel lane was excised into 20 bands followed by in-gel trypsin digestion (8). The resulting peptides were analyzed by LC-MS/MS (2 h) on an LTQ-Orbitrap mass spectrometer (Thermo). A total of ~640 h MS running time was spent in this project. MS/MS spectra were searched against a human reference database from the National Center for Biotechnology Information using the SEQUEST Sorcerer algorithm (version 2.0, SAGE-N) (9) as previously described (6).

MS/MS spectra searching parameters included mass tolerance of precursor ions (± 20 ppm) and product ion (± 0.5 Da), partial tryptic restriction, fixed mass shift for modification of carboxyamidomethylated Cys (+ 57.0215 Da), dynamic mass shifts for oxidized Met (+ 15.9949 Da), three maximal modification sites and three maximal missed cleavages. Only *b* and *y* ions were considered during the database match. To evaluate false discovery rate during the spectrum-peptide matching, all original protein sequences were reversed to generate a decoy database that was concatenated to the original database (1, 2). False discovery rate (FDR) was estimated by the number of decoy matches (nd) and total number of assigned matches (nt), according to

$$\mathrm{FDR} = 2 \times \mathrm{nd}/\mathrm{nt},$$

assuming mismatches in the original database were the same as in the decoy database. To remove false positive matches, assigned peptides were grouped by charge state and then filtered by minimal peptide length (7 amino acid), mass-to-charge accuracy (± 5 ppm) and matching scores (XCorr and deltaCn) to reduce protein FDR to below 1%. Furthermore, we removed all proteins identified by a single spectral count, which eliminated all decoy matches. If peptides were shared by multiple members of a protein family, the matched members were clustered into a single group. Based on the principle of parsimony, the group was represented by the protein with the highest number of assigned peptides, and by other proteins if they were matched by unique peptide(s), resulting in the acceptance of 4,216 proteins in two control pools and two AD pools. Raw MS files are uploaded to the ProteomeXchange consortium (www.proteomexchange.org, identifier PXD000067).

Label-free Protein Quantification and Statistical Inference. To identify differences between the control and AD cases, we quantified the proteins in multiple samples based on spectral counts (SCs) (10). The SCs were first normalized to ensure that the average SC per protein was the same in all datasets (11). We used two statistical approaches, a straightforward G-test analysis and a one-sided z-test analysis, to evaluate protein alteration.

A G-test was previously used to judge statistical significance of protein abundance difference (3). Briefly, the G-value of each protein was calculated as shown in the equation below:

$$G = 2 \times (S1 \times \ln[S1 \div ((S1 + S2) \div 2)] + S2 \times \ln[S2 \div ((S1 + S2) \div 2)]),$$

where S1 and S2 are the detected spectral counts of a given protein in any of two samples for comparison, respectively, and "ln" is the natural logarithm. Although theoretical distribution of the G values is complex, these values approximately fit to the $\chi 2$ distribution (one degree of freedom), allowing the calculation of related *P*-values (3).

We then set up a reliable *P*-value threshold to identify protein changes with statistical significance as previously reported (4). Ideally, the threshold should accept a very small number of proteins (i.e. false discoveries) in null experiments (e.g. comparison of control 1 versus control 2; or comparison of AD 1 versus AD 2). When the same threshold was used for AD-control comparison, the list is deemed acceptable with a low false discovery rate. To find the appropriate threshold, we dynamically adjusted the *P*-value from 0.4 to 0.001, and determined that *P*-value of 0.04 was a reasonable threshold with balanced sensitivity and specificity (false discovery rate ~5%), resulting in the acceptance of 63 proteins. We manually examined these proteins and removed protein paralogs, reducing the list to 43 proteins.

In addition, we developed a z-test analysis to analyze the data in multiple steps. (i) The spectral counts were standardized (5) and square root of spectral counts was used to stabilize the variance within each group (i.e. control or AD). (ii) For each group, a parameter phi was estimated to represent technical variance plus minimal biological variance. This was accomplished by a trimmed average of the sample variances: trimming off the largest 5% and smallest 5% of the sample variances so that the estimated phi was resistant to outliers. (iii) Each protein's variance was estimated using a shrinkage estimator as previously reported(6), in which a given protein's variance was based on a weighted average of phi and the protein-specific sample variance in only two observations (i.e. two pools). The weights were calculated using an empirical Bayes approach (w1 = 0.8 for phi and w2 = 0.2 for the protein-specific sample variance). (iv) We derived *P*-values under the assumption that z-tests were independent and normally distributed, and then used the original FDR controlling procedure of Benjamini and Hochberg (7) to set a threshold corresponding to an estimated FDR of 5%. (v) After manually examination and removal of protein paralogs, a list of 61 proteins were accepted.

Finally, we accepted 36 proteins (Dataset 1) passing the thresholds of both statistical approaches.

Antibodies. Two polyclonal rabbit U1-70K antibodies were developed and purified using synthetic peptides GDAFKTLFVARVNYDTTESKLR (N-terminal amino acid 99-120) and GGDGYLAPENGYLMEAAPE (C-terminal amino acid 419 to 437). Other commercial antibodies include: APP (22C11, Millipore; Y188, Epitomics), tau (AT8, Pierce), U1A (WH0006626M1, Sigma), hnRNP A/B (98273, Santa Cruz), SRRM2 (122719, Abcam), 2,2,7-trimethylguanosine (K121, Millipore), actin (6276, Abcam), and NF-H (Sigma).

Immunohistochemical Staining. The staining was performed as previously reported (4, 5, 12). Semi-quantitative analysis across brain regions was performed by a blinded rater to score U1-70K cytoplasmic aggregate and neurofibrillary tangle density in hippocampus and temporal, frontal and occipital cortex as absent, sparse, moderate or frequent in AD and control cases (Fig. S4*O*).

RNA Deep Sequencing Data Acquisition. The mRNA-seq was performed according to the Illumina standard kit protocol on human control and AD specimens from the Emory University and University of Kentucky brain banks (Dataset S1). TRIzol (Invitrogen) extracted RNA was used for poly(A) RNA purification and converted to cDNA. The double stranded cDNA fragments were ligated to Illumina paired end adaptors, followed by size selection (~200 bp). Finally, the libraries were enriched using PCR and analyzed by HiSeq 2000 sequencing systems (Illumina). The initial RNA quality was evaluated by the values of RNA integrity number (RIN). It was a challenge to obtain RNA samples from port-mortem human brain specimens. We screened over 20 human brain samples from the Emory brain banks and finally selected 5 AD and 4 control cases (RIN 4.4-7.7) for RNA-seq analysis. Approximately 34-52 million reads were acquired for each sample. To replicate the analysis, we obtained samples with much shorter postmortem interval from the University of Kentucky brain bank. We isolated high quality RNA samples (RIN 7.8-8.8) and performed deep RNA-seq analysis. Approximately 78-108 million reads were acquired for each sample.

RNA-seq Sequencing Alignment and Analysis. Paired end reads were mapped to University of California Santa Cruz (UCSC) human reference genome hg19 using Illumina iGenomes pre-built indexes (http://tophat.cbcb.umd.edu/igenomes.html) and TopHat programs (13): TopHat and Bowtie. Default parameters were used except that a gene transfer format file with known transcripts was also provided (–G parameter). This additional file permitted TopHat (v2.0.3) to map reads in multiple stages. Initially, all reads were mapped to a virtual transcriptome (i.e. a UCSC "knownCanonical" set of 27,297 transcripts). Only if the reads were not fully mapped to the transcriptome, they would be mapped to the genome (hg19). Finally, the reads mapped to the transcriptome were converted to genomic mapping, and merged together in the final output Binary Sequence Alignment/Map (BAM) files. During the transcriptome-to-genome conversion, the skipped regions of the genome (due to introns) were captured in the concise idiosyncratic gapped alignment report string of the resulting BAM files.

To extract the reads mapped to whole genes, including exons and introns, we converted the BAM to Browser Extensible Data (BED) files using bedtools (http://code.google.com/p/bedtools, bamToBed, v2.16.1), and used an in-house perl program to generate three BED files: (i) knownCanonical Genes, (ii) knownCanonical Exons and (iii) knownCanonicalIntrons. Finally, we used intersectBed (v2.16.1) to define the intersections between uniquely mapped reads and the three knownCanonical BED files.

The global splicing deficiency was first evaluated by the percentage of reads uniquely mapped to introns, after normalized to the total reads uniquely mapped to whole genes. The two-tailed student *t*-test analysis was performed to evaluate the *P*-values (Fig. 3*A*). Moreover, we defined a splicing deficiency (Sd) score for each gene as the ratio of length-corrected read counts aligned to introns and exons:

$$\mathrm{Sd} = (\text{no. of intronic reads/total intronic length}) \div (\text{no. of exonic reads/total exonic length}).$$

A high Sd value indicated low splicing efficiency. The histogram of the Sd value distribution was shown for every case (Fig. 3*B*). The Kolmogorov-Smirnov test was used to analyze statistical significance of the comparison between AD and control cases. Finally, we used the method of Significance Analysis of Microarrays (SAM)(8) to compute *P*-values and FDR and analyzed the effect of FDR on the acceptance of false positives and false negatives. As the sample size in this RNA-seq study was relatively small, we found that 5% FDR showed a reasonable balance between false positives and false negatives, leading to the acceptance of 6,976 genes in the Emory group and 6,036 genes in the UKY group, in which 3,614 genes were overlapped.

In addition, we used another experimental approach to identify gene changed in both Emory and UKY groups with statistical significance as previously reported (4) (Dataset S2). (i) For every gene detected in both groups (n = 10,253), we calculated $\log_2$-ratio for splicing deficiency score:

$$\log_2(\mathrm{AD/control}) = \log_2(\text{Sd score average of all AD cases} \div \text{Sd score average of all controls}).$$

(ii) We established a reliable cutoff using the values of $\log_2$Ratio. Four null experiments were performed to analyze the distribution of $\log_2$Ratio (i.e. intra-control comparison and intra-AD comparison in either Emory or UKY group). The data were centered on almost zero with a consistent standard deviation (0.49±0.04, Dataset S2), reflecting the sum of biological and experimental variations. Ideally, the cutoff should accept a few genes (i.e. false discoveries) in null experiments, which was used to derive FDR when applying the same cutoff to filter AD-control comparisons. We then adjusted the $\log_2$Ratio value from one standard deviation to more than two standard deviation, and found that $\log_2$Ratio of 0.78 led to ~5% FDR with the acceptance of 3,514 genes shared in the Emory and UKY groups (Dataset S2). This result was highly consistent with the SAM-based analysis.

To further improve the stringency of threshold, we only accepted genes that survived during both SAM-based and null hypothesis-based methods. A total of 3,027 (~85%) genes remained, in which only two (0.06%) genes had lower Sd scores (removed), 11 (0.36%) genes showed inconsistent data between Emory and UKY groups (removed), and 3014 (99.6%) genes exhibited higher Sd scores in AD in both groups, clearly indicating that a large portion (29.4%, 3014/10,253) of genes were altered in AD (Dataset S2).

In addition, we found that both the percentage intronic reads and the Sd scores between the Emory and UKY groups were different. As the Emory and UKY samples were processed independently, the batch discrepancy may be due to the difference in sample quality and other technical variations, including experimental settings in brain sample collection, genomic DNA contamination, and poly(A) RNA purification. Nevertheless, during the comparison of AD and control cases in the same batch, the results were highly consistent and reproducible in two groups of samples. Raw RNA-seq files are uploaded to NCBI's Sequence Read Archive database (www.ncbi.nlm.nih.gov/sra, SRA060572).

A program was developed to analyze cleavage and polyadenylation sites. Reads with a poly(A) tail need to have at least 20 consecutive adenines at the 3' end. Similarly, reads with a poly(T) stretch (at least 20 consecutive thymines at the 5' end) were counted as reverse complement strands. Poly(A) tails were then trimmed in every read, and the 3' end of a trimmed read indicated a potential cleavage and polyadenylation site. If the length of a trimmed read was shorter than 25 nt, the read was discarded. Trimmed reads were aligned to the human genome (hg19) with Bowtie program (version 1.0.0; parameters: -q -p 5 -k 2 –best -v 2). The uniquely mapped reads were subjected to a quality control filtering, in which the 20 nt genomic region downstream of potential poly(A) sites was examined. If the 20 nt region contained more than 12 adenines or 8 consecutive adenines, the sites were removed. Because the cleavage and polyadenylation events for transcripts usually occur in a sequence region instead of one precise RNA site, we iteratively clustered the reads carrying polyadenylation sites within 24 nt on the same strand of a chromosome. In one cluster, the position of poly(A) site was represented by the mode that was defined as the position with maximum reads.

To summarize polyadenylation sites for every transcript, we normalized each gene region (0-100 from start codon to stop codon) and its 3' UTR region (100-200) independently, and then divided the full-length gene sequence into 20 bins. In each bin, the occurrence of poly(A) sites was indicated by the percentage of the corresponding reads among all poly(A) reads of the transcript. Finally, to summarize all transcripts in every sample, the occurrence of poly(A) sites in each bin was averaged.

Amplification-Free Counter Assay and qRT-PCR for Relative Quantitation of Pre- and Mature mRNA. Total RNA was extracted from frontal cortices (0.5-1.0 g per sample) using TRIzol (Invitrogen), and assayed by the N-Counter gene expression system (NanoString Technologies, Seattle WA, 100 ng total RNA per sample, RIN 7.8-8.8) using capture and reporter probes complementary to a 100 bp target sequence for each RNA species as previously described (14). Each of the target sequences (Dataset S3) was unique to spliced (i.e., exon1-exon2 junction) and pre-spliced (i.e., exon1-intron1 junction) mRNA from selected genes, plus loading control RNAs of varying abundance (CEP170, EEF1A1 and RPL27, for which only mature mRNA species were counted). Counts for target RNAs were subtracted by background, which was determined by negative control target sequences not present in the human transcriptome. The counts were then normalized according to the abundant three control RNAs. To further improve the dataset, we required that the minimal normalized counts were at least 2-fold of the maximal standard deviation. To control for sampling heterogeneity, two-tailed Dixon's Q outlier removal was performed with $\alpha = 0.05$(9). Finally, relative pre-mRNA level was calculated based on the equation below:

$$\text{Relative pre} - \text{mRNA} = \text{pre} - \text{mRNA} \div \text{mRNA},$$

where "mRNA" and "pre-mRNA" represent the counts measured in the control or AD cases. To simplify the dataset, relative pre-mRNA level was normalized by setting the value in the controls to 100.

TaqMan quantitative RT-PCR was also used for analyzing transcripts and U1 snRNA (Dataset S3). The pre- and mature mRNA levels are represented by the PCR products spanning exon1-intron1 and exon1-exon2 junctions, respectively. We used RNA samples of high quality (Mean $RIN_{Control} = 8.6$, range 7.9-8.8; Mean $RIN_{AD} = 8.5$, range 8.5-8.8). Total RNA (2 μg) was used for cDNA synthesis by High Capacity cDNA Reverse Transcription Kit (Life Technologies), followed by qRT-PCR in triplicate (Applied Biosystems 7500 Fast Real-Time PCR System). Multiplex reactions were performed with additional detection of the house-keeping gene TBP. RNA expression was calculated by the $2^{-\Delta\Delta CT}$ method(10). The relative pre-mRNA level was derived using the equation above. Quantitative RT-PCR of U1-snRNA was performed as above with 150 ng of total RNA extracted from 80 μg of control and AD insoluble fractions with 0.5 ml TRIzol reagent (Invitrogen). An additional chloroform rinse (200 μl) was added to remove residual phenol from the aqueous phase.

Knockdown of U1-70K and AMO Inhibition of U1 snRNP. U1-70K in HEK293 and SH-SY5Y cells was knocked down by an equally mixed siRNA pool or individual siRNAs. The U1 AMO treatment was performed as previously reported (15). ON-TARGETplus of nontargeting control and U1-70K siRNA were purchased from Thermo Scientific Dharmacon. U1-70K siRNA pool was an equal mix of 4 siRNAs: 05-GCCGUACAUUCGAGAGUUU, 06-ACACGCAGAUGGCAAGAAG, 07-UACACAUGGUCUACAGUAA, 08-GAGAGUGAAUUAUGACACA. The HEK293 cells were cultured in DMEM/F12 media supplemented with 10% FBS, with 2 $x10^5$ cells in each well of 12-well plates. Next day cells were transfected with 10 nM siRNA by Lipofectamine RNAiMax (Life technologies), incubated for two days, and then changed into a low serum medium (1% FBS) for indicated time. The cells and media were harvested for Western blotting and Aβ40 ELISA (Millipore), respectively. The Lentiviral vectors of microRNA-adapted shRNAs for nontargeting control (GIPZ-NTC) and U1-70K shRNA (GIPZ-643682: CGGAGAGAGTTTGAGGTGT) were purchased from Thermo Scientific Open Biosystems. Cells were infected with Lentiviral particles at a multiplicity of infection of 10, incubated for two days followed by the change of the low serum medium with additional two day incubation before harvest. HEK293 cells were treated by U1 AMO (30 μM) as previously reported (11), incubated for one day and then changed into low serum medium (1% FBS) for another two day incubation before harvest.

Differentiation and Knockdown of U1-70K in Neuroblastoma SH-SY5Y Cells. SH-SY5Y cells were treated with 10 μM all-*trans*-retinoic acid (RA, Sigma) in DMEM/F12 with 10% FBS for 5 days, and then incubated in serum-free DMEM/F12 supplemented with 10 μM RA and 50 ng/ml brain-derived neurotrophic factor (BDNF, Alomone Labs) for another 3 days. For U1-70K knockdown, tandem transfections of 10 nM siRNA pool of nontargeting control or U1-70K were performed by Lipofectamine RNAiMax at day 1, 3, and 5 during the differentiation process.

RT-PCR for Selected Transcripts in Cultured Cells. Total RNA (2 μg) was extracted by RNeasy Mini Kit (Qiagen) followed by cDNA synthesis by High Capacity cDNA Reverse Transcription Kit (Life Technologies) and PCR reactions (see primers in TaqMan quantitative RT-PCR was also used for analyzing transcripts and U1 snRNA Dataset S3). The PCR products were resolved by electrophoresis on 10% Novex polyacrylamide TBE (Tris/Boric acid/ EDTA) Gels (Life Technologies), and probed with SYBR Safe DNA Gel Stain (Life Technologies).

1. Hynd MR, Lewohl JM, Scott HL, Dodd PR (2003) Biochemical and molecular studies using human autopsy brain tissue. *J Neurochem* 85(3):543–562.
2. Allison DB, Cui X, Page GP, Sabripour M (2006) Microarray data analysis: From disarray to consolidation and consensus. *Nat Rev Genet* 7(1):55–65.
3. Kendziorski CM, Zhang Y, Lan H, Attie AD (2003) The efficiency of pooling mRNA in microarray experiments. *Biostatistics (Oxford, England)* 4(3):465–477.
4. Gozal YM, et al. (2009) Proteomics analysis reveals novel components in the detergent-insoluble subproteome in Alzheimer's disease. *J Proteome Res* 8(11):5069–5079.
5. Gozal YM, et al. (2011) Aberrant septin 11 is associated with sporadic frontotemporal lobar degeneration. *Mol Neurodegener* 6:82.
6. Xu P, Duong DM, Peng J (2009) Systematical optimization of reverse-phase chromatography for shotgun proteomics. *J Proteome Res* 8(8):3944–3950.

7. Xu P, et al. (2009) Quantitative proteomics reveals the function of unconventional ubiquitin chains in proteasomal degradation. *Cell* 137(1):133–145.
8. Shevchenko A, Wilm M, Vorm O, Mann M (1996) Mass spectrometric sequencing of proteins silver-stained polyacrylamide gels. *Anal Chem* 68(5):850–858.
9. Eng J, McCormack AL, Yates JR, 3rd (1994) An approach to correlate tandem mass spectral data of peptides with amino acid sequences in a protein database. *J Am Soc Mass Spectrom* 5:976–989.
10. Liu H, Sadygov RG, Yates JR, 3rd (2004) A model for random sampling and estimation of relative protein abundance in shotgun proteomics. *Anal Chem* 76(14):4193–4201.
11. Kislinger T, et al. (2006) Global survey of organ and organelle protein expression in mouse: Combined proteomic and transcriptomic profiling. *Cell* 125(1):173–186.
12. Gozal YM, et al. (2011) Proteomic analysis of hippocampal dentate granule cells in frontotemporal lobar degeneration: Application of laser capture technology. *Front Neurol* 2:24.
13. Trapnell C, et al. (2010) Transcript assembly and quantification by RNA-Seq reveals unannotated transcripts and isoform switching during cell differentiation. *Nat Biotechnol* 28(5):511–515.
14. Geiss GK, et al. (2008) Direct multiplexed measurement of gene expression with color-coded probe pairs. *Nat Biotechnol* 26(3):317–325.
15. Berg MG, et al. (2012) U1 snRNP determines mRNA length and regulates isoform expression. *Cell* 150(1):53–64.

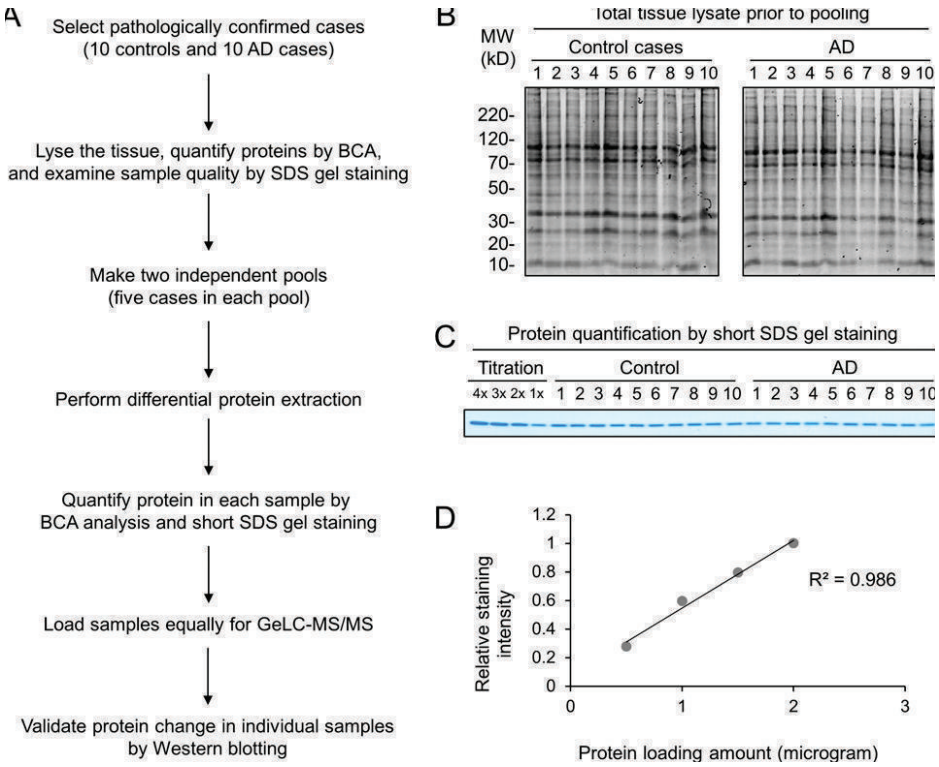

Fig. S1. Proteomic discovery scheme. (*A*) Overview of the discovery and validation scheme using protein quantification strategies. To ensure accurate protein loading, samples were measured using both the bicinchoninic acid (BCA) protein assay and short SDS gel electrophoresis followed by Coomassie staining. (*B*) One-dimensional SDS gel staining was used to examine sample quality (e.g., extensive protein degradation or blood contamination that may alter protein staining patterns). (*C*) Stained SDS gels were used to confirm the BCA results. A short (~2 mm) gel was run to compress all proteins into a single band, allowing accurate quantification during Coomassie staining, which allowed equal loading during MS and Western analysis. (*D*) Quantitative working curve based on the short SDS gel staining, demonstrating linear correlation between titrated protein levels and Coomassie dye intensities. The square of the correlation coefficient (R^2) is shown.

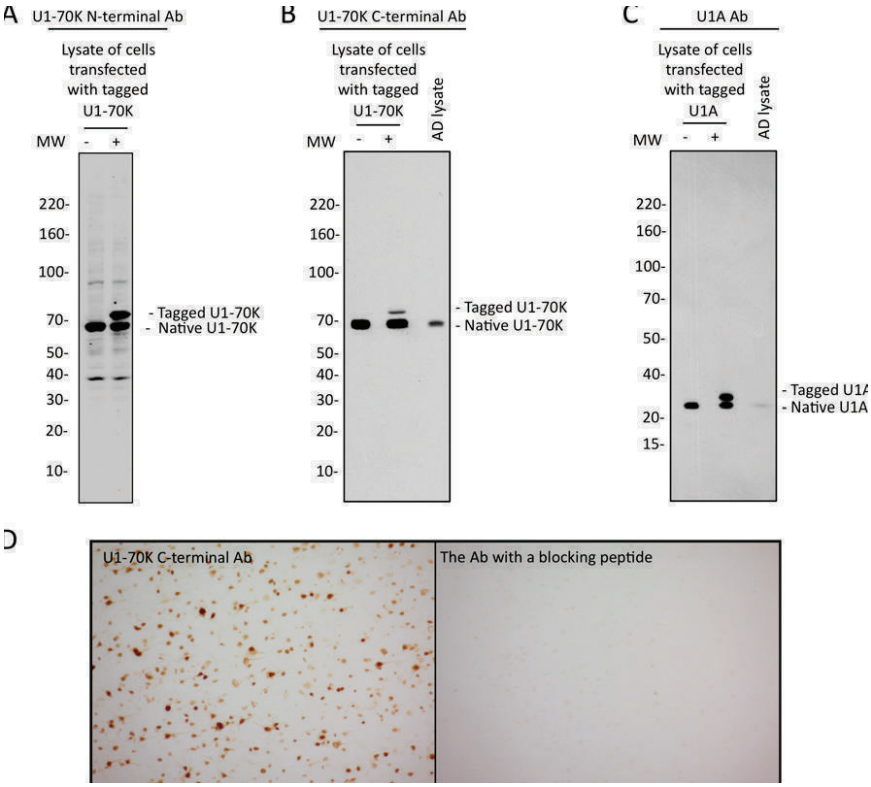

Fig. S2. Antibody specificity demonstrated by Western blotting and tissue staining. The Abs were tested using three protein samples: total cell lysate from human HEK293 cells without or with transfection of U1-70K or U1A with tandem Myc- and FLAG-tags at the C terminus and an AD detergent-insoluble fraction. (*A*) Antibodies recognizing the N-terminal epitope (amino acids 99–120) of U1-70K. (*B*) Antibodies recognizing the C-terminal epitope (amino acids 419–437) of U1-70K. (*C*) A commercial antibody against U1A. The U1A signal is typically weak in brain samples. (*D*) U1-70K diaminobenzidine staining of a human brain specimen was abolished by the addition of the epitope peptide.

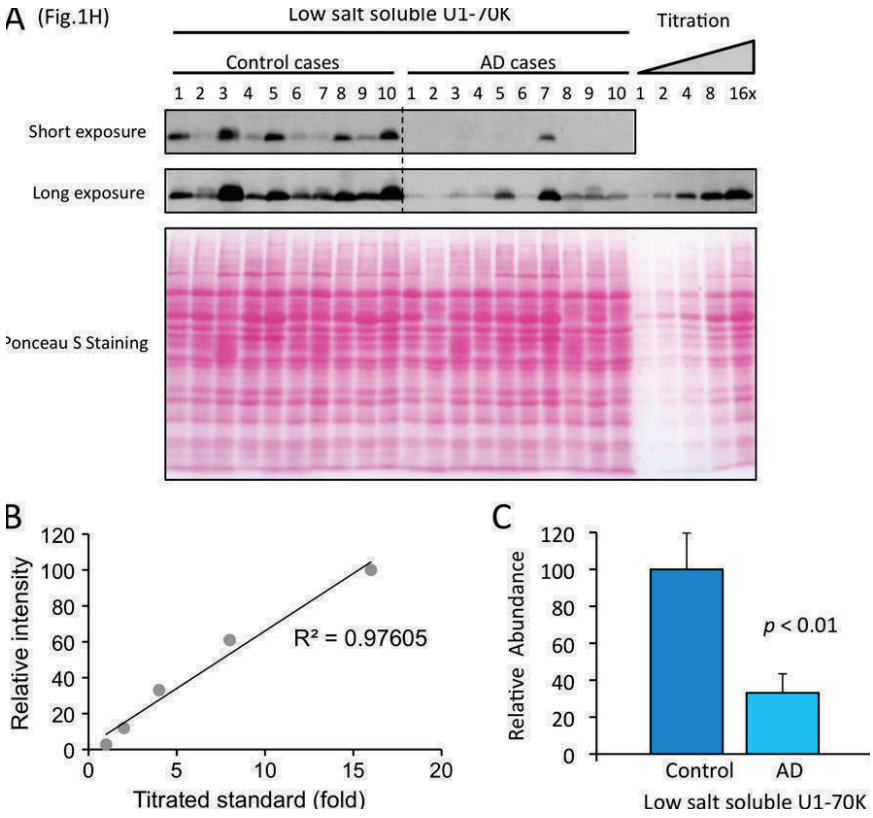

Fig. S3. Quantification of low salt-soluble U1-70K in control and AD cases by Western blotting. (*A*) Technical duplicate of the Western blotting analysis in Fig. 1*H* with titrated standards (1× to 16×). (*B*) Quantification of the standards for a working curve. (*C*) Analysis of the U1-70K level shows a statistically significant difference between control and AD cases (~threefold, $P < 0.01$, Student *t* test). The error bars indicate SEMs.

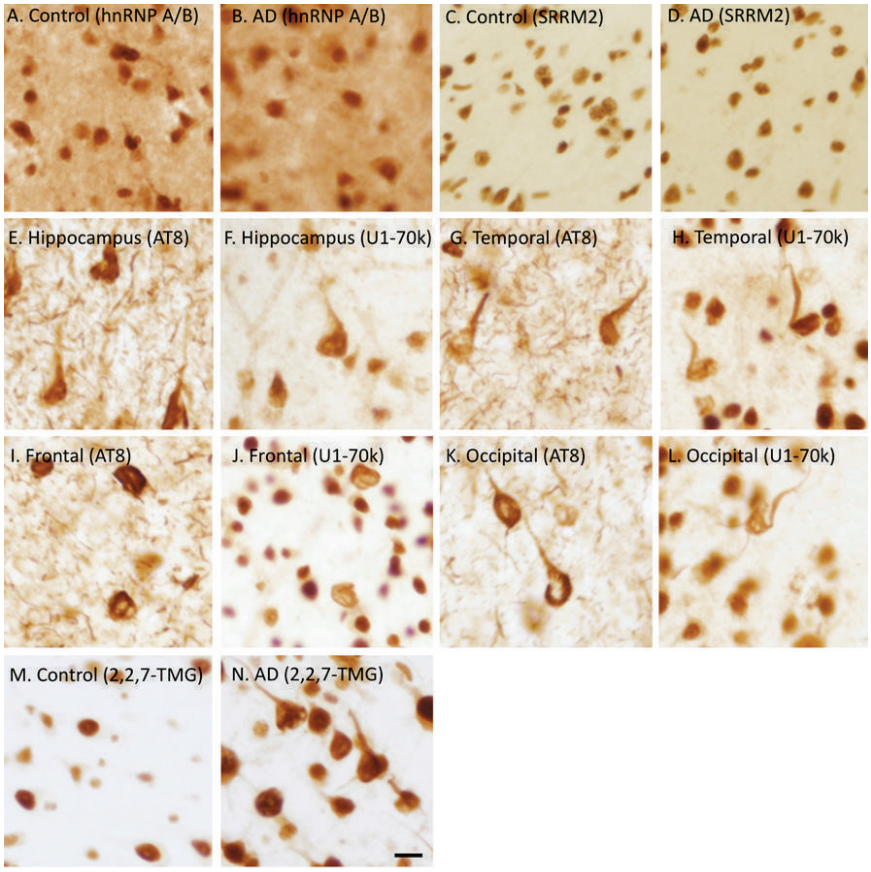

O.

	Braak 0			Braak III			Braak VI		
Brain Region	PHF-1	U1-70K	p-value	PHF-1	U1-70K	p-value	PHF-1	U1-70K	p-value
Hippocampus	0.00	0.25	0.36	3.00	1.00	0.05	5.00	2.75	0.01*
Temporal cortex	0.00	0.00	NA	1.75	1.25	0.55	5.00	4.75	0.36
Frontal cortex	0.00	0.00	NA	0.03	0.00	0.36	5.00	4.75	0.36
Occipital cortex	0.00	0.00	NA	0.00	0.00	NA	5.00	4.25	0.17

Fig. S4. Specificity of U1 small nuclear ribonucleoprotein (snRNP) component pathology. Immunohistochemistry staining of 50-μm free-floating sections. (*A–D*) Staining of other splicing factors (heterogeneous nuclear ribonucleoprotein A/B and serine/arginine repetitive matrix protein 2) in control and AD cases does not show pathological changes. (Scale bar, 20 μm.) (*E–J*) Representative sections ($n = 4$; Braak stage IV AD cases) demonstrating moderate to frequent U1-70K cytoplasmic aggregations throughout different brain regions (*F*, *H*, *J*, and *L*) with frequent neurofibrillary tangles (paired helical filament, AT8) from adjacent sections shown as reference (*E*, *G*, *I*, and *K*). Control cases ($n = 4$, Braak stage 0) were also evaluated and they demonstrated normal nuclear U1-70K staining across all cases and brain regions except for one case with sparse aggregates in the hippocampus. The control cases did not demonstrate pathological tau (PHF-1, AT8) immunoreactivity. (*M* and *N*) The 2,2,7-trimethylguanoisine (2,2,7-TMG) cap antibody labeled U-snRNA cytoplasmic aggregations in AD (*N*, representative section, $n = 3$) but maintained normal nuclear distribution in controls (*M*, representative section, $n = 3$). (*O*) Mean density of neurofibrillary tangles (PHF-1, AT8) and U1-70K tangles across four brain regions from four cases for each Braak stage. Tangles were scored semiquantitatively as 0, absent; 1, sparse; 3, moderate; and 5, frequent. *P* value was calculated with Student's *t* test for tangle density within each brain region. Asterisk denotes statistical significance between PHF-1 and U1-70K cases within hippocampus of Braak VI. NA, could not calculate *P* value because all values were zero.

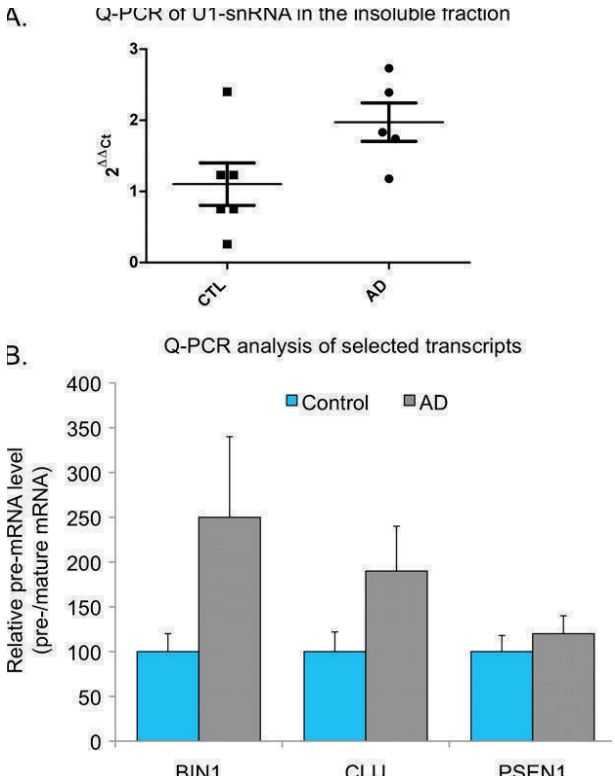

Fig. S5. Quantitative PCR of (*A*) U1 snRNA in the insoluble fraction from AD (n = 5) and controls (n = 6), and (*B*) the relative splicing efficiency of selected transcripts from AD (n = 7) and control cases (n = 7).

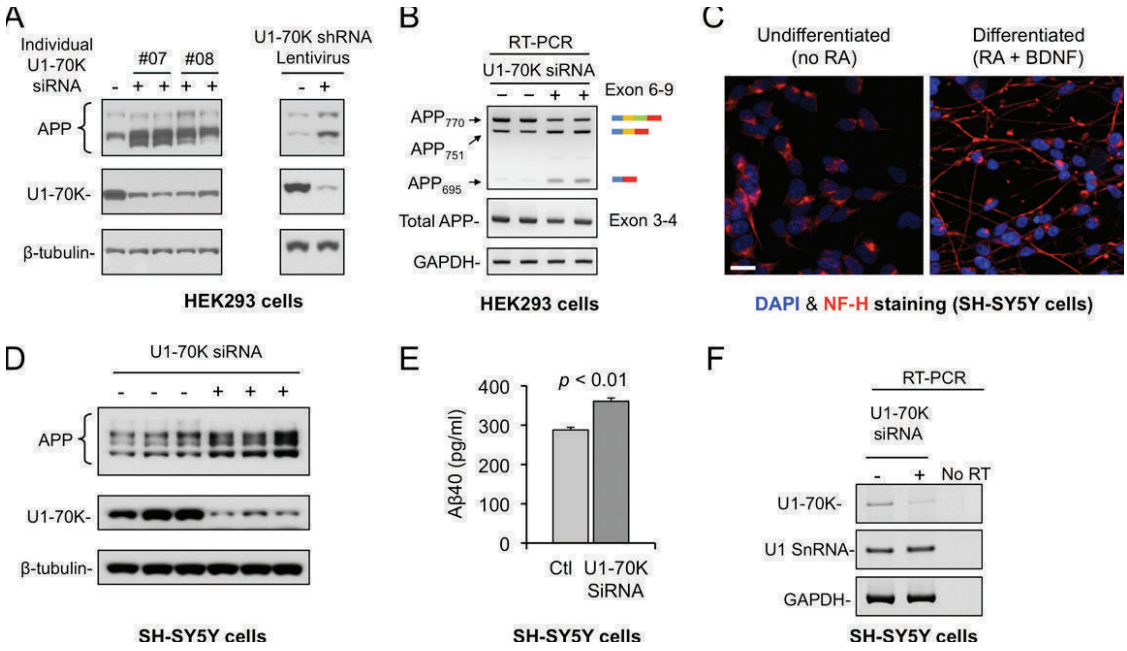

Fig. S6. (*A*) APP was up-regulated in cells in which U1-70K was knocked down by individual siRNA reagents, or U1-70K shRNA-expressing virus. (*B*) RT-PCR analysis of APP transcripts in HEK293 cells upon U1-70K knockdown. (*C*) Neuroblastoma SH-SY5Y cells were differentiated upon the treatment with RA and BDNF, and then stained with a neuronal marker, neurofilament heavy chain (NF-H) (Scale bar, 5 μm.) (*D* and *E*) APP and Aβ40 levels were increased upon U1-70K knockdown in differentiated SH-SY5Y cells. (*F*) RT-PCR showed that U1-70K knockdown did not alter the level of U1 snRNA in cells.

Dataset S1. Demographic information of patients in this study

Dataset S1

Dataset S2. The list of genes showing significant change in splicing efficiency (overlapped in both Emory and UKY groups)

Dataset S2

Dataset S3. RNA probes and RT-PCR primers

Dataset S3

Chapter 3:
INTEGRATED APPROACHES FOR ANALYZING U1-70K CLEAVAGE IN ALZHEIMER'S DISEASE

Journal of proteome research

Article

pubs.acs.org/jpr

Integrated Approaches for Analyzing U1-70K Cleavage in Alzheimer's Disease

Bing Bai,[†] Ping-Chung Chen,[†] Chadwick M. Hales,[§] Zhiping Wu,[†] Vishwajeeth Pagala,[‡] Anthony A. High,[‡] Allan I. Levey,[§] James J. Lah,[§] and Junmin Peng*[,†,‡]

[†]Departments of Structural Biology and Developmental Neurobiology, [‡]St. Jude Proteomics Facility, St. Jude Children's Research Hospital, Memphis, Tennessee 38105, United States

[§]Department of Neurology, Center for Neurodegenerative Diseases, Emory University, Atlanta, Georgia 30322, United States

Supporting Information

ABSTRACT: The accumulation of pathologic protein fragments is common in neurodegenerative disorders. We have recently identified in Alzheimer's disease (AD) the aggregation of the U1-70K splicing factor and abnormal RNA processing. Here, we present that U1-70K can be cleaved into an N-terminal truncation (N40K) in ~50% of AD cases, and the N40K abundance is inversely proportional to the total level of U1-70K. To map the cleavage site, we compared tryptic peptides of N40K and stable isotope labeled U1-70K by liquid chromatography−tandem mass spectrometry (MS), revealing that the proteolysis site is located in a highly repetitive and hydrophilic domain of U1-70K. We then adapted Western blotting to map the cleavage site in two steps: (i) mass spectrometric analysis revealing that U1-70K and N40K share the same N-termini and contain no major modifications; (ii) matching N40K with a series of six recombinant U1-70K truncations to define the cleavage site within a small region (Arg300 ± 6 residues). Finally, N40K expression led to substantial degeneration of rat primary hippocampal neurons. In summary, we combined multiple approaches to identify the U1-70K proteolytic site and found that the N40K fragment might contribute to neuronal toxicity in Alzheimer's disease.

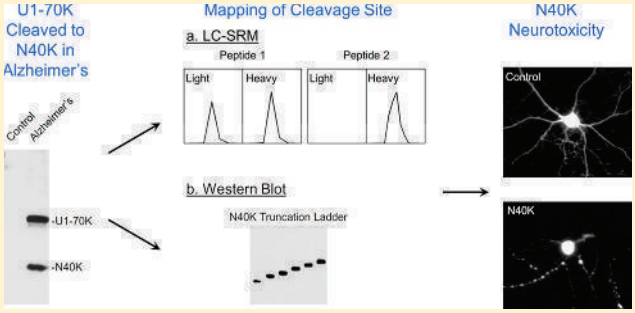

KEYWORDS: *mass spectrometry, LC−MS/MS, proteomics, neurodegenerative disease, Alzheimer's disease, stable isotope labeling, proteolytic cleavage, U1 snRNP, U1-70K, RNA splicing*

INTRODUCTION

Alzheimer's disease (AD) is the most common form of dementia and the sixth-leading cause of death in the U. S., affecting ~5 million people in the U. S., with a care cost of ~$200 billion in 2012.[1] However, no treatment is available to slow memory decline in AD. Analysis of familial early onset AD patients identified the association of three disease genes,[2] including amyloid β (Aβ) precursor protein (APP), presenilin 1, and presenilin 2, the mutations of which are thought to alter the cleavage of APP to accelerate the production of neurotoxic Aβ peptides. Genetic susceptibility, such as ApoE-ε4[3] and a TREM2 variant,[4,5] and environmental factors also influence the onset and progression of AD. Pathologically, AD is manifested by amyloid plaques and neurofibrillary tangles mainly composed of Aβ and tau, respectively.[6−9] The resulting amyloid[10] and tau hypotheses[11] have dominated AD research. However, the precise disease mechanism is still not fully understood.[12]

The advent of proteomics technology[13−15] provides an unprecedented opportunity to characterize human AD brain tissues. Highly sensitive liquid chromatography−tandem mass spectrometry (LC−MS/MS) has become the mainstream platform in proteomics.[16] We have been using this advanced platform to analyze AD specimens,[17−25] and recently discovered the aggregation of U1 small nuclear ribonucleoprotein complex (snRNP),[26,27] a spliceosome complex consisting of U1-70K, U1A, U1C, Sm proteins, and U1 snRNA.[28] Both U1-70K and U1A form cytoplasmic tangle-like structures in AD but not in other neurodegenerative disorders. Deep RNA sequencing revealed global dysregulation of RNA splicing in AD brains. Moreover, U1-70K knockdown or antisense oligonucleotide inhibition of U1 snRNP increases the levels of APP and Aβ in cellular models. Importantly, U1-70K aggregates are present in cases of mild cognitive impairment, a prodromal stage of AD, suggesting that U1 snRNP alteration occurs early in AD development. These results support specific U1 snRNP pathology and implicate dysfunctional RNA processing in AD pathogenesis.[26,27]

Special Issue: Proteomics of Human Diseases: Pathogenesis, Diagnosis, Prognosis, and Treatment

Received: April 11, 2014

   dx.doi.org/10.1021/pr5003593 | J. Proteome Res. XXXX, XXX, XXX−XXX

During our analysis of the aggregation-enriched proteome in AD by 1D SDS gel coupled with LC−MS/MS, U1-70K peptides were detected in two gel regions (~70 kDa and ~40 kDa), corresponding to the full length protein and a truncation form, respectively. The truncation contained only N-terminal peptides and was thus named N40K.[26] The N-terminal sequence in N40K was further confirmed by immunoblotting using antibodies specific to either the N-terminus or C-terminus of U1-70K. As the N40K truncation cannot be explained by the alternative splicing isoforms of U1-70K, the data indicate that U1-70K is internally cleaved to produce the N40K fragment in AD.

Protein cleavage is common in neurodegeneration, with the resulting proteolytic fragments forming aggregates and contributing to pathogenesis,[6,29] we sought to fully characterize the N40K fragment in AD. In the present study, we evaluated the N40K occurrence in AD cases and mapped the cleavage site of N40K by combining quantitative MS and Western blotting. Finally, the neuronal toxicity of the N40K fragments was investigated in cultured primary neuronal cells.

MATERIALS AND METHODS

AD Sample Analysis and Protein Preparation

Cortical Brain Tissues. Human frozen tissues from prefrontal cortical regions were provided by the brain bank of AD Research Center at Emory University. The cases (Supporting Information Table S1) were clinically and pathologically characterized in accordance with established criteria.[30]

Sequential Protein Extraction. The brain samples were sequentially extracted with increasingly stringent detergents.[26] Briefly, the cortical tissues were homogenized in a low salt buffer (10 mM Tris−HCl, pH 7.5, 5 mM EDTA, 1 mM DTT, 10% sucrose, and Sigma protease inhibitor cocktail), with 10mL buffer per gram of tissue, yielding the "total homogenate". After centrifugation at 180 000*g* for 30 min, the pellet was re-extracted with the same volume of the low salt buffer with the addition of 1% Triton X-100 and sonication. The extraction was further performed with the low salt buffer plus 1% sarkosyl (*N*-lauroylsarcosine) twice. Finally, the pellet was dissolved in 8 M urea with 2% SDS, generating the "detergent insoluble fraction".

Western Blotting. Protein samples were analyzed by NuPAGE Bis−Tris gel (Invitrogen) polyacrylamide gel electrophoresis and then transferred to nitrocellulose membrane. The membrane was blocked with 5% dry milk, incubated with antibodies, and followed by chemiluminescent detection (Thermo Fisher Scientific). The specificity of antibodies used in this study was previously characterized.[26] The band intensities of selected proteins were quantified by the ImageJ program (National Institutes of Health).

Generation of N40K Truncations and Neuronal Toxicity Analysis

DNA Plasmids and HEK293 Cell Transfection. Full-length U1-70K and its truncations were cloned from a commercial plasmid (U1-70K-*myc*-DDK, pCMV6, Origene, RC201713). The PCR products were inserted into the mammalian expression vector "pcDNA3.1(+)" between *Bam*HI and *Eco*RI sites using "Quick Ligation" kit (New England Biolabs). All DNA plasmids were validated by restrictive enzymatic digestion patterns and DNA sequencing. To express the recombinant proteins in HEK293 cells, the plasmids were transfected by the phospholipid-based transfection reagent FuGENE HD (Promega).

Recombinant U1-70K Expression and Purification. Full-length U1-70K-*myc*-DDK (FLAG tag) was overexpressed in HEK293 cells for 48 h after transfection. The cells were harvested and lysed in the Tris-buffered saline (TBS, 50 mM Tris−HCl, pH 7.5, and 100 mM NaCl) plus 1% Triton X-100 and Sigma protease inhibitor cocktail. After centrifugation at ~20 000*g* for 3 min, the pellet was dissolved with sonication in the radioimmunoprecipitation assay buffer (RIPA, 50 mM Tris−HCl, pH 7.4, 100 mM NaCl, 1% Triton X-100, 0.5% sodium deoxycholate, 0.1% SDS, and Sigma protease inhibitor cocktail). FLAG-tagged U1-70K was purified by M2 anti-FLAG beads (Sigma), and confirmed by Western blotting and mass spectrometry.

Rat Primary Hippocampal Neuron Culture, Transfection, and Toxicity Assays. Hippocampal neurons were isolated from Sprague−Dawley rat embryos at E18, and cultured in completed Neurobasal A (Life Technologies) supplemented with B27 complex and GlutaMAX. Transfection was carried out using the calcium phosphate method (CalPhos, Clontech) in the complete medium Hibernate E for 3 h without CO_2 in the incubator. The morphology of neurons was imaged after 2 day transfection. Transfection efficiency was optimized by using high quality plasmids (EndoFree Plasmid Maxi Kit, Qiagen) and adjusting the ratio of plasmids to calcium phosphate. Approximately 80 neurons were transfected per well in one 12-well plate for analyzing the degree of neuronal degeneration. Neuronal toxicity was also measured by the MTT assay (Thermo Fisher Scientific) upon 12 day Lentiviral infection (the multiplicity of infection of 10), in which mitochondrial activity in living cells converts the tetrazolium dye MTT 3-(4,5-dimethylthiazol-2-yl)-2,5-diphenyltetrazolium bromide to insoluble formazan crystals for detection.

Quantitative Mass Spectrometry

Metabolic Labeling of U1-70K and Purification. Full-length U1-70K-myc-DDK (FLAG tag) was expressed in HEK293 cells labeled with heavy isotopes: [$^{13}C_6{}^{15}N_4$] arginine (+10.0083 Da) and [$^{13}C_6$] lysine (+6.0201 Da) from Cambridge Isotope Laboratories, following our previous protocol.[24] The U1-70K was affinity purified and validated by Western blotting.

Targeted LC−SRM Analysis. The purified labeled U1-70K was analyzed on an SDS gel, together with N40K isolated from AD brain. The corresponding gel bands were excised for standard in-gel digestion (12.5 ng/μL trypsin in 50 mM NH_4HCO_3 overnight). Small peptide aliquots of heavy isotope labeled U1-70K and native N40K were mixed at different ratios to examine their relative amounts. Then the two samples were mixed at an equal molar ratio for LC−SRM analysis, in which a number of peptide pairs were coeluted by nanoscale reverse phase LC−MS. During selected reaction monitoring (SRM), the peptide ion pairs were selected for fragmentation and quantified according to the signal ratio of coeluting product ion pairs. The analysis was performed on an LTQ-Velos Orbitrap (Thermo Fisher Scientific). The optimized parameters for the peptide pairs are included in Supporting Information (Supporting Information Table S2).

LC−MS/MS Analysis of Recombinant U1-70K to Confirm the N-Terminal Acetylated Peptide. Purified recombinant U1-70K sample was resolved on an SDS gel

dx.doi.org/10.1021/pr5003593 | *J. Proteome Res.* XXXX, XXX, XXX−XXX

followed by in-gel digestion. The resulting peptides were analyzed on our optimized platform,[31] which includes an LTQ-Velos Orbitrap (Thermo Fisher Scientific), Nano Acquity UPLC (Waters), and a C_{18} reverse phase column (75 μm ID × 20 cm, 2.7 μm HALO beads, Michrom Biosources). The buffer system consisted of buffer A (0.1% formic acid) and buffer B (0.1% formic acid plus 70% AcN). The peptides were eluted by a gradient of 15−50% buffer B in 35 min at 0.3 μL per min. The MS settings included one survey scan (60 000 resolution in the Orbitrap, 10^6 automatic gain control (AGC), and 50 ms maximal ion time), and top 10 low resolution (linear ion trap) MS/MS scans (5000 AGC, 250 ms maximal ion time, 3 m/z isolation window, default collision-induced dissociation, and 15 s dynamic exclusion). Charge state screening was enabled to exclude precursor ions of singly charged or unassigned charge states.

Acquired MS/MS raw files were searched against Uniprot human databases by the Sequest algorithm (v28, revision 13) with the target−decoy strategy to analyze false discovery rate (FDR).[32,33] Spectra were matched with a mass tolerance of ± 10 ppm for precursor ions and ± 0.5 Da for product ions, with partially tryptic restriction and three maximal missed cleavages. Dynamic mass shift parameters were oxidized Met (+15.9949) and N-terminal acetylation (+42.0106), and four maximal modification sites. Only b and y ions were scored. Matched peptides were first refined by mass accuracy (±4 standard deviations, defined by all empirical good matches of doubly charged peptides with Xcorr of at least 2.5). These good matches were also utilized for mass recalibration. The refined matches were classified by precursor ion charge state and further filtered by Xcorr and ΔCn values until a protein FDR below 1% was reached. When peptides were matched to multiple proteins, these peptides were assigned to the proteins with the highest spectral counts based on the rule of parsimony.

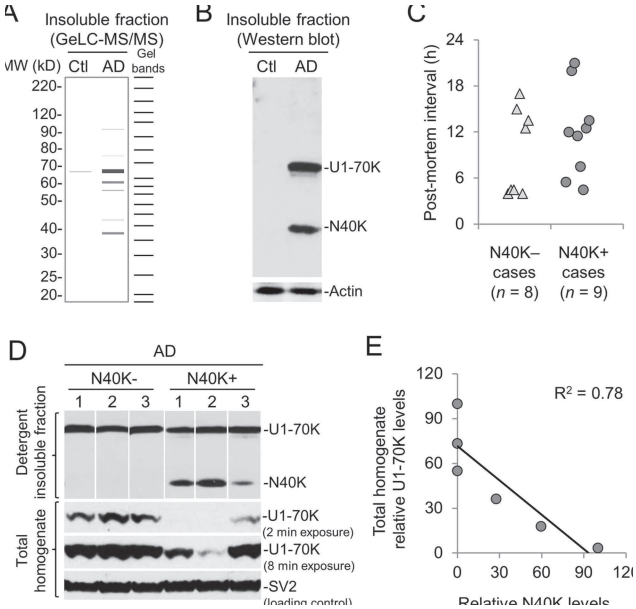

Figure 1. N40K occurrence is independent of the postmortem interval and correlates with the decrease of the U1-70K level in AD. (A) Identification of N40K in the detergent insoluble fraction of AD brain by 1D SDS gel and LC−MS/MS. Ctl: control case. (B) Validation of N40K only in AD (case 8 in Supporting Information Table S1) by Western blotting. (C) No statistically significant difference in postmortem intervals between the N40K negative and positive cases. (D) Western blotting to show reduced U1-70K level in the total homogenate in N40K positive cases. The numbers above the gel indicate the corresponding case numbers in Supporting Information Table S1. (E) Quantitation of the Western blotting intensity in panel D to indicate an inverse correlation of U1-70K in total homogenate with insoluble N40K. Relative intensities of U1-70K and N40K were normalized by setting the maximal values to 100, respectively.

RESULTS

N40K, a Proteolytic Product of U1-70K, Occurs Frequently in AD

To probe AD disease mechanism, we performed a comprehensive GeLC−MS/MS analysis of detergent insoluble proteome and found unique U1-70K pathology in AD.[26,27] In the analysis, U1-70K was identified by a large number of spectral counts and distributed in two main gel areas shown in a MS-based virtual Western blot image[34] (Figure 1A and Supporting Information Figure S1A), including 10 spectral counts in the ~40 kDa region and 33 spectral counts near its full-length 70 kDa region. Western blot demonstrated the presence of detergent insoluble U1-70K and the fragment (N40K) only in the diseased sample, whereas the nonspecific actin was found at an equal level in the control and AD samples (Figure 1B).

We further examined the prevalence of N40K in AD cases (n = 17, disease onset age of 58.7 ± 7.8 years old, age of death of 67.7 ± 8.6 years old, postmortem interval of 10.1 ± 5.7 h, Supporting Information Table S1). Approximately half of the cases (9/17, ~52.9%) exhibited N40K, and there was no significant difference between N40K negative ($N40K^-$) and N40K positive ($N40K^+$) AD cases when comparing the age of disease onset ($N40K^-$: 58.5 ± 7.7 y; $N40K^+$: 58.9 ± 8.4 y) or the age of death ($N40K^-$: 66.8 ± 9.7 y; $N40K^+$: 68.5 ± 8.1 y). Although the postmortem interval of the two AD groups appears to display a difference ($N40K^-$: 8.1 ± 5.3 h; $N40K^+$: 12 ± 5.8 h), it is not statistically significant (p = 0.165, Student's t-test, Figure 1C). The results suggest that the generation of N40K is unlikely caused by prolonged postmortem interval during the collection of brain tissues.

When extracting proteins from AD brain tissues, we observed that the U1-70K level was low in total homogenate of some cases.[26] Interestingly, the occurrence of N40K in the detergent insoluble fraction was concomitant with the reduction of total U1-70K (Figure 1D and Supporting Information Figure S1B), and the two protein abundances showed an inverse correlation (Figure 1E).

We then sought to determine whether N40K is an alternative splicing isoform or a cleaved fragment of full-length U1-70K. In the UniProt/Swiss-Prot database, U1-70K has four different splicing isoforms of 437 (full length, Figure 2), 428, 341, and 166 residues. None of these four isoforms fit the size of N40K. To explore potential new U1-70K splicing isoforms in AD, we analyzed RNA-seq data sets of multiple AD brains[26] but did not identify any additional isoforms. All exon reads of U1-70K were evenly distributed along the transcript, consistent with only one major RNA form of the full length U1-70K. In addition, U1 SnRNP deficiency may cause premature cleavage and polyadenylation in AD,[26] leading to shortened RNA transcripts. However, we did not find any premature polyadenylation in the exons of U1-70K. Therefore, N40K is most likely produced by the proteolysis of full length U1-70K.

dx.doi.org/10.1021/pr5003593 | J. Proteome Res. XXXX, XXX, XXX−XXX

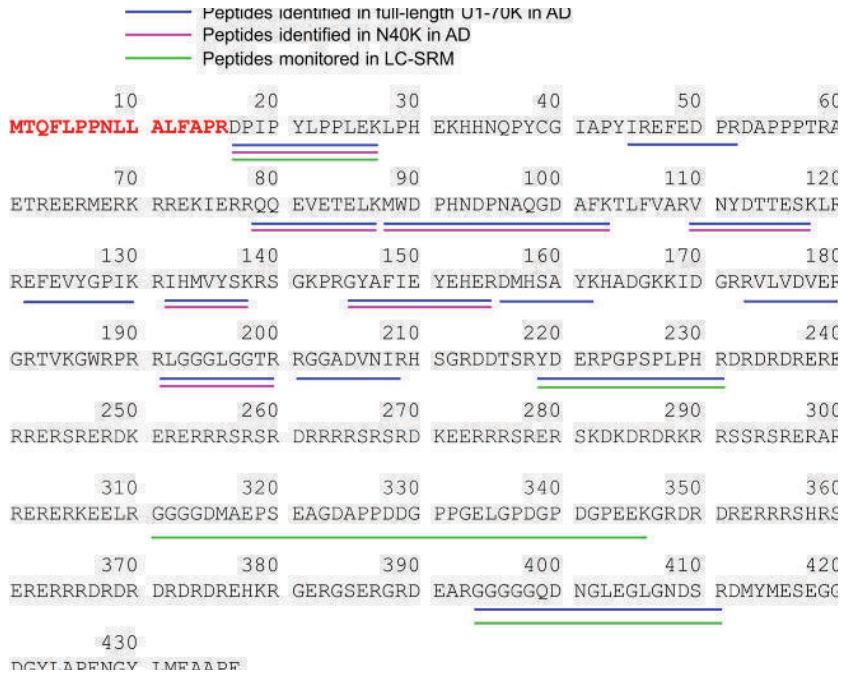

Figure 2. Identification of U1-70K and N40K peptides in AD. These peptides are shown in different colors in the protein sequence, together with peptides monitored in LC−SRM.

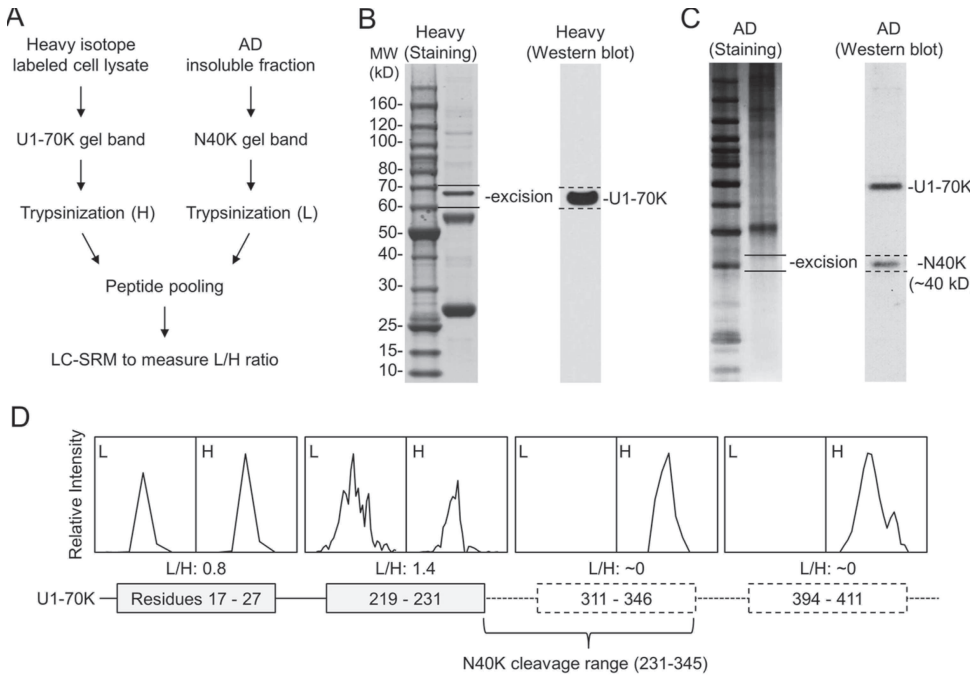

Figure 3. Analysis of the N40K C-terminus by LC−SRM. (A) Work flow of the method. (B) Identification and size confirmation of purified recombinant U1-70K by Western blotting, followed by band excision and in-gel digestion. (C) Identification of a N40K-containing gel band by Western blotting. The 10 kDa ladder was also used for precise alignment of immunoblotting images with stained gel. (D) The intensity ratios of light/heavy (L/H) of U1-70K peptide pairs, leading to the predicted cleavage region.

Analysis of N40K Termini by Mass Spectrometry

We attempted to determine both termini of N40K protein by mass spectrometry. First, shotgun MS analysis[26] identified seven peptides in N40K in the region from Asp17 to Arg200 (Figure 2), but N40K is clearly larger than a protein of 200 amino acids. Additional database search for protein modifications did not uncover any modified peptides. Some N40K peptides may be missed in the analysis, possibly due to the low level of N40K, undersampling of shotgun proteomics, or the incompatibility with LC−MS/MS.

To address the undersampling problem of shotgun MS, we then performed a systematic LC−SRM screening of N40K tryptic peptides using stable isotope labeled, recombinant U1-70K protein as an internal standard (Figure 3A). Compared to

dx.doi.org/10.1021/pr5003593 | J. Proteome Res. XXXX, XXX, XXX−XXX

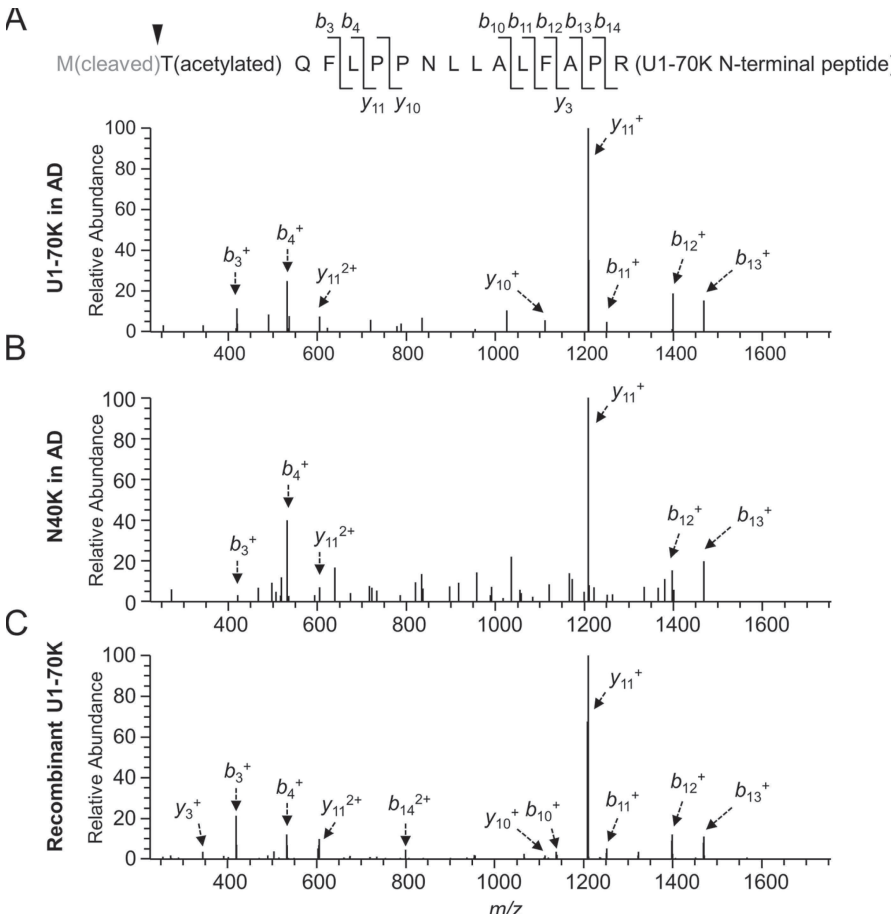

Figure 4. Analysis of the N40K N-terminus by MS. (A–C) MS/MS spectra for identifying the N-terminal peptide with methionine removal and threonine acetylation in U1-70K, N40K, and purified U1-70K in HEK293 cells, respectively. Matched ions were assigned by arrows indicating specific *b* or *y* ions.

precursor ion quantification on survey MS scans that may be interfered by coeluted isobaric ions, the SRM enables targeted analysis of product ions from precursor ion fragmentation (Supporting Information Table S2), typically showing better specificity and sensitivity. Theoretically, when U1-70K peptides are equally mixed with N40K peptides, shared peptides have a 1:1 ratio and unique peptides have a 1:0 or 0:1 ratio. On the basis of this principle, we purified heavy Lys and Arg labeled U1-70K from HEK293 cells and validated by immunoblotting. The sample was resolved on an SDS gel, and the U1-70K-containing band was excised for in-gel trypsin digestion (Figure 3B). Meanwhile, N40K extracted from the AD insoluble fraction was similarly processed (Figure 3C). The two samples were mixed at a nearly 1:1 ratio for LC–SRM, in which four selected peptides were monitored according to MS/MS spectra of purified U1-70K (Supporting Information Figure S2–S5). Two peptides (residues 17–27 and 219–231) showed roughly 1:1 ratio, whereas the other two peptides (residues 311–346 and 394~411) were not detected in the light forms, suggesting that the C-terminus of N40K is between amino acids 231 and 345 (Figure 3D).

Additional attempts to analyze putative peptides between residues 231 and 345 were futile, as the region is highly repetitive and hydrophilic, enriched in Lys, Arg, Asp, and Glu residues (Figure 2). Any peptides digested by available proteases are either too small or too hydrophilic for LC–MS/MS analysis using standard methodology. Thus, we decided to use Western blotting to narrow down the range of N40K C-terminus. Prior to the Western blotting analysis, we needed to ensure that full length U1-70K and N40K have the same N-terminus (Figure 2) and lack other post-translational modifications that may affect protein migration.

As the N-terminal amino acid of proteins is usually modified,[35] we tested multiple modification possibilities and found that U1-70K and N40K have the first Met removed and the second Thr acetylated (Figure 4A). The MS/MS pattern of the resulting tryptic peptide (residues 2–16) was detected for both U1-70K and N40K in AD (Figure 4A and B). Importantly, the MS/MS pattern was fully recapitulated in the analysis of recombinant U1-70K purified from HEK293 cells (Figure 4C). Moreover, the precursor ions in these three independent LC–MS/MS runs showed highly similar isotopic patterns and LC retention properties (i.e., eluted by ~33% acetonitrile, Supporting Information Figure S6). These data strongly support that N40K has the identical N-terminus as the full length U1-70K.

N40K C-Terminus Is Around Arg300 Based on Western Blotting

Protein migration during Western blotting is determined by its amino acid sequence and post-translational modifications. Our MS analysis did not identify any major post-translational modification sites with high occupancy in N40K. RNA-seq analysis did not reveal any alternative splicing isoforms similar

dx.doi.org/10.1021/pr5003593 | J. Proteome Res. XXXX, XXX, XXX–XXX

to N40K. To ensure the comparison of proteins with the same amino acid composition, we constructed serial U1-70K N-terminal truncations (N272, N282, N289, N300, N306, and N316, without any tag) based on the MS-mapped C-terminal range. When expressed in HEK293 cells, these proteins showed a ladder on Western blot using U1-70K polyclonal antibodies[26] that recognize a peptide antigen of residues 99−120 (Figure 5A). After multiple rounds of analyses, the cleavage site was

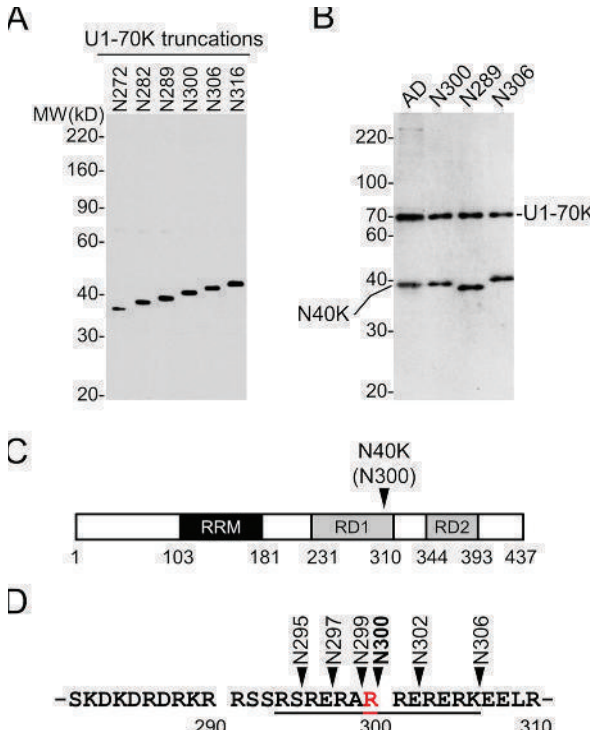

Figure 5. Determination of N40K C-terminus by Western blotting. (A) Expression of U1-70K N-terminal truncations in HEK293 cells. (B) Analysis of N40K in AD and three recombinant truncations. (C) Diagram of U1-70K domains and predicted N40K cleavage region. (D) N40K truncations covering all possible cleavage products with different C-terminal residues.

determined to be Arg300 [±0.8 kDa (six residues)] (Figure 5B; only the three closest truncations are shown). As most proteases exhibit residue specificity, we generated six N-terminal truncations including all possible C-terminal residues for subsequent functional studies (Figure 5C-5D).

N40K Fragment Expression Induces Neuronal Toxicity

As proteolytic cleavage may result in neurotoxic fragments in neurodegeneration,[6,29] we examined the toxicity of the full-length U1-70K and six N40K truncations (N295, N297, N299, N300, N302, and N306) in cultured primary neurons. To test the expression efficiency of these recombinant proteins, we transfected equal amounts of DNA plasmids (Figure 6A) in HEK293 cells and detected highly similar levels of recombinant proteins (Figure 6B). These plasmids were then cotransfected into rat primary hippocampal neurons that were cultured for 14 days in vitro, together with a vector expressing red fluorescent protein (RFP) to monitor neuronal morphology. Interestingly, at two days after transfection, all six truncations caused neuritic beading and dystrophy, reminiscent of neuronal morphologies observed in degeneration.[36−38] In contrast, the effects of mock vector and expression of enhanced green fluorescent protein (EGFP) were mild, and the expression of U1-70K showed a moderate toxicity (Figure 6C). This conclusion was further confirmed by statistical analysis of quantitative data (i.e., counting morphologically altered neurons, Figure 6D).

As all of the six N40K truncations showed almost identical effect during the morphology analysis, we selected a representative construct N300 and U1-70K to perform the MTT cell viability assay,[39] in which mitochondrial activity in living cells converts MTT to formazan crystals for detection. Dying cells have less mitochondrial activity and, thus, produce weaker signals. Because this biochemical assay requires a large number of neurons expressing targeted proteins, we generated recombinant Lentivirus to infect hippocampal neurons. The U1-70K expression exhibited a moderate neurotoxity to decrease cellular viability by ∼35%, whereas the N300 expression resulted in ∼50% decrease compared to the control virus (Figure 6E). These results strongly support that N40K expression in cultured neurons induces cellular death.

CONCLUSIONS AND DISCUSSION

In this study, we have demonstrated that N40K, a cleaved fragment of U1-70K, occurs frequently in Alzheimer's disease. Whereas the N-terminus of N40K is identical to that of U1-70K, N40K C-terminus is approximately Arg300 ± 6 residues. Extremely repetitive, hydrophilic residues in the C-terminal area raise a challenge to precisely define the cleavage site. All putative N40K truncations exhibit similar molecular properties, with respect to protein expression level and neuronal toxicity, suggesting that the accumulation of N40K in human brain may contribute to neuronal degeneration in Alzheimer's disease.

Interestingly, we have found that the N40K level is inversely correlated with the total level of full length U1-70K, which might result in the loss of function of U1-70K in addition to the toxic gain of function of N40K. It is notable that expression of C-terminal fragment of TDP-43,[40] another RNA processing factor involved in the pathogenesis of ALS, also caused similar suppression of endogenous full-length protein.[41] Both N40K and the TDP-43 fragments contain RNA recognition motifs, suggesting a common self-regulation mechanism of RNA binding proteins. Indeed, another U1 snRNP subunit U1A binds to U1 snRNA to maintain its expression level.[42] It is also possible that the reduction of U1-70K level is primarily caused by proteolytic cleavage because numerous proteases are activated in AD, such as caspases, calpains, and cathepsins.[43−45] Moreover, it is known that U1-70K is cleaved by caspase-3, granzyme B, and Cu/H_2O_2 oxidation reactions.[46−48] However, these protease-derived fragments are larger than N40K. Further investigation of the protease responsible for N40K cleavage is important to elucidate its involvement in AD.

In addition, we have used several approaches for mapping N40K proteolytic site. N40K was first identified by virtual Western blotting reconstructed from GeLC−MS/MS and then validated by traditional Western blotting (Figure 1A and B). It needs to be mentioned that the virtual Western blot image showed a more complex pattern than conventional Western blot, partially because of ambiguity during gel excision. In addition, the GeLC−MS/MS detects proteins in a large dynamic range (∼10 000), whereas Western blot only displays proteins in a narrow dynamic range (<100). These features contribute to the different images from the two semi-quantitative methods.

To overcome the undersampling problem for proteins of low abundance in shotgun LC−MS/MS analysis, we have

dx.doi.org/10.1021/pr5003593 | J. Proteome Res. XXXX, XXX, XXX−XXX

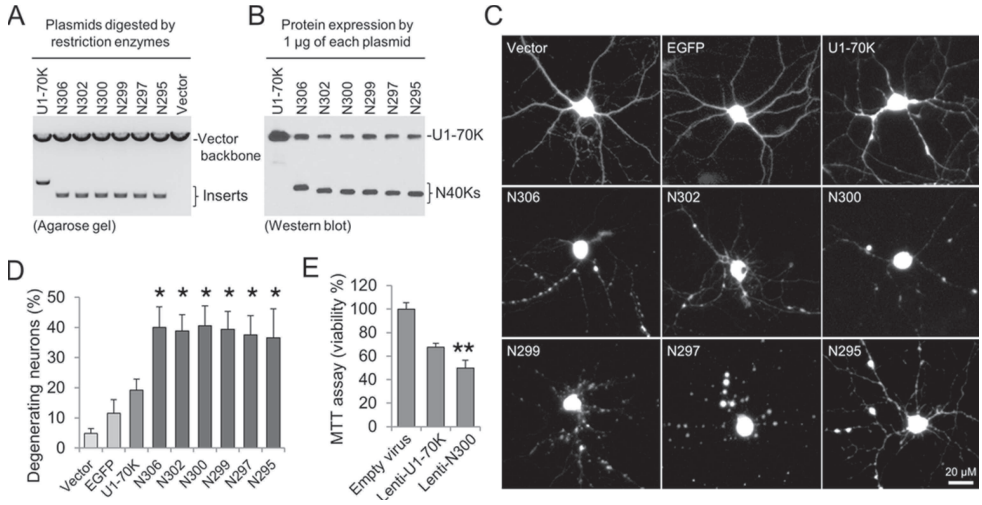

Figure 6. Toxicity analysis of N40K in rat hippocampal primary neurons. (A) Restriction enzyme digestion at the cloning sites by *Bam*HI and *Eco*RI to show equal levels of the plasmids of U1-70K and six N40K truncations. (B) Western blotting to show similar protein expression in HEK293 cells. (C) Co-transfection of nine plasmids each with RFP by the calcium phosphate method. (D) Quantitative analysis by counting degenerating neurons. Error bars represent standard errors of mean (SEM) of analyzed neurons in duplicated plates of the same batch of neuronal culture. The experiments were repeated three times with different batches of culture, all showing similar results. The asterisks indicate $p < 0.05$ by the ANOVA and Tukey range test. (E) The MTT assay of neuronal viability upon Lentiviral N40K transfection. Error bars represent SEM. The double asterisks indicate $p < 0.01$ by Student's *t*-test.

developed an LC−SRM method to determine the N40K C-terminus. The direct monitoring of U1-70K peptides based on pre-existing recombinant protein data greatly enhanced the sensitivity of detection, which was critical for the analysis of N40K in a limited amount of human samples. Because of irregular amino acid composition of N40K C-terminus, no suitable peptides are compatible with standard LC−MS/MS settings. We fully explored the usage of Western blotting using a ladder of recombinant proteins, which restricted the C-terminus in a small region.

We have further tested a series of putative N40K truncations in HEK293 cells and primary neuronal culture. All N40K proteins had no obvious influence on HEK293 cells but clearly demonstrated toxicity in rat primary neurons. Although full length U1-70K also led to a moderate toxicity, reminiscent of cell death caused by the expression of the RNA processing factor TDP-43,[49] U1-70K had less effect than the N40K fragments. Apoptosis is a fundamental process essential for tissue homeostasis and its dysfunction is involved in AD pathogenesis.[50] Neuronal apoptosis results in neuritic degeneration manifested by beading, thinning, and breakage, as well as the destruction of mitochondria.[36−38] N40K-expressing neurons displayed these morphological changes reported in apoptotic neurons and showed mitochondrial deficit in the MTT assay, suggesting that the toxicity in cell culture might be mediated by apoptotic events, although other alternative cell death mechanisms cannot be excluded.

In summary, we have identified that the N40K fragment in AD not only is associated with the reduction of full length U1-70K but also directly exerts toxic effects in cultured neurons, providing lines of evidence to support that the U1-70K cleavage event occurs in human AD brain and might contribute to the neurodegeneration in AD.

■ ASSOCIATED CONTENT

Supporting Information

Demographic information, LC−SRM analysis, Western blots, MS/MS spectra, and retention time data. This material is available free of charge via the Internet at http://pubs.acs.org.

■ AUTHOR INFORMATION

Corresponding Author

*J. Peng. Tel.: 901-336-1083. E-mail: junmin.peng@stjude.org.

Notes

The authors declare no competing financial interest.

■ ACKNOWLEDGMENTS

The authors thank all of the lab members for helpful discussion. This work was partially supported by NIH grants P50AG005136, and American Academy of Neurology Foundation Clinical Research Training Fellowship to C.M.H. J.P. is supported by ALSAC (American Lebanese Syrian Associated Charities). The MS analysis was performed in the St. Jude Children's Research Hospital Proteomics Facility, which is partially supported by NIH Cancer Center Support Grant (P30CA021765).

■ ABBREVIATIONS

LC, liquid chromatography; MS, mass spectrometer; U1 snRNP, U1 small nuclear ribonucleoprotein complex; AD, Alzheimer's disease

■ REFERENCES

(1) 2012 Alzheimer's disease facts and figures. *Alzheimer's Dementia* **2012**, *8* (2), 131−68.

(2) Tanzi, R. E., The genetics of Alzheimer disease. *Cold Spring Harbor Perspect. Med.* **2012**, *2* (10).

(3) Liu, C. C.; Kanekiyo, T.; Xu, H.; Bu, G. Apolipoprotein E and Alzheimer disease: risk, mechanisms and therapy. *Nat. Rev. Neurol.* **2013**, *9* (2), 106−18.

(4) Jonsson, T.; Stefansson, H.; Steinberg, S.; Jonsdottir, I.; Jonsson, P. V.; Snaedal, J.; Bjornsson, S.; Huttenlocher, J.; Levey, A. I.; Lah, J. J.; Rujescu, D.; Hampel, H.; Giegling, I.; Andreassen, O. A.; Engedal, K.; Ulstein, I.; Djurovic, S.; Ibrahim-Verbaas, C.; Hofman, A.; Ikram, M. A.; van Duijn, C. M.; Thorsteinsdottir, U.; Kong, A.; Stefansson, K. Variant of TREM2 associated with the risk of Alzheimer's disease. *N. Engl. J. Med.* **2013**, *368* (2), 107−16.
(5) Neumann, H.; Daly, M. J. Variant TREM2 as risk factor for Alzheimer's disease. *N. Engl. J. Med.* **2013**, *368* (2), 182−4.
(6) Taylor, J. P.; Hardy, J.; Fischbeck, K. H. Toxic proteins in neurodegenerative disease. *Science* **2002**, *296* (5575), 1991−5.
(7) Glenner, G. G.; Wong, C. W. Alzheimer's disease: initial report of the purification and characterization of a novel cerebrovascular amyloid protein. *Biochem. Biophys. Res. Commun.* **1984**, *120* (3), 885−90.
(8) Masters, C. L.; Simms, G.; Weinman, N. A.; Multhaup, G.; McDonald, B. L.; Beyreuther, K. Amyloid plaque core protein in Alzheimer disease and Down syndrome. *Proc. Natl. Acad. Sci. U. S. A.* **1985**, *82* (12), 4245−9.
(9) Lee, V. M.; Balin, B. J.; Otvos, L., Jr.; Trojanowski, J. Q. A68: a major subunit of paired helical filaments and derivatized forms of normal Tau. *Science* **1991**, *251* (4994), 675−8.
(10) Hardy, J.; Selkoe, D. J. The amyloid hypothesis of Alzheimer's disease: progress and problems on the road to therapeutics. *Science* **2002**, *297* (5580), 353−6.
(11) Ballatore, C.; Lee, V. M.; Trojanowski, J. Q. Tau-mediated neurodegeneration in Alzheimer's disease and related disorders. *Nat. Rev. Neurosci.* **2007**, *8* (9), 663−72.
(12) Pimplikar, S. W.; Nixon, R. A.; Robakis, N. K.; Shen, J.; Tsai, L. H. Amyloid-independent mechanisms in Alzheimer's disease pathogenesis. *J. Neurosci.* **2010**, *30* (45), 14946−54.
(13) Aebersold, R.; Mann, M. Mass spectrometry-based proteomics. *Nature* **2003**, *422* (6928), 198−207.
(14) Peng, J.; Gygi, S. P. Proteomics: the move to mixtures. *J. Mass Spectrom.* **2001**, *36* (10), 1083−91.
(15) Cravatt, B. F.; Simon, G. M.; Yates, J. R., 3rd The biological impact of mass-spectrometry-based proteomics. *Nature* **2007**, *450* (7172), 991−1000.
(16) Mann, M.; Kulak, N. A.; Nagaraj, N.; Cox, J. The coming age of complete, accurate, and ubiquitous proteomes. *Mol. Cell* **2013**, *49* (4), 583−90.
(17) Zhou, J. Y.; Jones, D. R.; Duong, D. M.; Levey, A. I.; Lah, J. J.; Peng, J. Proteomic Analysis of Postsynaptic Density in Alzheimer Disease. *Clin. Chim. Acta* **2013**, *420*, 62−8.
(18) Gozal, Y. M.; Duong, D. M.; Gearing, M.; Cheng, D.; Hanfelt, J. J.; Funderburk, C.; Peng, J.; Lah, J. J.; Levey, A. I. Proteomics analysis reveals novel components in the detergent-insoluble subproteome in Alzheimer's disease. *J. Proteome Res.* **2009**, *8* (11), 5069−79.
(19) Gozal, Y. M.; Dammer, E. B.; Duong, D. M.; Cheng, D.; Gearing, M.; Rees, H. D.; Peng, J.; Lah, J. J.; Levey, A. I. Proteomic analysis of hippocampal dentate granule cells in frontotemporal lobar degeneration: application of laser capture technology. *Front. Neurol.* **2011**, *2*, 24.
(20) Gozal, Y. M.; Seyfried, N. T.; Gearing, M.; Glass, J. D.; Heilman, C. J.; Wuu, J.; Duong, D. M.; Cheng, D.; Xia, Q.; Rees, H. D.; Fritz, J. J.; Cooper, D. S.; Peng, J.; Levey, A. I.; Lah, J. J. Aberrant septin 11 is associated with sporadic frontotemporal lobar degeneration. *Mol. Neurodegener.* **2011**, *6*, 82.
(21) Dammer, E. B.; Na, C. H.; Xu, P.; Seyfried, N. T.; Duong, D. M.; Cheng, D.; Gearing, M.; Rees, H.; Lah, J. J.; Levey, A. I.; Rush, J.; Peng, J. Polyubiquitin linkage profiles in three models of proteolytic stress suggest the etiology of Alzheimer disease. *J. Biol. Chem.* **2011**, *286* (12), 10457−65.
(22) Xia, Q.; Cheng, D.; Duong, D. M.; Gearing, M.; Lah, J. J.; Levey, A. I.; Peng, J. Phosphoproteomic analysis of human brain by calcium phosphate precipitation and mass spectrometry. *J. Proteome Res.* **2008**, *7* (7), 2845−51.
(23) Liao, L.; Cheng, D.; Wang, J.; Duong, D. M.; Losik, T. G.; Gearing, M.; Rees, H. D.; Lah, J. J.; Levey, A. I.; Peng, J. Proteomic characterization of postmortem amyloid plaques isolated by laser capture microdissection. *J. Biol. Chem.* **2004**, *279* (35), 37061−8.
(24) Seyfried, N. T.; Gozal, Y. M.; Dammer, E. B.; Xia, Q.; Duong, D. M.; Cheng, D.; Lah, J. J.; Levey, A. I.; Peng, J. Multiplex SILAC analysis of a cellular TDP-43 proteinopathy model reveals protein inclusions associated with SUMOylation and diverse polyubiquitin chains. *Mol. Cell. Proteomics* **2010**, *9* (4), 705−18.
(25) Zhou, J. Y.; Afjehi-Sadat, L.; Asress, S.; Duong, D. M.; Cudkowicz, M.; Glass, J. D.; Peng, J. Galectin-3 Is a Candidate Biomarker for Amyotrophic Lateral Sclerosis: Discovery by a Proteomics Approach. *J. Proteome Res.* **2010**, *9* (10), 5133−41.
(26) Bai, B.; Hales, C. M.; Chen, P. C.; Gozal, Y.; Dammer, E. B.; Fritz, J. J.; Wang, X.; Xia, Q.; Duong, D. M.; Street, C.; Cantero, G.; Cheng, D.; Jones, D. R.; Wu, Z.; Li, Y.; Diner, I.; Heilman, C. J.; Rees, H. D.; Wu, H.; Lin, L.; Szulwach, K. E.; Gearing, M.; Mufson, E. J.; Bennett, D. A.; Montine, T. J.; Seyfried, N. T.; Wingo, T. S.; Sun, Y. E.; Jin, P.; Hanfelt, J.; Willcock, D. M.; Levey, A.; Lah, J. J.; Peng, J. U1 small nuclear ribonucleoprotein complex and RNA splicing alterations in Alzheimer's disease. *Proc. Natl. Acad. Sci. U. S. A.* **2013**, *110* (41), 16562−7.
(27) Hales, C. M.; Dammer, E. B.; Diner, I.; Yi, H.; Seyfried, N. T.; Gearing, M.; Glass, J. D.; Montine, T. J.; Levey, A. I.; Lah, J. J. Aggregates of small nuclear ribonucleic acids (snRNAs) in Alzheimer's disease. *Brain Pathol.* **2014**, No. 10.1111/bpa.12133.
(28) Staley, J. P.; Guthrie, C. Mechanical devices of the spliceosome: motors, clocks, springs, and things. *Cell* **1998**, *92* (3), 315−26.
(29) Ross, C. A.; Poirier, M. A. Protein aggregation and neurodegenerative disease. *Nat. Med.* **2004**, *10* (Suppl), S10−7.
(30) Hyman, B. T.; Trojanowski, J. Q. Consensus recommendations for the postmortem diagnosis of Alzheimer disease from the National Institute on Aging and the Reagan Institute Working Group on diagnostic criteria for the neuropathological assessment of Alzheimer disease. *J. Neuropathol. Exp. Neurol.* **1997**, *56* (10), 1095−7.
(31) Xu, P.; Duong, D. M.; Peng, J. Systematical optimization of reverse-phase chromatography for shotgun proteomics. *J. Proteome Res.* **2009**, *8* (8), 3944−50.
(32) Peng, J.; Elias, J. E.; Thoreen, C. C.; Licklider, L. J.; Gygi, S. P. Evaluation of multidimensional chromatography coupled with tandem mass spectrometry (LC/LC−MS/MS) for large-scale protein analysis: the yeast proteome. *J. Proteome Res.* **2003**, *2*, 43−50.
(33) Elias, J. E.; Gygi, S. P. Target-decoy search strategy for increased confidence in large-scale protein identifications by mass spectrometry. *Nat. Methods* **2007**, *4* (3), 207−14.
(34) Seyfried, N. T.; Xu, P.; Duong, D. M.; Cheng, D.; Hanfelt, J.; Peng, J. Systematic approach for validating the ubiquitinated proteome. *Anal. Chem.* **2008**, *80* (11), 4161−9.
(35) Bonissone, S.; Gupta, N.; Romine, M.; Bradshaw, R. A.; Pevzner, P. A. N-terminal protein processing: a comparative proteogenomic analysis. *Mol. Cell. Proteomics* **2013**, *12* (1), 14−28.
(36) Kuchibhotla, K. V.; Goldman, S. T.; Lattarulo, C. R.; Wu, H. Y.; Hyman, B. T.; Bacskai, B. J. Abeta plaques lead to aberrant regulation of calcium homeostasis in vivo resulting in structural and functional disruption of neuronal networks. *Neuron* **2008**, *59* (2), 214−25.
(37) Jin, M.; Shepardson, N.; Yang, T.; Chen, G.; Walsh, D.; Selkoe, D. J. Soluble amyloid beta-protein dimers isolated from Alzheimer cortex directly induce Tau hyperphosphorylation and neuritic degeneration. *Proc. Natl. Acad. Sci. U. S. A.* **2011**, *108* (14), 5819−24.
(38) Nikolaev, A.; McLaughlin, T.; O'Leary, D. D.; Tessier-Lavigne, M. APP binds DR6 to trigger axon pruning and neuron death via distinct caspases. *Nature* **2009**, *457* (7232), 981−9.
(39) Lobner, D. Comparison of the LDH and MTT assays for quantifying cell death: validity for neuronal apoptosis? *J. Neurosci. Methods* **2000**, *96* (2), 147−52.
(40) Neumann, M.; Sampathu, D. M.; Kwong, L. K.; Truax, A. C.; Micsenyi, M. C.; Chou, T. T.; Bruce, J.; Schuck, T.; Grossman, M.; Clark, C. M.; McCluskey, L. F.; Miller, B. L.; Masliah, E.; Mackenzie, I. R.; Feldman, H.; Feiden, W.; Kretzschmar, H. A.; Trojanowski, J. Q.; Lee, V. M. Ubiquitinated TDP-43 in frontotemporal lobar

degeneration and amyotrophic lateral sclerosis. *Science* **2006**, *314* (5796), 130−3.
(41) Nonaka, T.; Kametani, F.; Arai, T.; Akiyama, H.; Hasegawa, M. Truncation and pathogenic mutations facilitate the formation of intracellular aggregates of TDP-43. *Hum. Mol. Genet.* **2009**, *18* (18), 3353−64.
(42) Kambach, C.; Mattaj, I. W. Intracellular distribution of the U1A protein depends on active transport and nuclear binding to U1 snRNA. *J. Cell Biol.* **1992**, *118* (1), 11−21.
(43) Gervais, F. G.; Xu, D.; Robertson, G. S.; Vaillancourt, J. P.; Zhu, Y.; Huang, J.; LeBlanc, A.; Smith, D.; Rigby, M.; Shearman, M. S.; Clarke, E. E.; Zheng, H.; Van Der Ploeg, L. H.; Ruffolo, S. C.; Thornberry, N. A.; Xanthoudakis, S.; Zamboni, R. J.; Roy, S.; Nicholson, D. W. Involvement of caspases in proteolytic cleavage of Alzheimer's amyloid-beta precursor protein and amyloidogenic A beta peptide formation. *Cell* **1999**, *97* (3), 395−406.
(44) Saito, K.; Elce, J. S.; Hamos, J. E.; Nixon, R. A. Widespread activation of calcium-activated neutral proteinase (calpain) in the brain in Alzheimer disease: a potential molecular basis for neuronal degeneration. *Proc. Natl. Acad. Sci. U. S. A.* **1993**, *90* (7), 2628−32.
(45) Cataldo, A. M.; Nixon, R. A. Enzymatically active lysosomal proteases are associated with amyloid deposits in Alzheimer brain. *Proc. Natl. Acad. Sci. U. S. A.* **1990**, *87* (10), 3861−5.
(46) Casciola-Rosen, L.; Nicholson, D. W.; Chong, T.; Rowan, K. R.; Thornberry, N. A.; Miller, D. K.; Rosen, A. Apopain/CPP32 cleaves proteins that are essential for cellular repair: a fundamental principle of apoptotic death. *J. Exp. Med.* **1996**, *183* (5), 1957−64.
(47) Casciola-Rosen, L.; Andrade, F.; Ulanet, D.; Wong, W. B.; Rosen, A. Cleavage by granzyme B is strongly predictive of autoantigen status: implications for initiation of autoimmunity. *J. Exp. Med.* **1999**, *190* (6), 815−26.
(48) Casciola-Rosen, L.; Wigley, F.; Rosen, A. Scleroderma autoantigens are uniquely fragmented by metal-catalyzed oxidation reactions: implications for pathogenesis. *J. Exp. Med.* **1997**, *185* (1), 71−9.
(49) Lee, E. B.; Lee, V. M.; Trojanowski, J. Q. Gains or losses: molecular mechanisms of TDP43-mediated neurodegeneration. *Nat. Rev. Neurosci.* **2012**, *13* (1), 38−50.
(50) Yuan, J.; Yankner, B. A. Apoptosis in the nervous system. *Nature* **2000**, *407* (6805), 802−9.

Integrated Approaches for Analyzing U1-70K Cleavage in Alzheimer's disease

Bing Bai[*], Ping-Chung Chen[*], Chadwick M. Hales[#], Zhiping Wu[*], Vishwajeeth Pagala[%], Anthony A. High[%], Allan I. Levey[#], James J. Lah[#], and Junmin Peng[*, %, &]

Supporting Information:

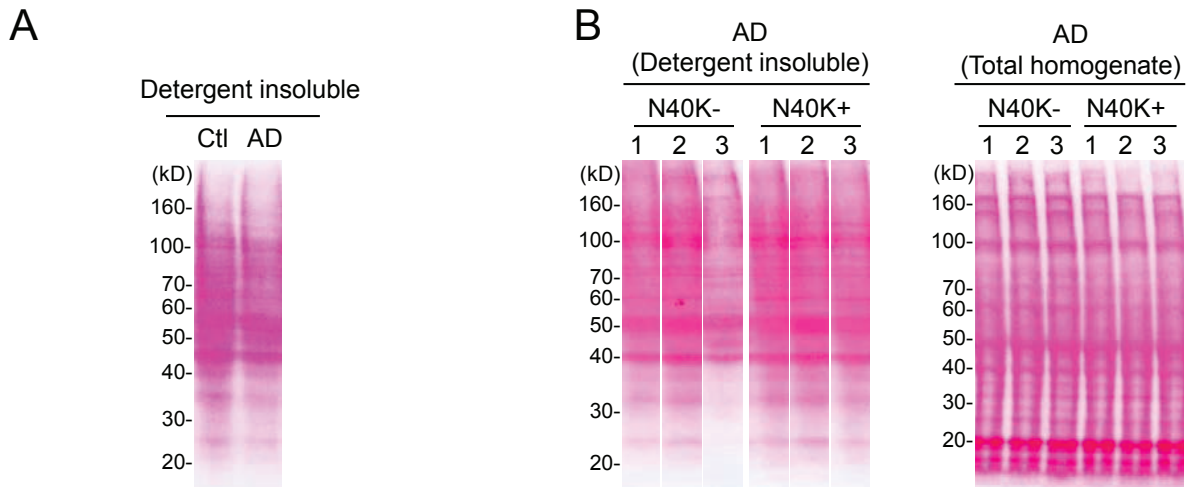

Ponceau S staining for figure 1B

Ponceau S staining for figure 1D

Figure S1. Protein loading on Western blots shown by Ponceau S staining.

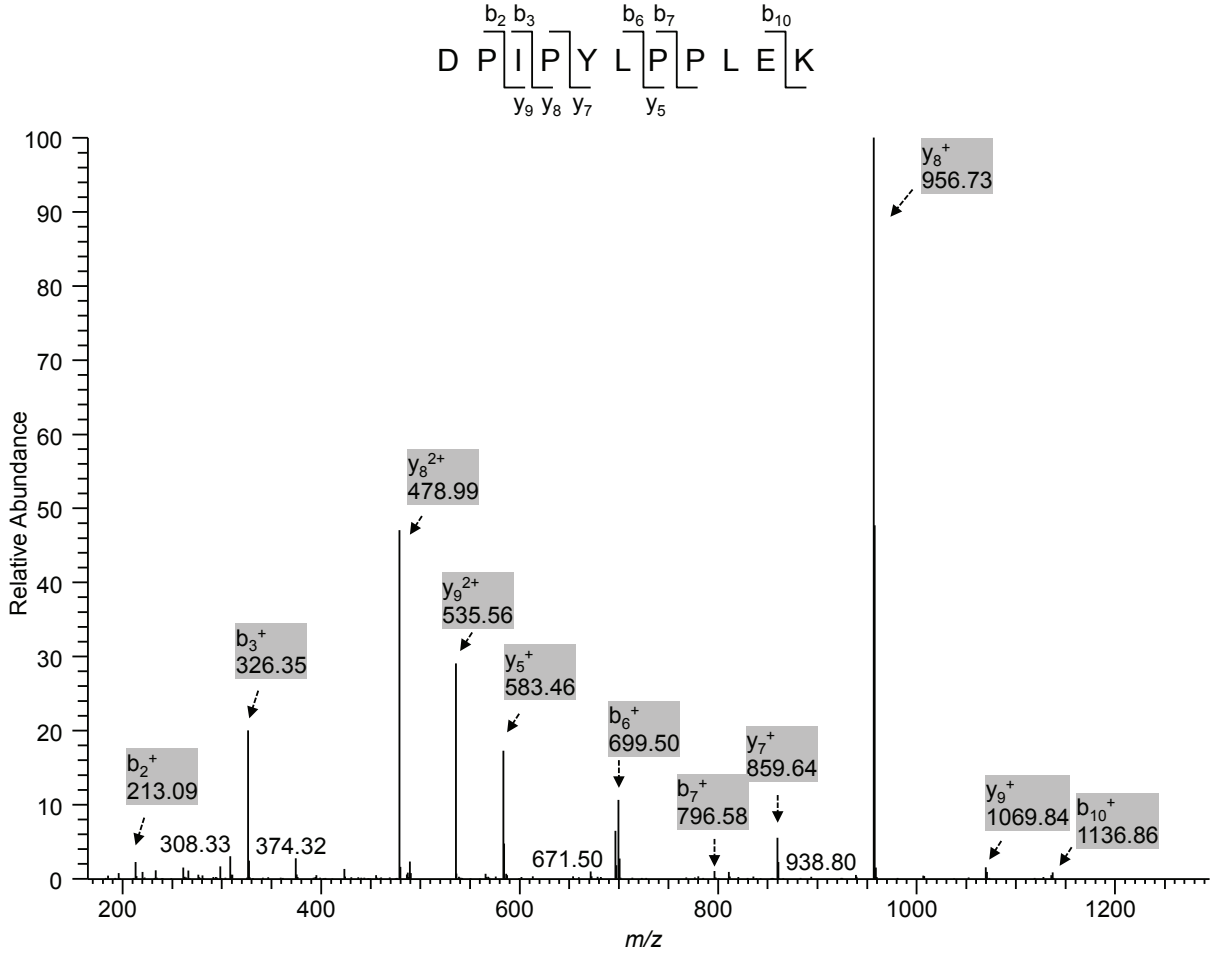

Figure S2. MS/MS spectrum from recombinant U1-70K.

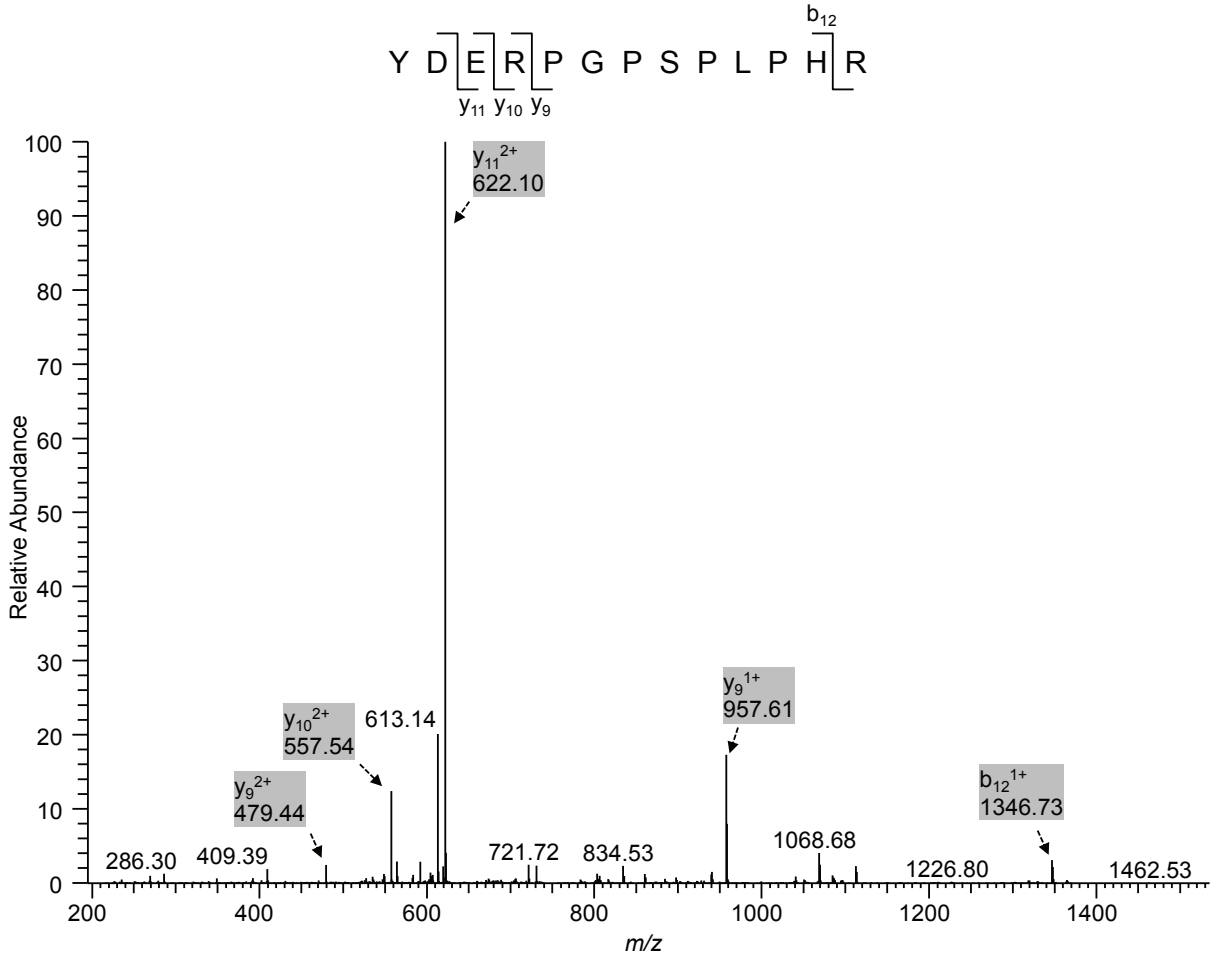

Figure S3.MS/MS spectrum from recombinant U1-70K.

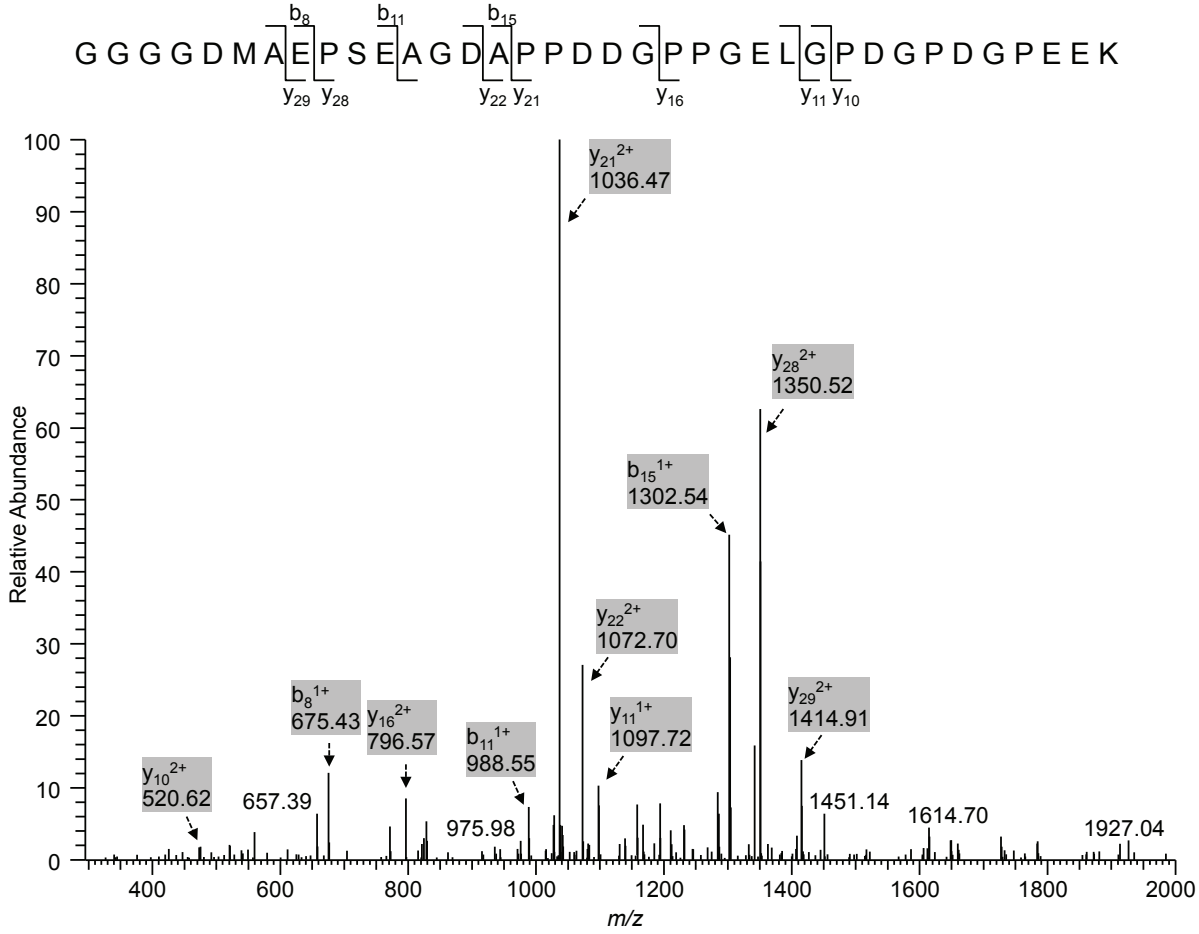

Figure S4. MS/MS spectrum from recombinant U1-70K.

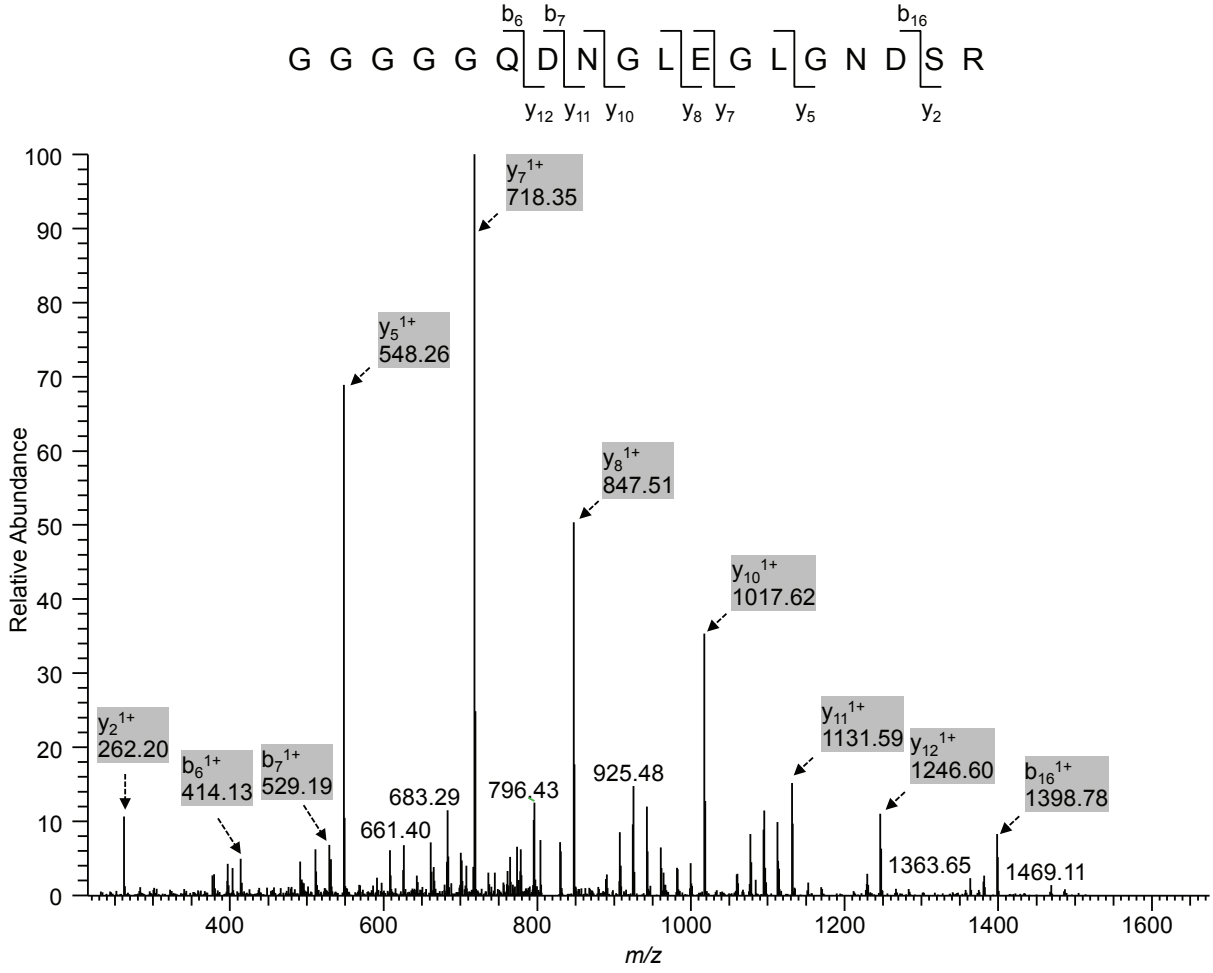

Figure S5. MS/MS spectrum from recombinant U1-70K.

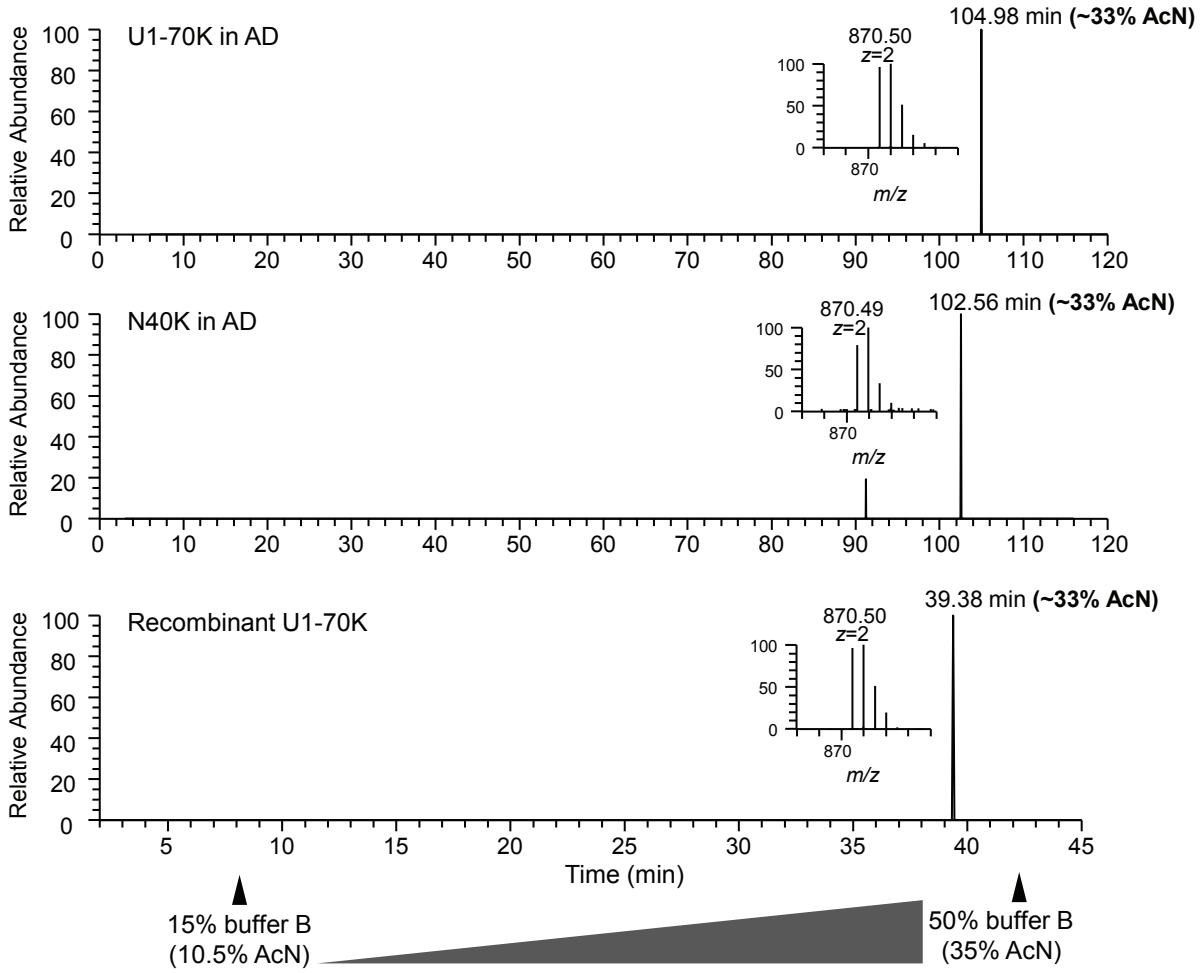

Figure S6. Retention times of the N-terminal peptide during LC-MS/MS analysis of three samples: AD U1-70K, AD N40K and recombinant U1-70K. The AD samples were eluted in a 100 min gradient and the recombinant protein was analyzed in a 35 min gradient. The N-terminal peptide was eluted at the same concentration of acetonitrile (~33% AcN). The isotopic patterns of the peptide in the three runs were similar as well (inserted images).

Table S1: Demographic information of patients in this study

	Sample number	Case Number	PMI (hr)[1]	Age of Onset	Age at Death	Duration (yr)[2]	ApoE Status[3]	Race[4]/Sex[5]
Control		OS00-23	11		68		E3/3	wf
AD (N40K-)	1	E04-68	4	69	85	16	E3/4	wf
	2	E05-179	10	57	67	10	E4/4	wm
	3	E06-37	5.5	57	66	9	E4/4	wm
	4	OS00-11	4	49	55	6	E3/3	wm
	5	OS03-163	4.5	<52	55	>3	E3/4	wf
	6	E05-04	4.5	52	64	12	E3/4	wf
	7	E05-194	15	69	71	2	E3/4	wm
	8	E05-56	17	63	71	8	E3/4	wm
AD (N40K+)	1	OS01-02	5.5	~48	69	~21	E4/4	wf
	2	OS03-66	12	69	81	12	E3/4	wf
	3	E04-33	20	50	57	7	E3/4	bf
	4	OS00-28	7.5	68	72	4	E3/4	bf
	5	E04-49	4.5	60	70	10	E4/4	bf
	6	E05-132	12.5	52	58	6	E3/3	wm
	7	E06-15	13.5	67	72	5	E3/4	wm
	8	E05-195	21	64	76	12	E2/3	wf
	9	E05-67	11.5	52	62	10	E3/4	wm

[1]Postmortem interval; [2]Duration of disease from diagnosis to death; [3]ApoE genotype; [4]Race: w (white/Caucasian), b (black/African American), a (Asian), h (Hispanic), and n (not available); [5]Sex: m (male), f (female), and n (not available).

Chapter 4:
GENERAL DISCUSSION AND FUTURE DIRECTIONS

1. Summary of the dissertation work

This study was initiated in ~2007 by Drs James Lah, Allan Levey and Junmin Peng, and involved 8 different case categories: AD (Alzheimer's disease), MCI (mild cognitive impairment), DLB (Dementia with Lewy bodies), FTLD-U (frontotemporal dementia with ubiquitin positive), CBD (corticobasal dementia), PD (Parkinson's disease), ALS (amyloid lateral sclerosis) and non-demented controls. It attempted to discover novel proteins that can potentially be involved in AD pathogenesis, because of the fact that Aβ, Tau and some other proteins or pathways fail to provide sufficient rationale for fully understanding of AD.

From the brain insoluble proteome where the Aβ and Tau were historically identified, 4,216 proteins were identified using label-free quantitative analysis by mass spectrometry, and 36 among them showed significant enrichment in AD compared to controls cases, including Aβ, Tau, ApoE, complement C3 as commonly known, validating the accuracy of the whole proteomic analysis.

In addition, several novel proteins were also identified in the enrichment list, including U1-70K, U1A and DDX46. All three belong to RNA splicing factors with U1-70K and U1A from the same spliceosomal complex U1. This is particularly interesting because during that time, TDP-43, also a RNA binding protein, has been just demonstrated to be the major component in the aggregates of brains with two neurodegenerative diseases, FTLD-U (frontotemporal lobe dementia with ubiquitin positive) and ALS (amyloid lateral sclerosis)(2), and its causal role was quickly supported by genetic evidence in familial cases(3-6). According to the discovery of TDP-43, it was very reasonable to determine whether the three RNA splicing factors is similarly play involved in AD pathogenesis. Therefore, my dissertational work is to validate the U1 spliceosomal pathology and to examine the consequential effect on RNA splicing.

I first made three different polyclonal antibodies in rabbit that target N-terminal, middle, and C-terminal regions of U1-70K, and validated their specificity using HEK cells overexpressing C-terminally tagged U1-70K. The antibodies for U1A and other proteins were purchased from commercial vendors

as they are less frequently used in this study. All these antibodies were validated using the similar approach.

With the specific antibodies, I western-blotted the insoluble U1-70K and U1A in the insoluble extraction from all cases recruited in the initial MS analysis. As expected, U1-70K is remarkably increased in almost all AD cases, but not in any other disease cases. Intriguingly, it is also elevated in MCI cases, often considered the early stage of AD. The wide-spread, highly specific, early-occurring U1-70K alteration strongly suggests its possible causative role.

My colleagues, Howard Rees and Chadwick Hales, performed immunohistochemical staining of the brain cortex slides and revealed tangle-like structures in the cytoplasm of neurons in AD in a manner consistent to the Western blot results. Those structures co-localize well with Tau tangles. Similar tangle-like structures were also found on other U1 spliceosomal components in AD.

U1 complex is one of the five major spliceosomes essentially exerting RNA splicing in mammalian cells. Loss-of-function of U1 complex by knocking out U1-70K in drosophila is embryonically lethal. It is, therefore, very reasonable to think U1 dysfunction is involved in AD pathogenesis as a novel mechanism. In this study, I focused on the possible RNA splicing deficiency as a consequential effect of U1 dysfunction, and my colleagues, Ping-Chung Chen, mainly engaged in establishing a mouse models to study the potential dementia phenotype upon U1 disruption.

I used RNA-seq to examine whether RNA splicing is affected in AD. Two batches of RNA with different quality and RNA-seq protocol were done. Three analyses were performed to evaluate the splicing function, including pre-RNA accumulation (normalized exon-to-intron ratio for each gene), exon junction alteration and PCPA (premature cleavage and polyadenylation, occurs when U1 spliceosomal function is inhibited). All showed positive results that supported RNA splicing deficiency in AD. Two different batches of experiments showed consistent results.

Besides U1-70K aggregation, I also observed that U1-70K appeared to have a fragment in the ~40 kDa region in addition to its full-length region about ~70kD.

This fragment was then validated by western blot using an N-terminal antibody. We then named if as N40K. As protein proteolytic cleavage is common in brains with neurodegenerative diseases and the fragments are often toxic to neurons. Therefore, we sought to determine if N40K is similarly toxic to neurons.

I first found N40K was present in more than 50% AD cases and was not likely a product from global sample degradation due to delayed brain preservation at room temperature. Interestingly, N40K-positive brains demonstrated reduced level of full-length U1-70K, suggesting a proteolytic event of U1-70K. Then, I analyzed the N40K both N- and C-terminus using mass spectrometric and biochemical approaches. After that, I made serial recombinant N40K proteins accordingly. Expression of these proteins in cultured rat primary hippocampal neurons caused neuronal death, suggesting the potential toxic effect of N40K.

In summary, this dissertation work utilized comprehensive proteome and transcriptome analyses to thoroughly study the U1 spliceosomal alteration and RNA splicing efficiency in AD, and integrated approaches for analyzing U1-70K cleavage event. It introduces U1 spliceosomal alteration and RNA splicing deficiency as potentially novel mechanisms in AD (Figure 4.1).

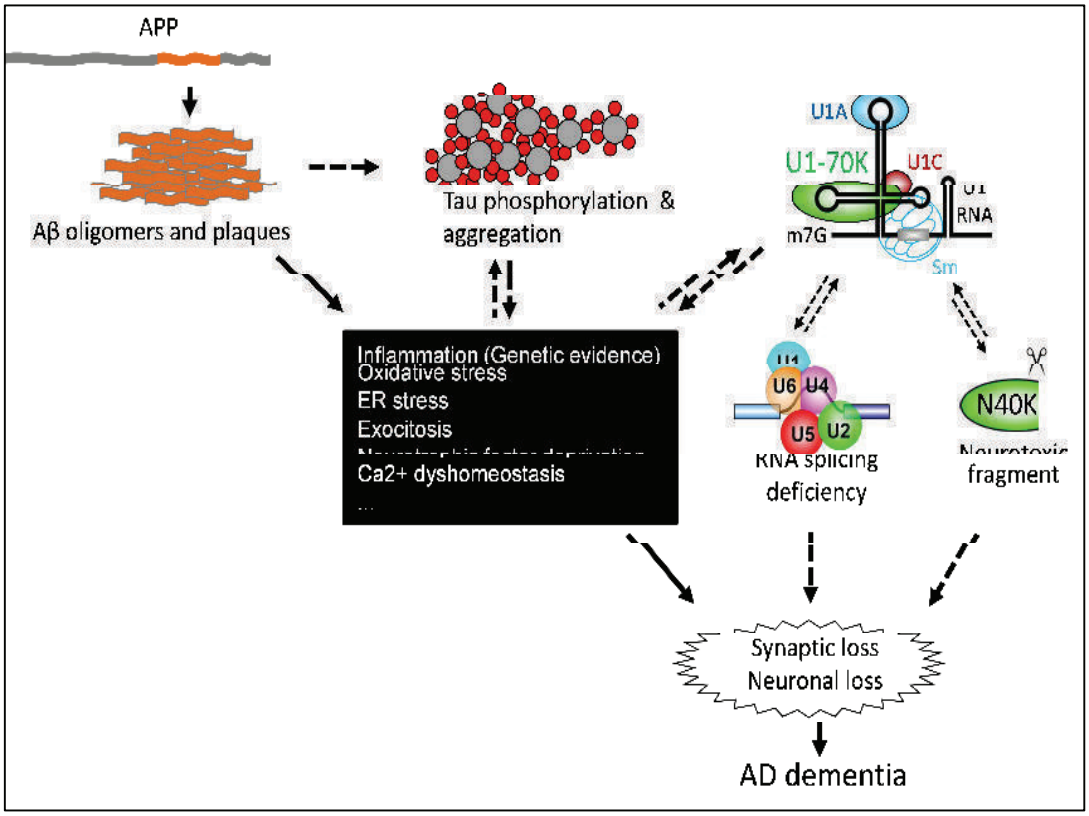

Figure 4.1 Summary of the dissertation study. Stress conditions in the black box may the conditions that cause U1 mislocalization and tangle-formation. This U1 alteration is co-existing with but independent of tau tangle formation. The defective RNA splicing is probably the consequence of dysfunctional U1, and might contribute to AD neuronal degeneration. Meanwhile, U1-70K can be cleaved into the neurotoxic fragment N40K, imposing extra neuronal insult. Based on the fact that U1 alteration is widespread, disease-specific, early-occurring and concomitant with dysfunctional events in AD, it can be speculated to a potentially causative player in AD.

2. Future directions

2.1. To determine if U1-70K can be causally involved in AD

The major concern in the field about the U1 pathology is about its causative role in AD pathogenesis, because it could be just a phenomenon of neuronal death in the end stage. This can be addressed by looking at neurons to see whether death is triggered when they bear U1 pathology. I noticed that the neurons with U1 alteration still show normal-looking nuclei as visualized by the DNA binding dye "DAPI". To further address this concern, I can first co-stain some death makers with U1-70K. These include TUNEL to see DNA fragmentation, Cytochrome C to see mitochondrial integrity and cleaved caspase-3 to see apoptosis. Markers of oxidative stress, ER stress and others can also be used to see the functional status of these subcellular organisms or pathways. Neuronal viability can also be assessed by morphology of dendrites and expression of functional proteins like GluR, synatophysin, SV2, etc. The ultrastructure of neurons can provide definitive conclusions about the intracellular status of a neuron. Neurons bearing U1-70K pathology are expected to be at early stage of death.

If the U1 spliceosome pathology is a unique cellular event without involving other nuclear proteins, then it can speculated that a particular upstream pathway is disrupted and the RNA splicing is disrupted specifically. This will be easier for therapeutic intervention. It is shown in this thesis that the other U1 components U1A and U1 snRNA can form similar tangle-like structures in AD neurons. Despite of the absence of similar pathology in this study, some RNA binding proteins proteins do appear in cytoplasmic aggregations in certain neurodegenerative disorders. TDP-43 is known to be able to form cytoplasmic inclusion in frontotemporal dementia and ALS(2). Both hnRNPA2B1 and hnRNPA1 can also do the same in multisystem proteinopathy and ALS (8). In addition, hnRNP A/B is reduced in neurons in AD (9). Co-immunostaining of these proteins each with U1-70K in the same neuron will provide not only more confidence in the specificity of U1 alteration in AD, but also mechanistic clues to U1 dysregulation.

If U1-70K pathology is only present in AD specifically, but not in the most affected brain regions of other neurodegenerative diseases, then it can be suspected to be an initiator of neuronal degeneration. Otherwise, it is either a general dysregulation in the end stage of neuronal death, or involved in a common neuronal death pathway. Either outcome will provide useful information for better understanding of the mechanism of these neurodegenerative disorders.

If U1-70K pathology is a causal event, it is supposed to occur in the early affected brain regions. U1-70K pathology is largely overlapped with Tau tangles in the frontal cortex (10). Tau tangles usually start in the transentorhinal region and then spread diffusively to the adjacent medial temporal lobe including perirhinal, parahippocampal, and entorhinal neocortex and hippocampus, etc. This progression correlates well with AD dementia progression. We already showed that U1-70K can form tangle-like structure in the hippocampus in one AD case. Thorough analysis of the surrounding regions in more cases is required. If U1-70K pathology occurs early in these regions, then there is much higher possibility that it is casually involved in AD neurodeneration.

I observed that in some neurons U1-70K shows mislocalization but Tau phosphorylation or tangles are absent (Figure 4.2 A), indicating U1-70K alteration may be even earlier than Tau phosphorylation. If this is largely present in the transentorhinal region at early stage of dementia, then we can trace nearer to the initial pathway disruption that triggers neuronal death.

In order to determine whether the altered RNA splicing plays a causative role in AD pathogenesis, it is critical to demonstrate that genes identified with significant splicing alterations have neuronal toxicity. Altered RNA splicing may be causally involved in neurodegenerative disorders. For example, certain mutations on Tau cause the splice isoforms biased to the exon 10-including transcript which is more toxic, which is the etiological mechanism of frontotemporal dementia and parkinsonism linked to chromosome 17 (11). Some genes have been reported to have aberrant RNA splicing in AD such as presenilin-2 with exon-5 skipping (12, 13) and EAAT2 with exon 7 and 9 skipping (14). Although these aberrant splice events are not detected because of

insufficient reading depth, the RNA-seq data show abnormal splicing of other genes. More thorough analyses are required to provide the final list of these genes, and publications of their involvement in AD will be extensively searched. A neuronal culture system can be employed to examine their possible neurotoxic effect.

It is necessary to examine the pre-RNA and splicing alterations in neurons with mislocalized U1-70K by in-situ RNA hybridization. In this thesis, both U1 pathology and RNA splicing deficiency were demonstrated in AD. However, to provide more evidence to link these two directly, it is better to show U1 cytoplasmic aggregation and the nuclear accumulation of pre-RNA in the same neuron by in situ RNA hybridization using both U1 snRNA and intron-exon junction specific fluorescent probes. This method can also be used to validate the aberrant splice events indicated in the RNA-seq data, in order to strengthen the direct link between them and the U1 alteration.

It would be very convincing if the AD-specific splicing alterations can be induced by U1 spliceosomal inhibition. The causal connection of U1 pathology to aberrant splice events can be determined in a cell culture system by reducing the U1 spliceosomal function by siRNA mediated knockdown of U1-70K or by morpholino antisense oligomer induced inhibition of U1 snRNA in human neuronal cell line SH-SY5Y or rat primary hippocampal neurons, to see those splicing alterations can be recapitulated. This would facilitate in our understanding of whether U1 pathology and splicing alteration are causally related or just independently co-existing in AD brains.

It is necessary to study of potential involvement of U1 snRNP in Aβ-Tau axis. We have already shown that U1 dysfunction by U1-70K knockdown or U1 snRNA inhibition causes increased production of Aβ (10). This indicates U1-70K might contribute to the regulation of Aβ generation. However, to strengthen this, it would be necessary to show increased intracellular Aβ or plaques surrounding the neurons that bear tangle-like structures or mislocalization of U1-70K, or its nuclear reduction in AD, compared to nondemented healthy controls.

We also looked whether Aβ plaques are the insult that induces the U1 alteration. Immunostaining of U1-70K in the brain of APP transgenic mice that

bear heavy load of Aβ plaques shows no aggregation, mislocation, or any difference from the wildtype controls, suggesting that Aβ accumulation and aggregation cannot cause U1 pathology directly.

It is also interesting to examine the relationship between U1 and Tau dysregulation. It was already shown in this study that U1-70K pathology is not likely the result of Tau aggregation because of its absence in corticobasal dementia and frontotemporal dementia diseases which have plenty of Tau phosphorylation and aggregation. As U1-70K and Tau are largely overlapped in the AD brain cortex, it probably indicates that they share the same upstream regulating protein or pathway. However, U1-70K depletion from the nuclei and redistribution to the cytoplasm can be present in the absence of Tau aggregation (Figure 4.2 A), suggesting it might be an earlier event than Tau dysregulation. Besides, the amount of Tau phosphorylation in the insoluble fraction is correlated to the reduced amount of U1-70K low salt fraction (Figure 4.2 B, C). Moreover, in the U1-70K knockdown cells, the Tau phosphorylation kinase GSK-3β is increased and appears with an extra isoform (Figure 4.2 D). These results indicate that reduced protein level of U1-70K might have a promoting effect on Tau phosphorylation and aggregation in AD.

However, when U1-70K is knocked down, human Tau shows decreased phosphorylation (Figure 4.2 E), suggesting that U1-70K pathology and Tau phosphorylation might be separate events in AD. Because U1-70K can also interact with GSK-3β (15), it is possible that U1 and Tau are both regulated by the same upstream pathway. However, a neuronal culture system should be applied to further clarify the relationship between U1-70K knockdown and Tau phosphorylation.

The Tau splice isoform that includes exon 10 is more toxic to neurons and it is causally involved in frontotemporal dementia and parkinsonism linked to chromosome 17 (FTDP-17) (11, 16, 17). However, U1-70K knockdown showed no effect on Tau splicing (Figure 4.3 A-F). This negative result is consistent with the fact that Tau has no splicing alteration in AD (16, 18, 19).

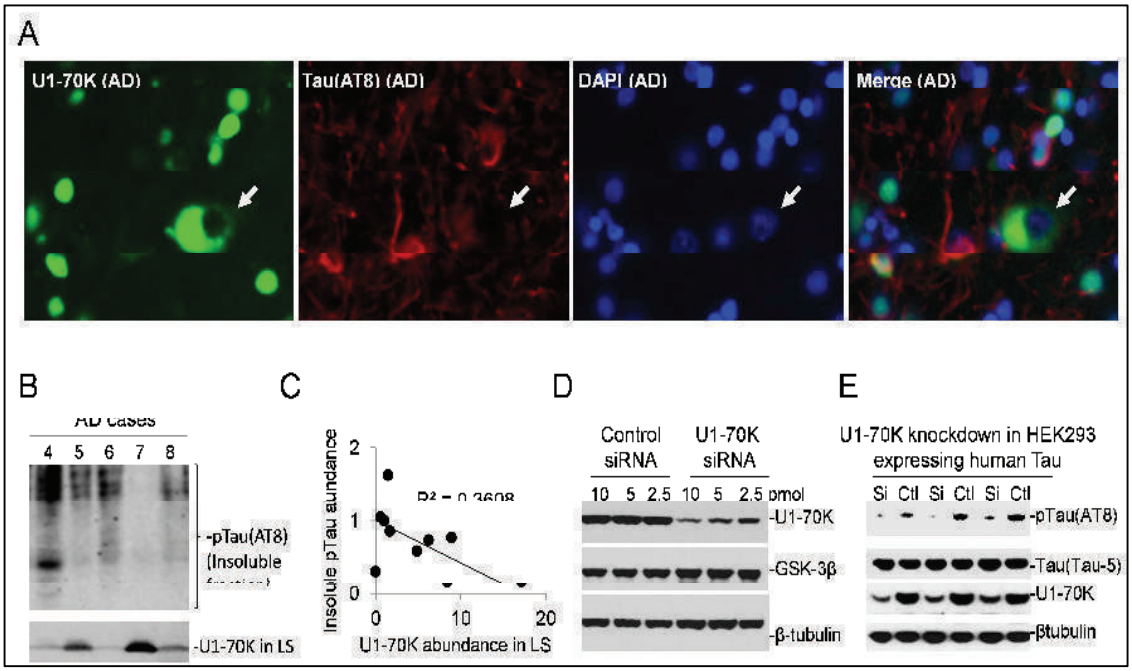

Figure 4.2 Correlation of insoluble Tau and U1-70K in AD and effect of U1-70K knockdown on Tau phosphorylation. A) U1-70K mislocalization can be earlier than Tau phosphorylation. Co-immunostaining of U1-70K and Tau in the cortex of a AD postmortem brain. B) AD with lower U1-70K in the low salt fraction (LS) demonstrates more hyperphosphorylation and aggregation of Tau. C) Correlation of U1-70K in LS with phosphorylated Tau in the insoluble fraction. D) Knockdown of U1-70K causes increased amount of GSK-3β and an extra form. E) Knockdown of U1-70K results in reduced Tau phosphorylation. Tau is cloned from the human neuronal cell line SH-SY5Y.

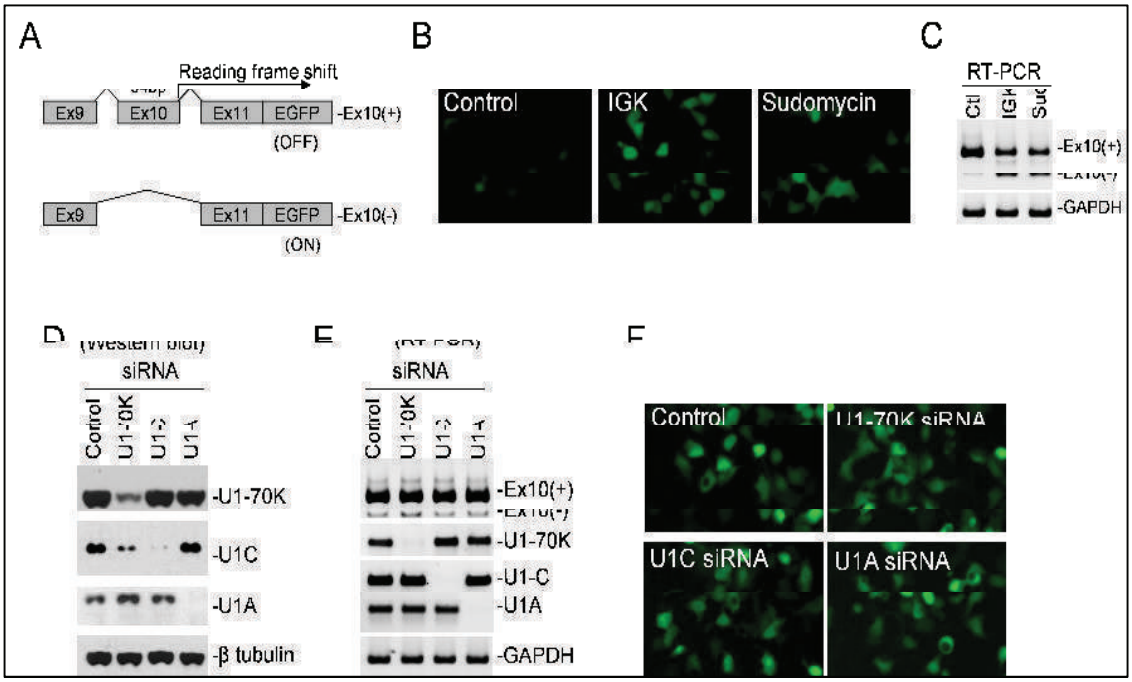

Figure 4.3 Effect of U1-70K knockdown on Tau splicing. A) In the Tau splicing reporter design, exon 10 (Ex10) has 94bp instead of 93bp (endogenous), causing a downstream framing shift when included. Therefore, when Ex10 is included, then no EGFP expression occurs due to reading frame shift. In contrast, EGFP will start to express when Tau Ex10 is skipped due to no reading frame shift. B) GFP expression before harvesting for RT-PCR in C). C) RT-PCR to show Ex10 skipping of the Tau splicing reporter under RNA splicing inhibition (IGK, Isoginikgetin, 33uM; Sud, Sudomycin, 2uM; 6h after knockdown). C) GFP expression before harvesting for RT-PCR in B). D) Western blotting to demonstrate successful knockdown of U1 components. E) RT-PCR to show Tau minigene splicing isoforms. F) No obvious GFP expression in the EHK293 cells before harvesteding for RT-PCR in and E).

2.2. To study the mechanism of U1-70K pathology

As mentioned before, U1 pathology mainly includes the formation of tangle-like structures and the mislocalization to perinuclear distribution. Presence of U1-70K tangle-like structures is occurs only when Tau tangles exist in the cell and is always overlapping with Tau, while U1-70K mislocalization in a neuron without a Tau tangle. This implies U1 mislocalization is the early stage of the formation of tangle-like structure. Thus, mechanistic studies should focus on the mislocalization.

Redistribution of U1 in the cytoplasm can be the result of two possible events: one is the interrupted translocation of newly synthesized protein from ER-Golgi system to the nuclei, and the other is its translocation from nuclei. The studies will be designed accordingly to address these possibilities.

ER stress might be the reason for U1 mislocalization. U1-70K is first synthesized in the ER and then transported to the nuclei for the assembly of a mature spliceosome (20). The distribution pattern of U1 in the cytoplasm looks like the shape of ER in cortical neurons (21). ER is known to be under stress even before the Tau tangle formation (22). Besides, the small GTPase Rab6, which is responsible for retrograde Golgi–ER trafficking for possible protein post-ER quality control, has a similar overlapping pattern with Tau in the temporal cortex of AD brains (23). Therefore, it is highly likely that this perinuclear distribution is caused by ER dysfunction. Therefore, it will be necessary to perform co-immunostaining of Rab6 (23), ER marker Calnexin (21), Golgi marker TGN-38 (21), mitochondria marker COX I (24), late endosomal marker LAMP2 (25) each together with U1-70K on AD cortical and hippocampal slides.

U1 mislocalization might be underlined by activated cell cycle reentry. The U1 cytoplasmic distribution could be a result of activation of cell cycle reentry. It is known that U1 proteins moves out of nuclei during mitosis (26). In this study, the U1 redistribution that surrounds nuclei in the cytoplasm looks very similar to the pattern of a transcription factor Sp1 during prometaphase of mitosis (27). There is already ample evidence of cell cycle reentry in AD brain neurons (28-31). It is very likely that U1 depletion from nuclei is a reflection of initiated mitosis. Tau

can be phosphorylated during mitosis (32, 33). Therefore, the co-existent aggregation of both Tau and U1 may reflect the reentry of neuronal cell cycle. To test whether this is true, the mitosis markers such as Ki-67, PCNA, cyclines, CDKs can be used to be co-immunostained with U1-70K and Tau in the AD brain neurons, to see if the cell cycle reentry event co-exists with the pathology of U1 or Tau in the same neuron.

The insoluble form of U1-70K might be due to abnormal modification. The major modification of U1-70K that has been intensely studied is phosphorylation. It will be phosphorylated during cellular apoptosis (34), cell cycle (35) and RNA splicing (36). Because AD neurons with U1 tangle-like structure are probably undergoing cell cycle progression and apoptosis, the cytoplasmic U1-70K is probably phosphorylated, or added with other modifications. This can be determined by measuring the protein intact mass of purified U1-70K using mass spectrometry. U1-70K in the insoluble fraction is expected to have a different mass spectrum as compared to U1-70K in the soluble fraction using non-demented healthy individuals as controls. The suspected modifications can be further analyzed by both MS and biochemical approaches.

U1-70K interactome study might be the essential approach for discovering critical clues to its pathological change. There are about 99 interacting proteins of U1-70K that have been identified so far according to BioGRID (http://thebiogrid.org/112509). The unique cytoplasmic distribution of U1-70K in AD should be regulated by proteins that are very likely still associated with it.The interactome of U1-70K in AD is certainly different from that in non-demented healthy brains. Using specific antibody with high binding affinity to co-immuoprecipitate U1-70K and identify associated proteins by LC-MS/MS can probably reveal mechanistic proteins for understanding of U1 mislocalization and potentially aggregation.

REFERENCES

1. Ross CA & Poirier MA (2004) Protein aggregation and neurodegenerative disease. *Nat Med* 10 Suppl:S10-17.
2. Forno LS (1996) Neuropathology of Parkinson's disease. *Journal of neuropathology and experimental neurology* 55(3):259-272.
3. Ross CA & Tabrizi SJ (2011) Huntington's disease: from molecular pathogenesis to clinical treatment. *Lancet neurology* 10(1):83-98.
4. Kuemmerle S*, et al.* (1999) Huntington aggregates may not predict neuronal death in Huntington's disease. *Annals of neurology* 46(6):842-849.
5. Cleveland DW & Rothstein JD (2001) From Charcot to Lou Gehrig: deciphering selective motor neuron death in ALS. *Nature reviews. Neuroscience* 2(11):806-819.
6. Neumann M*, et al.* (2006) Ubiquitinated TDP-43 in frontotemporal lobar degeneration and amyotrophic lateral sclerosis. *Science* 314(5796):130-133.
7. Sreedharan J*, et al.* (2008) TDP-43 mutations in familial and sporadic amyotrophic lateral sclerosis. *Science* 319(5870):1668-1672.
8. Prusiner SB (2001) Shattuck lecture--neurodegenerative diseases and prions. *The New England journal of medicine* 344(20):1516-1526.
9. Rumble B*, et al.* (1989) Amyloid A4 protein and its precursor in Down's syndrome and Alzheimer's disease. *The New England journal of medicine* 320(22):1446-1452.
10. Singleton AB*, et al.* (2003) alpha-Synuclein locus triplication causes Parkinson's disease. *Science* 302(5646):841.
11. Conway KA, Rochet JC, Bieganski RM, & Lansbury PT, Jr. (2001) Kinetic stabilization of the alpha-synuclein protofibril by a dopamine-alpha-synuclein adduct. *Science* 294(5545):1346-1349.
12. Ballatore C, Lee VM, & Trojanowski JQ (2007) Tau-mediated neurodegeneration in Alzheimer's disease and related disorders. *Nature reviews. Neuroscience* 8(9):663-672.
13. Poirier MA*, et al.* (2002) Huntingtin spheroids and protofibrils as precursors in polyglutamine fibrilization. *The Journal of biological chemistry* 277(43):41032-41037.
14. Goedert M & Spillantini MG (2006) A century of Alzheimer's disease. *Science* 314(5800):777-781.
15. Roberson ED & Mucke L (2006) 100 years and counting: prospects for defeating Alzheimer's disease. *Science* 314(5800):781-784.
16. Dubois B*, et al.* (2010) Revising the definition of Alzheimer's disease: a new lexicon. *Lancet neurology* 9(11):1118-1127.

17. Forstl H & Kurz A (1999) Clinical features of Alzheimer's disease. *European archives of psychiatry and clinical neuroscience* 249(6):288-290.

18. McKhann G*, et al.* (1984) Clinical diagnosis of Alzheimer's disease: report of the NINCDS-ADRDA Work Group under the auspices of Department of Health and Human Services Task Force on Alzheimer's Disease. *Neurology* 34(7):939-944.

19. Thies W & Bleiler L (2013) 2013 Alzheimer's disease facts and figures. *Alzheimer's & dementia : the journal of the Alzheimer's Association* 9(2):208-245.

20. Hebert LE, Weuve J, Scherr PA, & Evans DA (2013) Alzheimer disease in the United States (2010-2050) estimated using the 2010 census. *Neurology* 80(19):1778-1783.

21. Reitz C, Brayne C, & Mayeux R (2011) Epidemiology of Alzheimer disease. *Nature reviews. Neurology* 7(3):137-152.

22. Holtzman DM, Mandelkow E, & Selkoe DJ (2012) Alzheimer disease in 2020. *Cold Spring Harb Perspect Med* 2(11).

23. Blennow K, de Leon MJ, & Zetterberg H (2006) Alzheimer's disease. *Lancet* 368(9533):387-403.

24. Braak H & Braak E (1991) Demonstration of amyloid deposits and neurofibrillary changes in whole brain sections. *Brain Pathol* 1(3):213-216.

25. Braak H & Braak E (1991) Neuropathological stageing of Alzheimer-related changes. *Acta neuropathologica* 82(4):239-259.

26. Perry G*, et al.* (2003) Oxidative damage in the olfactory system in Alzheimer's disease. *Acta neuropathologica* 106(6):552-556.

27. Jobst KA*, et al.* (1992) Detection in life of confirmed Alzheimer's disease using a simple measurement of medial temporal lobe atrophy by computed tomography. *Lancet* 340(8829):1179-1183.

28. Jobst KA*, et al.* (1994) Rapidly progressing atrophy of medial temporal lobe in Alzheimer's disease. *Lancet* 343(8901):829-830.

29. Bobinski M*, et al.* (1996) Neurofibrillary pathology--correlation with hippocampal formation atrophy in Alzheimer disease. *Neurobiology of aging* 17(6):909-919.

30. Jack CR*, et al.* (2008) Atrophy rates accelerate in amnestic mild cognitive impairment. *Neurology* 70(19):1740-1752.

31. Jack CR*, et al.* (2008) C-II PiB and structural MRI provide complementary information in imaging of Alzheimers disease and amnestic mild cognitive impairment. *Brain : a journal of neurology* 131:665-680.

32. Gomez-Isla T*, et al.* (1997) Neuronal loss correlates with but exceeds neurofibrillary tangles in Alzheimer's disease. *Annals of neurology* 41(1):17-24.

33. Gomez-Isla T*, et al.* (1996) Profound loss of layer II entorhinal cortex neurons occurs in very mild Alzheimer's disease. *The Journal of neuroscience : the official journal of the Society for Neuroscience* 16(14):4491-4500.

34. Whitehouse PJ*, et al.* (1982) Alzheimer's disease and senile dementia: loss of neurons in the basal forebrain. *Science* 215(4537):1237-1239.

35. Selkoe DJ (2002) Alzheimer's disease is a synaptic failure. *Science* 298(5594):789-791.

36. Davies CA, Mann DM, Sumpter PQ, & Yates PO (1987) A quantitative morphometric analysis of the neuronal and synaptic content of the frontal and temporal cortex in patients with Alzheimer's disease. *Journal of the neurological sciences* 78(2):151-164.

37. Scheff SW, DeKosky ST, & Price DA (1990) Quantitative assessment of cortical synaptic density in Alzheimer's disease. *Neurobiology of aging* 11(1):29-37.

38. Terry RD*, et al.* (1991) Physical basis of cognitive alterations in Alzheimer's disease: synapse loss is the major correlate of cognitive impairment. *Annals of neurology* 30(4):572-580.

39. DeKosky ST & Scheff SW (1990) Synapse loss in frontal cortex biopsies in Alzheimer's disease: correlation with cognitive severity. *Annals of neurology* 27(5):457-464.

40. Scheff SW, Price DA, Schmitt FA, & Mufson EJ (2006) Hippocampal synaptic loss in early Alzheimer's disease and mild cognitive impairment. *Neurobiology of aging* 27(10):1372-1384.

41. Arnold SE, Hyman BT, Flory J, Damasio AR, & Van Hoesen GW (1991) The topographical and neuroanatomical distribution of neurofibrillary tangles and neuritic plaques in the cerebral cortex of patients with Alzheimer's disease. *Cereb Cortex* 1(1):103-116.

42. Small DH, Mok SS, & Bornstein JC (2001) Alzheimer's disease and Abeta toxicity: from top to bottom. *Nature reviews. Neuroscience* 2(8):595-598.

43. Wisniewski HM, Merz PA, & Iqbal K (1984) Ultrastructure of paired helical filaments of Alzheimer's neurofibrillary tangle. *Journal of neuropathology and experimental neurology* 43(6):643-656.

44. Selkoe DJ, Ihara Y, & Salazar FJ (1982) Alzheimer's disease: insolubility of partially purified paired helical filaments in sodium dodecyl sulfate and urea. *Science* 215(4537):1243-1245.

45. Ksiezak-Reding H*, et al.* (1994) Ultrastructure and biochemical composition of paired helical filaments in corticobasal degeneration. *The American journal of pathology* 145(6):1496-1508.

46. Ohm TG, Muller H, Braak H, & Bohl J (1995) Close-meshed prevalence rates of different stages as a tool to uncover the rate of Alzheimer's disease-related neurofibrillary changes. *Neuroscience* 64(1):209-217.

47. Glenner GG & Wong CW (1984) Alzheimer's disease: initial report of the purification and characterization of a novel cerebrovascular amyloid protein. *Biochemical and biophysical research communications* 120(3):885-890.

48. Vassar R*, et al.* (1999) Beta-secretase cleavage of Alzheimer's amyloid precursor protein by the transmembrane aspartic protease BACE. *Science* 286(5440):735-741.

49. Yan R*, et al.* (1999) Membrane-anchored aspartyl protease with Alzheimer's disease beta-secretase activity. *Nature* 402(6761):533-537.

50. Haass C, Kaether C, Thinakaran G, & Sisodia S (2012) Trafficking and Proteolytic Processing of APP. *Cold Spring Harbor perspectives in medicine* 2(5).

51. Lammich S*, et al.* (1999) Constitutive and regulated alpha-secretase cleavage of Alzheimer's amyloid precursor protein by a disintegrin metalloprotease. *Proceedings of the National Academy of Sciences of the United States of America* 96(7):3922-3927.

52. Thinakaran G & Koo EH (2008) Amyloid precursor protein trafficking, processing, and function. *The Journal of biological chemistry* 283(44):29615-29619.

53. Mackenzie IR & Miller LA (1994) Senile plaques in temporal lobe epilepsy. *Acta neuropathologica* 87(5):504-510.

54. Ehehalt R, Keller P, Haass C, Thiele C, & Simons K (2003) Amyloidogenic processing of the Alzheimer beta-amyloid precursor protein depends on lipid rafts. *The Journal of cell biology* 160(1):113-123.

55. Cordy JM, Hussain I, Dingwall C, Hooper NM, & Turner AJ (2003) Exclusively targeting beta-secretase to lipid rafts by GPI-anchor addition up-regulates beta-site processing of the amyloid precursor protein. *Proceedings of the National Academy of Sciences of the United States of America* 100(20):11735-11740.

56. Cordy JM, Hooper NM, & Turner AJ (2006) The involvement of lipid rafts in Alzheimer's disease. *Mol Membr Biol* 23(1):111-122.

57. Bates KA*, et al.* (2009) Clearance mechanisms of Alzheimer's amyloid-beta peptide: implications for therapeutic design and diagnostic tests. *Mol Psychiatry* 14(5):469-486.

58. Kuperstein I*, et al.* (2010) Neurotoxicity of Alzheimer's disease Abeta peptides is induced by small changes in the Abeta42 to Abeta40 ratio. *EMBO J* 29(19):3408-3420.

59. Games D*, et al.* (1995) Alzheimer-type neuropathology in transgenic mice overexpressing V717F beta-amyloid precursor protein. *Nature* 373(6514):523-527.

60. Selkoe DJ (2011) Resolving controversies on the path to Alzheimer's therapeutics. *Nat Med* 17(9):1060-1065.

61. Shankar GM*, et al.* (2008) Amyloid-beta protein dimers isolated directly from Alzheimer's brains impair synaptic plasticity and memory. *Nat Med* 14(8):837-842.

62. Cleary JP*, et al.* (2005) Natural oligomers of the amyloid-beta protein specifically disrupt cognitive function. *Nat Neurosci* 8(1):79-84.

63. Walsh DM & Selkoe DJ (2007) A beta oligomers - a decade of discovery. *J Neurochem* 101(5):1172-1184.

64. Cavallucci V, D'Amelio M, & Cecconi F (2012) Abeta toxicity in Alzheimer's disease. *Mol Neurobiol* 45(2):366-378.

65. Manczak M*, et al.* (2006) Mitochondria are a direct site of A beta accumulation in Alzheimer's disease neurons: implications for free radical generation and oxidative damage in disease progression. *Human molecular genetics* 15(9):1437-1449.

66. Goedert M, Spillantini MG, Jakes R, Rutherford D, & Crowther RA (1989) Multiple Isoforms of Human Microtubule-Associated Protein-Tau - Sequences and Localization in Neurofibrillary Tangles of Alzheimers-Disease. *Neuron* 3(4):519-526.

67. Grundkeiqbal I*, et al.* (1986) Microtubule-Associated Protein-Tau - a Component of Alzheimer Paired Helical Filaments. *Journal of Biological Chemistry* 261(13):6084-6089.

68. Kosik KS, Joachim CL, & Selkoe DJ (1986) Microtubule-Associated Protein Tau (Tau) Is a Major Antigenic Component of Paired Helical Filaments in Alzheimer-Disease. *Proceedings of the National Academy of Sciences of the United States of America* 83(11):4044-4048.

69. Grundkeiqbal I*, et al.* (1986) Abnormal Phosphorylation of the Microtubule-Associated Protein-Tau (Tau) in Alzheimer Cytoskeletal Pathology. *Proceedings of the National Academy of Sciences of the United States of America* 83(13):4913-4917.

70. Ballatore C, Lee VMY, & Trojanowski JQ (2007) Tau-mediated neurodegeneration in Alzheimer's disease and related disorders. *Nature Reviews Neuroscience* 8(9):663-672.

71. Santacruz K*, et al.* (2005) Tau suppression in a neurodegenerative mouse model improves memory function. *Science* 309(5733):476-481.

72. Gotz J, Ittner LM, & Kins S (2006) Do axonal defects in tau and amyloid precursor protein transgenic animals model axonopathy in Alzheimer's disease? *Journal of neurochemistry* 98(4):993-1006.

73. Ittner LM, Ke YD, & Gotz J (2009) Phosphorylated Tau interacts with c-Jun N-terminal kinase-interacting protein 1 (JIP1) in Alzheimer disease. *The Journal of biological chemistry* 284(31):20909-20916.

74. Rapoport M, Dawson HN, Binder LI, Vitek MP, & Ferreira A (2002) Tau is essential to beta -amyloid-induced neurotoxicity. *Proceedings of the National Academy of Sciences of the United States of America* 99(9):6364-6369.

75. Roberson ED*, et al.* (2007) Reducing endogenous tau ameliorates amyloid beta-induced deficits in an Alzheimer's disease mouse model. *Science* 316(5825):750-754.

76. Ittner LM*, et al.* (2010) Dendritic function of tau mediates amyloid-beta toxicity in Alzheimer's disease mouse models. *Cell* 142(3):387-397.

77. McGeer PL & McGeer EG (1995) The inflammatory response system of brain: implications for therapy of Alzheimer and other neurodegenerative diseases. *Brain research. Brain research reviews* 21(2):195-218.

78. Eikelenboom P & Stam FC (1982) Immunoglobulins and complement factors in senile plaques. An immunoperoxidase study. *Acta neuropathologica* 57(2-3):239-242.

79. Bai B*, et al.* (2013) U1 small nuclear ribonucleoprotein complex and RNA splicing alterations in Alzheimer's disease. *Proceedings of the National Academy of Sciences of the United States of America*.

80. Itagaki S, Akiyama H, Saito H, & McGeer PL (1994) Ultrastructural localization of complement membrane attack complex (MAC)-like immunoreactivity in brains of patients with Alzheimer's disease. *Brain research* 645(1-2):78-84.

81. Haga S, Akai K, & Ishii T (1989) Demonstration of microglial cells in and around senile (neuritic) plaques in the Alzheimer brain. An immunohistochemical study using a novel monoclonal antibody. *Acta neuropathologica* 77(6):569-575.

82. Vehmas AK, Kawas CH, Stewart WF, & Troncoso JC (2003) Immune reactive cells in senile plaques and cognitive decline in Alzheimer's disease. *Neurobiology of aging* 24(2):321-331.

83. Akiyama H*, et al.* (2000) Inflammation and Alzheimer's disease. *Neurobiology of aging* 21(3):383-421.

84. Akiyama H*, et al.* (2000) Cell mediators of inflammation in the Alzheimer disease brain. *Alzheimer disease and associated disorders* 14 Suppl 1:S47-53.

85. Wyss-Coray T*, et al.* (2003) Adult mouse astrocytes degrade amyloid-beta in vitro and in situ. *Nature medicine* 9(4):453-457.

86. Cartier L, Hartley O, Dubois-Dauphin M, & Krause KH (2005) Chemokine receptors in the central nervous system: role in brain inflammation and neurodegenerative diseases. *Brain research. Brain research reviews* 48(1):16-42.

87. Griffin WS*, et al.* (1989) Brain interleukin 1 and S-100 immunoreactivity are elevated in Down syndrome and Alzheimer disease. *Proceedings of the National Academy of Sciences of the United States of America* 86(19):7611-7615.

88. Jonsson T*, et al.* (2013) Variant of TREM2 associated with the risk of Alzheimer's disease. *N Engl J Med* 368(2):107-116.

89. Harold D*, et al.* (2009) Genome-wide association study identifies variants at CLU and PICALM associated with Alzheimer's disease. *Nat Genet* 41(10):1088-1093.

90. Naj AC*, et al.* (2011) Common variants at MS4A4/MS4A6E, CD2AP, CD33 and EPHA1 are associated with late-onset Alzheimer's disease. *Nat Genet* 43(5):436-441.

91. Guerreiro R, Bras J, & Hardy J (2013) SnapShot: genetics of Alzheimer's disease. *Cell* 155(4):968-968 e961.

92. Glass CK, Saijo K, Winner B, Marchetto MC, & Gage FH (2010) Mechanisms underlying inflammation in neurodegeneration. *Cell* 140(6):918-934.

93. Tacnet-Delorme P, Chevallier S, & Arlaud GJ (2001) Beta-amyloid fibrils activate the C1 complex of complement under physiological conditions: evidence for a binding site for A beta on the C1q globular regions. *J Immunol* 167(11):6374-6381.

94. Tahara K*, et al.* (2006) Role of toll-like receptor signalling in Abeta uptake and clearance. *Brain* 129(Pt 11):3006-3019.

95. Parvathenani LK*, et al.* (2003) P2X7 mediates superoxide production in primary microglia and is up-regulated in a transgenic mouse model of Alzheimer's disease. *The Journal of biological chemistry* 278(15):13309-13317.

96. Suzuki T*, et al.* (2004) Production and release of neuroprotective tumor necrosis factor by P2X7 receptor-activated microglia. *J Neurosci* 24(1):1-7.

97. Chakfe Y*, et al.* (2002) ADP and AMP induce interleukin-1beta release from microglial cells through activation of ATP-primed P2X7 receptor channels. *J Neurosci* 22(8):3061-3069.

98. Rogers J, Strohmeyer R, Kovelowski CJ, & Li R (2002) Microglia and inflammatory mechanisms in the clearance of amyloid beta peptide. *Glia* 40(2):260-269.

99. Wyss-Coray T & Mucke L (2002) Inflammation in neurodegenerative disease--a double-edged sword. *Neuron* 35(3):419-432.

100. Maxfield FR (2014) Role of endosomes and lysosomes in human disease. *Cold Spring Harbor perspectives in biology* 6(5):a016931.

101. Murthy VN & Stevens CF (1998) Synaptic vesicles retain their identity through the endocytic cycle. *Nature* 392(6675):497-501.

102. Sofroniew MV, Howe CL, & Mobley WC (2001) Nerve growth factor signaling, neuroprotection, and neural repair. *Annual review of neuroscience* 24:1217-1281.

103. Hollenbeck PJ (1993) Products of endocytosis and autophagy are retrieved from axons by regulated retrograde organelle transport. *The Journal of cell biology* 121(2):305-315.

104. Cataldo AM*, et al.* (2004) Abeta localization in abnormal endosomes: association with earliest Abeta elevations in AD and Down syndrome. *Neurobiology of aging* 25(10):1263-1272.

105. Choy RW, Cheng Z, & Schekman R (2012) Amyloid precursor protein (APP) traffics from the cell surface via endosomes for amyloid beta (Abeta) production in the trans-Golgi network. *Proceedings of the National Academy of Sciences of the United States of America* 109(30):E2077-2082.

106. Cataldo AM*, et al.* (2000) Endocytic pathway abnormalities precede amyloid beta deposition in sporadic Alzheimer's disease and Down syndrome: differential effects of APOE genotype and presenilin mutations. *The American journal of pathology* 157(1):277-286.

107. Butterfield DA, Perluigi M, & Sultana R (2006) Oxidative stress in Alzheimer's disease brain: new insights from redox proteomics. *European journal of pharmacology* 545(1):39-50.

108. Smith CD*, et al.* (1991) Excess brain protein oxidation and enzyme dysfunction in normal aging and in Alzheimer disease. *Proceedings of the National Academy of Sciences of the United States of America* 88(23):10540-10543.

109. Aksenov MY, Aksenova MV, Butterfield DA, Geddes JW, & Markesbery WR (2001) Protein oxidation in the brain in Alzheimer's disease. *Neuroscience* 103(2):373-383.

110. Butterfield DA, Drake J, Pocernich C, & Castegna A (2001) Evidence of oxidative damage in Alzheimer's disease brain: central role for amyloid beta-peptide. *Trends in molecular medicine* 7(12):548-554.

111. Butterfield DA & Lauderback CM (2002) Lipid peroxidation and protein oxidation in Alzheimer's disease brain: potential causes and consequences involving amyloid beta-peptide-associated free radical oxidative stress. *Free radical biology & medicine* 32(11):1050-1060.

112. Lovell MA & Markesbery WR (2001) Ratio of 8-hydroxyguanine in intact DNA to free 8-hydroxyguanine is increased in Alzheimer disease ventricular cerebrospinal fluid. *Archives of neurology* 58(3):392-396.

113. Gabbita SP, Lovell MA, & Markesbery WR (1998) Increased nuclear DNA oxidation in the brain in Alzheimer's disease. *Journal of neurochemistry* 71(5):2034-2040.

114. Lovell MA, Gabbita SP, & Markesbery WR (1999) Increased DNA oxidation and decreased levels of repair products in Alzheimer's disease ventricular CSF. *Journal of neurochemistry* 72(2):771-776.

115. Mecocci P, MacGarvey U, & Beal MF (1994) Oxidative damage to mitochondrial DNA is increased in Alzheimer's disease. *Annals of neurology* 36(5):747-751.

116. Markesbery WR & Lovell MA (2006) DNA oxidation in Alzheimer's disease. *Antioxidants & redox signaling* 8(11-12):2039-2045.

117. Santos RX*, et al.* (2013) Mitochondrial DNA oxidative damage and repair in aging and Alzheimer's disease. *Antioxidants & redox signaling* 18(18):2444-2457.

118. Santos RX*, et al.* (2012) Nuclear and mitochondrial DNA oxidation in Alzheimer's disease. *Free radical research* 46(4):565-576.

119. Vitek MP*, et al.* (1994) Advanced glycation end products contribute to amyloidosis in Alzheimer disease. *Proceedings of the National Academy of Sciences of the United States of America* 91(11):4766-4770.

120. Balaban RS, Nemoto S, & Finkel T (2005) Mitochondria, oxidants, and aging. *Cell* 120(4):483-495.

121. Linnane AW, Marzuki S, Ozawa T, & Tanaka M (1989) Mitochondrial DNA mutations as an important contributor to ageing and degenerative diseases. *Lancet* 1(8639):642-645.

122. Trifunovic A*, et al.* (2004) Premature ageing in mice expressing defective mitochondrial DNA polymerase. *Nature* 429(6990):417-423.

123. Cadenas E & Davies KJ (2000) Mitochondrial free radical generation, oxidative stress, and aging. *Free Radic Biol Med* 29(3-4):222-230.

124. Caspersen C*, et al.* (2005) Mitochondrial Abeta: a potential focal point for neuronal metabolic dysfunction in Alzheimer's disease. *FASEB journal : official publication of the Federation of American Societies for Experimental Biology* 19(14):2040-2041.

125. Hansson Petersen CA*, et al.* (2008) The amyloid beta-peptide is imported into mitochondria via the TOM import machinery and localized to mitochondrial cristae. *Proceedings of the National Academy of Sciences of the United States of America* 105(35):13145-13150.

126. Lustbader JW*, et al.* (2004) ABAD directly links Abeta to mitochondrial toxicity in Alzheimer's disease. *Science* 304(5669):448-452.

127. Busciglio J*, et al.* (2002) Altered metabolism of the amyloid beta precursor protein is associated with mitochondrial dysfunction in Down's syndrome. *Neuron* 33(5):677-688.

128. Lovell MA, Robertson JD, Teesdale WJ, Campbell JL, & Markesbery WR (1998) Copper, iron and zinc in Alzheimer's disease senile plaques. *Journal of the neurological sciences* 158(1):47-52.

129. Lee JY, Cole TB, Palmiter RD, Suh SW, & Koh JY (2002) Contribution by synaptic zinc to the gender-disparate plaque formation in human Swedish mutant APP transgenic mice. *Proceedings of the National Academy of Sciences of the United States of America* 99(11):7705-7710.

130. Bush AI (2000) Metals and neuroscience. *Current opinion in chemical biology* 4(2):184-191.

131. Barnham KJ, Masters CL, & Bush AI (2004) Neurodegenerative diseases and oxidative stress. *Nature reviews. Drug discovery* 3(3):205-214.

132. Bush AI (2003) The metallobiology of Alzheimer's disease. *Trends in neurosciences* 26(4):207-214.

133. Roberts BR, Ryan TM, Bush AI, Masters CL, & Duce JA (2012) The role of metallobiology and amyloid-beta peptides in Alzheimer's disease. *Journal of neurochemistry* 120 Suppl 1:149-166.

134. Hynd MR, Scott HL, & Dodd PR (2004) Glutamate-mediated excitotoxicity and neurodegeneration in Alzheimer's disease. *Neurochem Int* 45(5):583-595.

135. Choi DW (1988) Calcium-mediated neurotoxicity: relationship to specific channel types and role in ischemic damage. *Trends Neurosci* 11(10):465-469.

136. Dubinsky JM (1993) Intracellular calcium levels during the period of delayed excitotoxicity. *J Neurosci* 13(2):623-631.

137. Mattson MP*, et al.* (1992) beta-Amyloid peptides destabilize calcium homeostasis and render human cortical neurons vulnerable to excitotoxicity. *The Journal of neuroscience : the official journal of the Society for Neuroscience* 12(2):376-389.

138. Guo Q*, et al.* (1999) Increased vulnerability of hippocampal neurons to excitotoxic necrosis in presenilin-1 mutant knock-in mice. *Nature medicine* 5(1):101-106.

139. Koh JY, Yang LL, & Cotman CW (1990) Beta-amyloid protein increases the vulnerability of cultured cortical neurons to excitotoxic damage. *Brain research* 533(2):315-320.

140. Lipton SA (2006) Paradigm shift in neuroprotection by NMDA receptor blockade: memantine and beyond. *Nature reviews. Drug discovery* 5(2):160-170.

141. Li L, Sengupta A, Haque N, Grundke-Iqbal I, & Iqbal K (2004) Memantine inhibits and reverses the Alzheimer type abnormal hyperphosphorylation of tau and associated neurodegeneration. *FEBS Lett* 566(1-3):261-269.

142. Esclaire F, Lesort M, Blanchard C, & Hugon J (1997) Glutamate toxicity enhances tau gene expression in neuronal cultures. *J Neurosci Res* 49(3):309-318.

143. Amadoro G*, et al.* (2006) NMDA receptor mediates tau-induced neurotoxicity by calpain and ERK/MAPK activation. *Proceedings of the National Academy of Sciences of the United States of America* 103(8):2892-2897.

144. Rahman A*, et al.* (2009) The excitotoxin quinolinic acid induces tau phosphorylation in human neurons. *PLoS One* 4(7):e6344.

145. Matus S, Glimcher LH, & Hetz C (2011) Protein folding stress in neurodegenerative diseases: a glimpse into the ER. *Curr Opin Cell Biol* 23(2):239-252.

146. LaFerla FM (2002) Calcium dyshomeostasis and intracellular signalling in Alzheimer's disease. *Nature reviews. Neuroscience* 3(11):862-872.

147. Katayama T*, et al.* (2004) Induction of neuronal death by ER stress in Alzheimer's disease. *Journal of chemical neuroanatomy* 28(1-2):67-78.

148. van der Voorn JP*, et al.* (2005) The unfolded protein response in vanishing white matter disease. *Journal of neuropathology and experimental neurology* 64(9):770-775.

149. Hoozemans JJ*, et al.* (2005) The unfolded protein response is activated in Alzheimer's disease. *Acta neuropathologica* 110(2):165-172.

150. Elfrink HL*, et al.* (2012) Rab6 is a modulator of the unfolded protein response: implications for Alzheimer's disease. *Journal of Alzheimer's disease : JAD* 28(4):917-929.

151. Scheper W*, et al.* (2007) Rab6 is increased in Alzheimer's disease brain and correlates with endoplasmic reticulum stress. *Neuropathol Appl Neurobiol* 33(5):523-532.

152. Honjo Y, Ito H, Horibe T, Takahashi R, & Kawakami K (2010) Protein disulfide isomerase-immunopositive inclusions in patients with Alzheimer disease. *Brain research* 1349:90-96.

153. Hoozemans JJ*, et al.* (2009) The unfolded protein response is activated in pretangle neurons in Alzheimer's disease hippocampus. *The American journal of pathology* 174(4):1241-1251.

154. Bezprozvanny I & Mattson MP (2008) Neuronal calcium mishandling and the pathogenesis of Alzheimer's disease. *Trends Neurosci* 31(9):454-463.

155. Khachaturian ZS (1987) Hypothesis on the regulation of cytosol calcium concentration and the aging brain. *Neurobiology of aging* 8(4):345-346.

156. Siau C & Bennett GJ (2006) Dysregulation of cellular calcium homeostasis in chemotherapy-evoked painful peripheral neuropathy. *Anesthesia and analgesia* 102(5):1485-1490.

157. Kuchibhotla KV*, et al.* (2008) Abeta plaques lead to aberrant regulation of calcium homeostasis in vivo resulting in structural and functional disruption of neuronal networks. *Neuron* 59(2):214-225.

158. Saito K, Elce JS, Hamos JE, & Nixon RA (1993) Widespread activation of calcium-activated neutral proteinase (calpain) in the brain in Alzheimer disease: a potential molecular basis for neuronal degeneration. *Proceedings of the National Academy of Sciences of the United States of America* 90(7):2628-2632.

159. Nixon RA*, et al.* (1994) Calcium-activated neutral proteinase (calpain) system in aging and Alzheimer's disease. *Annals of the New York Academy of Sciences* 747:77-91.

160. Chard PS, Bleakman D, Christakos S, Fullmer CS, & Miller RJ (1993) Calcium buffering properties of calbindin D28k and parvalbumin in rat sensory neurones. *The Journal of physiology* 472:341-357.

161. Vecellio M, Schwaller B, Meyer M, Hunziker W, & Celio MR (2000) Alterations in Purkinje cell spines of calbindin D-28 k and parvalbumin knock-out mice. *The European journal of neuroscience* 12(3):945-954.

162. De Felice FG*, et al.* (2007) Abeta oligomers induce neuronal oxidative stress through an N-methyl-D-aspartate receptor-dependent mechanism that is blocked by the Alzheimer drug memantine. *The Journal of biological chemistry* 282(15):11590-11601.

163. Phillips HS*, et al.* (1991) BDNF mRNA is decreased in the hippocampus of individuals with Alzheimer's disease. *Neuron* 7(5):695-702.

164. Peng S, Wuu J, Mufson EJ, & Fahnestock M (2005) Precursor form of brain-derived neurotrophic factor and mature brain-derived neurotrophic factor are decreased in the pre-clinical stages of Alzheimer's disease. *Journal of neurochemistry* 93(6):1412-1421.

165. Murer MG, Yan Q, & Raisman-Vozari R (2001) Brain-derived neurotrophic factor in the control human brain, and in Alzheimer's disease and Parkinson's disease. *Progress in neurobiology* 63(1):71-124.

166. Murer MG*, et al.* (1999) An immunohistochemical study of the distribution of brain-derived neurotrophic factor in the adult human brain, with particular reference to Alzheimer's disease. *Neuroscience* 88(4):1015-1032.

167. Burbach GJ*, et al.* (2004) Induction of brain-derived neurotrophic factor in plaque-associated glial cells of aged APP23 transgenic mice. *The Journal of neuroscience : the official journal of the Society for Neuroscience* 24(10):2421-2430.

168. Ando S*, et al.* (2002) Animal model of dementia induced by entorhinal synaptic damage and partial restoration of cognitive deficits by BDNF and carnitine. *Journal of neuroscience research* 70(3):519-527.

169. Jones KR, Farinas I, Backus C, & Reichardt LF (1994) Targeted disruption of the BDNF gene perturbs brain and sensory neuron development but not motor neuron development. *Cell* 76(6):989-999.

170. Ernfors P, Kucera J, Lee KF, Loring J, & Jaenisch R (1995) Studies on the physiological role of brain-derived neurotrophic factor and neurotrophin-3 in knockout mice. *The International journal of developmental biology* 39(5):799-807.

171. Nagahara AH*, et al.* (2009) Neuroprotective effects of brain-derived neurotrophic factor in rodent and primate models of Alzheimer's disease. *Nature medicine* 15(3):331-337.

172. Zuccato C & Cattaneo E (2009) Brain-derived neurotrophic factor in neurodegenerative diseases. *Nature reviews. Neurology* 5(6):311-322.

173. Verdelho A*, et al.* (2007) Differential impact of cerebral white matter changes, diabetes, hypertension and stroke on cognitive performance among non-disabled elderly. The LADIS study. *Journal of neurology, neurosurgery, and psychiatry* 78(12):1325-1330.

174. Martins IJ*, et al.* (2006) Apolipoprotein E, cholesterol metabolism, diabetes, and the convergence of risk factors for Alzheimer's disease and cardiovascular disease. *Molecular psychiatry* 11(8):721-736.

175. de la Monte SM & Wands JR (2008) Alzheimer's disease is type 3 diabetes-evidence reviewed. *Journal of diabetes science and technology* 2(6):1101-1113.

176. Steen E*, et al.* (2005) Impaired insulin and insulin-like growth factor expression and signaling mechanisms in Alzheimer's disease--is this type 3 diabetes? *Journal of Alzheimer's disease : JAD* 7(1):63-80.

177. Rivera EJ*, et al.* (2005) Insulin and insulin-like growth factor expression and function deteriorate with progression of Alzheimer's disease: link to brain reductions in acetylcholine. *Journal of Alzheimer's disease : JAD* 8(3):247-268.

178. Craft S (2006) Insulin resistance syndrome and Alzheimer disease: pathophysiologic mechanisms and therapeutic implications. *Alzheimer disease and associated disorders* 20(4):298-301.

179. Craft S (2007) Insulin resistance and Alzheimer's disease pathogenesis: potential mechanisms and implications for treatment. *Current Alzheimer research* 4(2):147-152.

180. de la Monte SM, Tong M, Lester-Coll N, Plater M, Jr., & Wands JR (2006) Therapeutic rescue of neurodegeneration in experimental type 3 diabetes: relevance to Alzheimer's disease. *Journal of Alzheimer's disease : JAD* 10(1):89-109.

181. Pasquier F, Boulogne A, Leys D, & Fontaine P (2006) Diabetes mellitus and dementia. *Diabetes & metabolism* 32(5 Pt 1):403-414.

182. Buckner RL*, et al.* (2005) Molecular, structural, and functional characterization of Alzheimer's disease: evidence for a relationship between default activity, amyloid, and memory. *J Neurosci* 25(34):7709-7717.

183. Kamenetz F*, et al.* (2003) APP processing and synaptic function. *Neuron* 37(6):925-937.

184. Haass C, Kaether C, Thinakaran G, & Sisodia S (2012) Trafficking and proteolytic processing of APP. *Cold Spring Harbor perspectives in medicine* 2(5):a006270.

185. Dai W*, et al.* (2009) Mild cognitive impairment and alzheimer disease: patterns of altered cerebral blood flow at MR imaging. *Radiology* 250(3):856-866.

186. Hirao K*, et al.* (2005) The prediction of rapid conversion to Alzheimer's disease in mild cognitive impairment using regional cerebral blood flow SPECT. *NeuroImage* 28(4):1014-1021.

187. Pearlson GD*, et al.* (1992) Quantitative changes in mesial temporal volume, regional cerebral blood flow, and cognition in Alzheimer's disease. *Archives of general psychiatry* 49(5):402-408.

188. Montaldi D*, et al.* (1990) Measurements of regional cerebral blood flow and cognitive performance in Alzheimer's disease. *Journal of neurology, neurosurgery, and psychiatry* 53(1):33-38.

189. O'Brien JT, Eagger S, Syed GM, Sahakian BJ, & Levy R (1992) A study of regional cerebral blood flow and cognitive performance in Alzheimer's disease. *Journal of neurology, neurosurgery, and psychiatry* 55(12):1182-1187.

190. Craig AH*, et al.* (1996) Cerebral blood flow correlates of apathy in Alzheimer disease. *Archives of neurology* 53(11):1116-1120.

191. Bartenstein P*, et al.* (1997) Quantitative assessment of cerebral blood flow in patients with Alzheimer's disease by SPECT. *Journal of nuclear medicine : official publication, Society of Nuclear Medicine* 38(7):1095-1101.

192. Varvel NH*, et al.* (2008) Abeta oligomers induce neuronal cell cycle events in Alzheimer's disease. *The Journal of neuroscience : the official journal of the Society for Neuroscience* 28(43):10786-10793.

193. Herrup K & Yang Y (2007) Cell cycle regulation in the postmitotic neuron: oxymoron or new biology? *Nature reviews. Neuroscience* 8(5):368-378.

194. Andorfer C*, et al.* (2005) Cell-cycle reentry and cell death in transgenic mice expressing nonmutant human tau isoforms. *The Journal of neuroscience : the official journal of the Society for Neuroscience* 25(22):5446-5454.

195. Neve RL & McPhie DL (2006) The cell cycle as a therapeutic target for Alzheimer's disease. *Pharmacology & therapeutics* 111(1):99-113.

196. Webber KM*, et al.* (2005) The cell cycle in Alzheimer disease: a unique target for neuropharmacology. *Mechanisms of ageing and development* 126(10):1019-1025.

197. Bauer S & Patterson PH (2005) The cell cycle-apoptosis connection revisited in the adult brain. *The Journal of cell biology* 171(4):641-650.

198. Nagy Z, Esiri MM, & Smith AD (1997) Expression of cell division markers in the hippocampus in Alzheimer's disease and other neurodegenerative conditions. *Acta neuropathologica* 93(3):294-300.

199. Busser J, Geldmacher DS, & Herrup K (1998) Ectopic cell cycle proteins predict the sites of neuronal cell death in Alzheimer's disease brain. *J Neurosci* 18(8):2801-2807.

200. Yang Y, Geldmacher DS, & Herrup K (2001) DNA replication precedes neuronal cell death in Alzheimer's disease. *The Journal of neuroscience : the official journal of the Society for Neuroscience* 21(8):2661-2668.

201. Yang Y, Mufson EJ, & Herrup K (2003) Neuronal cell death is preceded by cell cycle events at all stages of Alzheimer's disease. *J Neurosci* 23(7):2557-2563.

202. Arendt T, Holzer M, & Gartner U (1998) Neuronal expression of cycline dependent kinase inhibitors of the INK4 family in Alzheimer's disease. *Journal of neural transmission* 105(8-9):949-960.

203. Hoozemans JJ*, et al.* (2002) Cyclin D1 and cyclin E are co-localized with cyclo-oxygenase 2 (COX-2) in pyramidal neurons in Alzheimer disease temporal cortex. *Journal of neuropathology and experimental neurology* 61(8):678-688.

204. Nagy Z, Esiri MM, Cato AM, & Smith AD (1997) Cell cycle markers in the hippocampus in Alzheimer's disease. *Acta neuropathologica* 94(1):6-15.

205. McShea A, Harris PL, Webster KR, Wahl AF, & Smith MA (1997) Abnormal expression of the cell cycle regulators P16 and CDK4 in Alzheimer's disease. *The American journal of pathology* 150(6):1933-1939.

206. Illenberger S*, et al.* (1998) The endogenous and cell cycle-dependent phosphorylation of tau protein in living cells: implications for Alzheimer's disease. *Mol Biol Cell* 9(6):1495-1512.

207. Preuss U, Doring F, Illenberger S, & Mandelkow EM (1995) Cell cycle-dependent phosphorylation and microtubule binding of tau protein stably transfected into Chinese hamster ovary cells. *Mol Biol Cell* 6(10):1397-1410.

208. Braak H & Del Tredici K (2011) The pathological process underlying Alzheimer's disease in individuals under thirty. *Acta neuropathologica* 121(2):171-181.

209. Grinberg LT*, et al.* (2009) The dorsal raphe nucleus shows phospho-tau neurofibrillary changes before the transentorhinal region in Alzheimer's disease. A precocious onset? *Neuropathol Appl Neurobiol* 35(4):406-416.

210. Jellinger KA (2001) Cell death mechanisms in neurodegeneration. *J Cell Mol Med* 5(1):1-17.

211. Lassmann H*, et al.* (1995) Cell-Death in Alzheimers-Disease Evaluated by DNA Fragmentation in-Situ. *Acta neuropathologica* 89(1):35-41.

212. Velez-Pardo C, Arroyave ST, Lopera F, Castano AD, & Jimenez Del Rio M (2001) Ultrastructure evidence of necrotic neural cell death in familial Alzheimer's disease brains bearing presenilin-1 E280A mutation. *Journal of Alzheimer's disease : JAD* 3(4):409-415.

213. Stadelmann C, Bruck W, Bancher C, Jellinger K, & Lassmann H (1998) Alzheimer disease: DNA fragmentation indicates increased neuronal vulnerability, but not apoptosis. *Journal of neuropathology and experimental neurology* 57(5):456-464.

214. Behl C, Davis JB, Klier FG, & Schubert D (1994) Amyloid beta peptide induces necrosis rather than apoptosis. *Brain Res* 645(1-2):253-264.

215. Nixon RA*, et al.* (2005) Extensive involvement of autophagy in Alzheimer disease: an immuno-electron microscopy study. *Journal of neuropathology and experimental neurology* 64(2):113-122.

216. Hayashi T, Shoji M, & Abe K (2006) Molecular mechanisms of ischemic neuronal cell death--with relevance to Alzheimer's disease. *Curr Alzheimer Res* 3(4):351-358.

217. Strittmatter WJ*, et al.* (1993) Apolipoprotein E: high-avidity binding to beta-amyloid and increased frequency of type 4 allele in late-onset familial Alzheimer disease. *Proceedings of the National Academy of Sciences of the United States of America* 90(5):1977-1981.

218. Guerreiro R*, et al.* (2013) TREM2 variants in Alzheimer's disease. *The New England journal of medicine* 368(2):117-127.

219. Kim J, Basak JM, & Holtzman DM (2009) The role of apolipoprotein E in Alzheimer's disease. *Neuron* 63(3):287-303.

220. Holtzman DM*, et al.* (2000) Apolipoprotein E isoform-dependent amyloid deposition and neuritic degeneration in a mouse model of Alzheimer's disease. *Proceedings of the National Academy of Sciences of the United States of America* 97(6):2892-2897.

221. Fagan AM*, et al.* (2002) Human and murine ApoE markedly alters A beta metabolism before and after plaque formation in a mouse model of Alzheimer's disease. *Neurobiology of disease* 9(3):305-318.

222. Lee JE & Han PL (2013) An update of animal models of Alzheimer disease with a reevaluation of plaque depositions. *Experimental neurobiology* 22(2):84-95.

223. Ashe KH (2001) Learning and memory in transgenic mice modeling Alzheimer's disease. *Learn Mem* 8(6):301-308.

224. Chen G*, et al.* (2000) A learning deficit related to age and beta-amyloid plaques in a mouse model of Alzheimer's disease. *Nature* 408(6815):975-979.

225. Selkoe DJ (2013) SnapShot: pathobiology of Alzheimer's disease. *Cell* 154(2):468-468 e461.

226. Jonsson T*, et al.* (2012) A mutation in APP protects against Alzheimer's disease and age-related cognitive decline. *Nature* 488(7409):96-99.

227. Aebersold R & Mann M (2003) Mass spectrometry-based proteomics. *Nature* 422(6928):198-207.

228. Peng J & Gygi SP (2001) Proteomics: the move to mixtures. *J Mass Spectrom* 36(10):1083-1091.

229. Price WD, Schnier PD, & Williams ER (1996) Tandem mass spectrometry of large biomolecule ions by blackbody infrared radiative dissociation. *Anal Chem* 68(5):859-866.

230. Karas M & Hillenkamp F (1988) Laser desorption ionization of proteins with molecular masses exceeding 10,000 daltons. *Anal Chem* 60(20):2299-2301.

231. Menon KN*, et al.* (2011) A novel unbiased proteomic approach to detect the reactivity of cerebrospinal fluid in neurological diseases. *Mol Cell Proteomics* 10(6):M110 000042.

232. Seyfried NT*, et al.* (2010) Multiplex SILAC analysis of a cellular TDP-43 proteinopathy model reveals protein inclusions associated with SUMOylation and diverse polyubiquitin chains. *Mol Cell Proteomics* 9(4):705-718.

233. Seyfried NT*, et al.* (2012) Quantitative analysis of the detergent-insoluble brain proteome in frontotemporal lobar degeneration using SILAC internal standards. *J Proteome Res* 11(5):2721-2738.

234. Gozal YM*, et al.* (2011) Proteomic analysis of hippocampal dentate granule cells in frontotemporal lobar degeneration: application of laser capture technology. *Front Neurol* 2:24.

235. Zhou J*, et al.* (2013) Proteomic analysis of postsynaptic density in Alzheimer's disease. *Clin Chim Acta* 420:62-68.

236. Gozal YM*, et al.* (2009) Proteomics analysis reveals novel components in the detergent-insoluble subproteome in Alzheimer's disease. *J Proteome Res* 8(11):5069-5079.

237. Di Domenico F*, et al.* (2011) Quantitative proteomics analysis of phosphorylated proteins in the hippocampus of Alzheimer's disease subjects. *J Proteomics* 74(7):1091-1103.

238. Na CH*, et al.* (2012) Synaptic protein ubiquitination in rat brain revealed by antibody-based ubiquitome analysis. *J Proteome Res* 11(9):4722-4732.

239. Dammer EB*, et al.* (2011) Polyubiquitin linkage profiles in three models of proteolytic stress suggest the etiology of Alzheimer disease. *The Journal of biological chemistry* 286(12):10457-10465.

240. Reed TT, Pierce WM, Jr., Turner DM, Markesbery WR, & Butterfield DA (2009) Proteomic identification of nitrated brain proteins in early Alzheimer's disease inferior parietal lobule. *J Cell Mol Med* 13(8B):2019-2029.

241. Castegna A*, et al.* (2003) Proteomic identification of nitrated proteins in Alzheimer's disease brain. *J Neurochem* 85(6):1394-1401.

242. Butterfield DA, Boyd-Kimball D, & Castegna A (2003) Proteomics in Alzheimer's disease: insights into potential mechanisms of neurodegeneration. *J Neurochem* 86(6):1313-1327.

243. Hye A*, et al.* (2006) Proteome-based plasma biomarkers for Alzheimer's disease. *Brain* 129(Pt 11):3042-3050.

244. Hsich G, Kenney K, Gibbs CJ, Lee KH, & Harrington MG (1996) The 14-3-3 brain protein in cerebrospinal fluid as a marker for transmissible spongiform encephalopathies. *The New England journal of medicine* 335(13):924-930.

245. Zhou JY*, et al.* (2010) Galectin-3 is a candidate biomarker for amyotrophic lateral sclerosis: discovery by a proteomics approach. *J Proteome Res* 9(10):5133-5141.

246. Zhou JY, Hanfelt J, & Peng J (2007) Clinical proteomics in neurodegenerative diseases. *Proteomics Clin Appl* 1(11):1342-1350.

247. Mortazavi A, Williams BA, McCue K, Schaeffer L, & Wold B (2008) Mapping and quantifying mammalian transcriptomes by RNA-Seq. *Nat Methods* 5(7):621-628.

248. Wang Z, Gerstein M, & Snyder M (2009) RNA-Seq: a revolutionary tool for transcriptomics. *Nat Rev Genet* 10(1):57-63.

249. Marioni JC, Mason CE, Mane SM, Stephens M, & Gilad Y (2008) RNA-seq: an assessment of technical reproducibility and comparison with gene expression arrays. *Genome Res* 18(9):1509-1517.

250. Costa V, Aprile M, Esposito R, & Ciccodicola A (2013) RNA-Seq and human complex diseases: recent accomplishments and future perspectives. *Eur J Hum Genet* 21(2):134-142.

251. Courtney E, Kornfeld S, Janitz K, & Janitz M (2010) Transcriptome profiling in neurodegenerative disease. *J Neurosci Methods* 193(2):189-202.

252. Polymenidou M*, et al.* (2011) Long pre-mRNA depletion and RNA missplicing contribute to neuronal vulnerability from loss of TDP-43. *Nat Neurosci* 14(4):459-468.

253. Tollervey JR*, et al.* (2011) Characterizing the RNA targets and position-dependent splicing regulation by TDP-43. *Nat Neurosci* 14(4):452-458.

254. Twine NA, Janitz K, Wilkins MR, & Janitz M (2011) Whole transcriptome sequencing reveals gene expression and splicing differences in brain regions affected by Alzheimer's disease. *PLoS One* 6(1):e16266.

255. Mills JD*, et al.* (2013) RNA-Seq analysis of the parietal cortex in Alzheimer's disease reveals alternatively spliced isoforms related to lipid metabolism. *Neurosci Lett* 536:90-95.

256. Kim KH, Moon M, Yu SB, Mook-Jung I, & Kim JI (2012) RNA-Seq analysis of frontal cortex and cerebellum from 5XFAD mice at early stage of disease pathology. *J Alzheimers Dis* 29(4):793-808.

257. Sutherland GT, Janitz M, & Kril JJ (2011) Understanding the pathogenesis of Alzheimer's disease: will RNA-Seq realize the promise of transcriptomics? *J Neurochem* 116(6):937-946.

258. Anonymous (2012) 2012 Alzheimer's disease facts and figures. *Alzheimers Dement.* 8(2):131-168.

259. Tanzi RE (2012) The genetics of Alzheimer disease. *Cold Spring Harb Perspect Med* 2(10).

260. Liu CC, Kanekiyo T, Xu H, & Bu G (2013) Apolipoprotein E and Alzheimer disease: risk, mechanisms and therapy. *Nat. Rev Neurol* 9(2):106-118.

261. Neumann H & Daly MJ (2013) Variant TREM2 as risk factor for Alzheimer's disease. *N Engl J Med* 368(2):182-184.

262. Taylor JP, Hardy J, & Fischbeck KH (2002) Toxic proteins in neurodegenerative disease. *Science* 296(5575):1991-1995.

263. Glenner GG & Wong CW (1984) Alzheimer's disease: initial report of the purification and characterization of a novel cerebrovascular amyloid protein. *Biochem. Biophys. Res. Commun.* 120(3):885-890.

264. Masters CL*, et al.* (1985) Amyloid plaque core protein in Alzheimer disease and Down syndrome. *Proc. Natl. Acad. Sci. U. S. A.* 82(12):4245-4249.

265. Lee VM, Balin BJ, Otvos L, Jr., & Trojanowski JQ (1991) A68: a major subunit of paired helical filaments and derivatized forms of normal Tau. *Science* 251(4994):675-678.

266. Hardy J & Selkoe DJ (2002) The amyloid hypothesis of Alzheimer's disease: progress and problems on the road to therapeutics. *Science* 297(5580):353-356.

267. Ballatore C, Lee VM, & Trojanowski JQ (2007) Tau-mediated neurodegeneration in Alzheimer's disease and related disorders. *Nat. Rev. Neurosci.* 8(9):663-672.

268. Pimplikar SW, Nixon RA, Robakis NK, Shen J, & Tsai LH (2010) Amyloid-independent mechanisms in Alzheimer's disease pathogenesis. *J Neurosci* 30(45):14946-14954.

269. Peng J & Gygi SP (2001) Proteomics: the move to mixtures. *J. Mass Spectrom.* 36(10):1083-1091.

270. Cravatt BF, Simon GM, & Yates JR, 3rd (2007) The biological impact of mass-spectrometry-based proteomics. *Nature* 450(7172):991-1000.

271. Mann M, Kulak NA, Nagaraj N, & Cox J (2013) The coming age of complete, accurate, and ubiquitous proteomes. *Mol Cell* 49(4):583-590.

272. Zhou JY*, et al.* (2013) Proteomic Analysis of Postsynaptic Density in Alzheimer Disease. *Clinica Chimica Acta* 420:62-68.

273. Gozal YM*, et al.* (2009) Proteomics analysis reveals novel components in the detergent-insoluble subproteome in Alzheimer's disease. *J. Proteome Res.* 8(11):5069-5079.

274. Gozal YM*, et al.* (2011) Proteomic analysis of hippocampal dentate granule cells in frontotemporal lobar degeneration: application of laser capture technology. *Front Neurol* 2:24.

275. Gozal YM*, et al.* (2011) Aberrant septin 11 is associated with sporadic frontotemporal lobar degeneration. *Mol Neurodegener* 6:82.

276. Xia Q*, et al.* (2008) Phosphoproteomic analysis of human brain by calcium phosphate precipitation and mass spectrometry. *J Proteome Res* 7(7):2845-2851.

277. Liao L*, et al.* (2004) Proteomic characterization of postmortem amyloid plaques isolated by laser capture microdissection. *J Biol Chem* 279(35):37061-37068.

278. Zhou JY*, et al.* (2010) Galectin-3 Is a Candidate Biomarker for Amyotrophic Lateral Sclerosis: Discovery by a Proteomics Approach. *J. Proteome Res.* 9(10):5133-5141.

279. Bai B*, et al.* (2013) U1 small nuclear ribonucleoprotein complex and RNA splicing alterations in Alzheimer's disease. *Proc Natl Acad Sci U S A* 110(41):16562-16567.

280. Hales CM*, et al.* (2014) Aggregates of small nuclear ribonucleic acids (snRNAs) in Alzheimer's disease. *Brain Pathol*.

281. Staley JP & Guthrie C (1998) Mechanical devices of the spliceosome: motors, clocks, springs, and things. *Cell* 92(3):315-326.

282. Ross CA & Poirier MA (2004) Protein aggregation and neurodegenerative disease. *Nat Med* 10 Suppl:S10-17.

283. Hyman BT & Trojanowski JQ (1997) Consensus recommendations for the postmortem diagnosis of Alzheimer disease from the National Institute on Aging and the Reagan Institute Working Group on diagnostic criteria for the neuropathological assessment of Alzheimer disease. *J Neuropathol Exp Neurol* 56(10):1095-1097.

284. Xu P, Duong DM, & Peng J (2009) Systematical optimization of reverse-phase chromatography for shotgun proteomics. *J. Proteome Res.* 8(8):3944-3950.

285. Peng J, Elias JE, Thoreen CC, Licklider LJ, & Gygi SP (2003) Evaluation of multidimensional chromatography coupled with tandem mass spectrometry (LC/LC-MS/MS) for large-scale protein analysis: the yeast proteome. *J. Proteome Res.* 2:43-50.

286. Elias JE & Gygi SP (2007) Target-decoy search strategy for increased confidence in large-scale protein identifications by mass spectrometry. *Nat. Methods* 4(3):207-214.

287. Seyfried NT*, et al.* (2008) Systematic approach for validating the ubiquitinated proteome. *Anal Chem* 80(11):4161-4169.

288. Bonissone S, Gupta N, Romine M, Bradshaw RA, & Pevzner PA (2013) N-terminal protein processing: a comparative proteogenomic analysis. *Mol Cell Proteomics* 12(1):14-28.

289. Jin M*, et al.* (2011) Soluble amyloid beta-protein dimers isolated from Alzheimer cortex directly induce Tau hyperphosphorylation and neuritic degeneration. *Proceedings of the National Academy of Sciences of the United States of America* 108(14):5819-5824.

290. Nikolaev A, McLaughlin T, O'Leary DD, & Tessier-Lavigne M (2009) APP binds DR6 to trigger axon pruning and neuron death via distinct caspases. *Nature* 457(7232):981-989.

291. Lobner D (2000) Comparison of the LDH and MTT assays for quantifying cell death: validity for neuronal apoptosis? *Journal of neuroscience methods* 96(2):147-152.

292. Neumann M*, et al.* (2006) Ubiquitinated TDP-43 in frontotemporal lobar degeneration and amyotrophic lateral sclerosis. *Science* 314(5796):130-133.

293. Nonaka T, Kametani F, Arai T, Akiyama H, & Hasegawa M (2009) Truncation and pathogenic mutations facilitate the formation of intracellular aggregates of TDP-43. *Hum Mol Genet* 18(18):3353-3364.

294. Kambach C & Mattaj IW (1992) Intracellular distribution of the U1A protein depends on active transport and nuclear binding to U1 snRNA. *The Journal of cell biology* 118(1):11-21.

295. Gervais FG*, et al.* (1999) Involvement of caspases in proteolytic cleavage of Alzheimer's amyloid-beta precursor protein and amyloidogenic A beta peptide formation. *Cell* 97(3):395-406.

296. Cataldo AM & Nixon RA (1990) Enzymatically active lysosomal proteases are associated with amyloid deposits in Alzheimer brain. *Proc Natl Acad Sci U S A* 87(10):3861-3865.

297. Casciola-Rosen L*, et al.* (1996) Apopain/CPP32 cleaves proteins that are essential for cellular repair: a fundamental principle of apoptotic death. *The Journal of experimental medicine* 183(5):1957-1964.

298. Casciola-Rosen L, Andrade F, Ulanet D, Wong WB, & Rosen A (1999) Cleavage by granzyme B is strongly predictive of autoantigen status: implications for initiation of autoimmunity. *The Journal of experimental medicine* 190(6):815-826.

299. Casciola-Rosen L, Wigley F, & Rosen A (1997) Scleroderma autoantigens are uniquely fragmented by metal-catalyzed oxidation reactions: implications for pathogenesis. *The Journal of experimental medicine* 185(1):71-79.

300. Will CL*, et al.* (2002) Characterization of novel SF3b and 17S U2 snRNP proteins, including a human Prp5p homologue and an SF3b DEAD-box protein. *EMBO J* 21(18):4978-4988.

301. Tamaoka A*, et al.* (2010) TDP-43 M337V mutation in familial amyotrophic lateral sclerosis in Japan. *Intern Med* 49(4):331-334.

302. Barmada SJ*, et al.* (2010) Cytoplasmic mislocalization of TDP-43 is toxic to neurons and enhanced by a mutation associated with familial amyotrophic lateral sclerosis. *J Neurosci* 30(2):639-649.

303. Lemmens R*, et al.* (2009) TDP-43 M311V mutation in familial amyotrophic lateral sclerosis. *J Neurol Neurosurg Psychiatry* 80(3):354-355.

304. Yokoseki A*, et al.* (2008) TDP-43 mutation in familial amyotrophic lateral sclerosis. *Annals of neurology* 63(4):538-542.

305. Kaida D*, et al.* (2010) U1 snRNP protects pre-mRNAs from premature cleavage and polyadenylation. *Nature* 468(7324):664-668.

306. Kim HJ*, et al.* (2013) Mutations in prion-like domains in hnRNPA2B1 and hnRNPA1 cause multisystem proteinopathy and ALS. *Nature* 495(7442):467-473.

307. Berson A*, et al.* (2012) Cholinergic-associated loss of hnRNP-A/B in Alzheimer's disease impairs cortical splicing and cognitive function in mice. *EMBO Mol Med* 4(8):730-742.

308. Hutton M*, et al.* (1998) Association of missense and 5'-splice-site mutations in tau with the inherited dementia FTDP-17. *Nature* 393(6686):702-705.

309. Sato N*, et al.* (1999) A novel presenilin-2 splice variant in human Alzheimer's disease brain tissue. *J Neurochem* 72(6):2498-2505.

310. Manabe T*, et al.* (2003) Induced HMGA1a expression causes aberrant splicing of Presenilin-2 pre-mRNA in sporadic Alzheimer's disease. *Cell Death Differ* 10(6):698-708.

311. Honig LS, Chambliss DD, Bigio EH, Carroll SL, & Elliott JL (2000) Glutamate transporter EAAT2 splice variants occur not only in ALS, but also in AD and controls. *Neurology* 55(8):1082-1088.

312. Ewing RM*, et al.* (2007) Large-scale mapping of human protein-protein interactions by mass spectrometry. *Mol Syst Biol* 3:89.

313. Hong M*, et al.* (1998) Mutation-specific functional impairments in distinct tau isoforms of hereditary FTDP-17. *Science* 282(5395):1914-1917.

314. Spillantini MG*, et al.* (1998) Mutation in the tau gene in familial multiple system tauopathy with presenile dementia. *Proceedings of the National Academy of Sciences of the United States of America* 95(13):7737-7741.

315. Goedert M, Spillantini MG, Jakes R, Rutherford D, & Crowther RA (1989) Multiple isoforms of human microtubule-associated protein tau: sequences and localization in neurofibrillary tangles of Alzheimer's disease. *Neuron* 3(4):519-526.

316. Ingelsson M*, et al.* (2006) No alteration in tau exon 10 alternative splicing in tangle-bearing neurons of the Alzheimer's disease brain. *Acta neuropathologica* 112(4):439-449.

317. Will CL & Luhrmann R (2001) Spliceosomal UsnRNP biogenesis, structure and function. *Curr Opin Cell Biol* 13(3):290-301.

318. Greenfield JP*, et al.* (1999) Endoplasmic reticulum and trans-Golgi network generate distinct populations of Alzheimer beta-amyloid peptides. *Proceedings of the National Academy of Sciences of the United States of America* 96(2):742-747.

319. Lindholm D, Wootz H, & Korhonen L (2006) ER stress and neurodegenerative diseases. *Cell Death Differ* 13(3):385-392.

320. Wang X*, et al.* (2009) Impaired balance of mitochondrial fission and fusion in Alzheimer's disease. *J Neurosci* 29(28):9090-9103.

321. Simard AR, Soulet D, Gowing G, Julien JP, & Rivest S (2006) Bone marrow-derived microglia play a critical role in restricting senile plaque formation in Alzheimer's disease. *Neuron* 49(4):489-502.

322. Spector DL & Smith HC (1986) Redistribution of U-snRNPs during mitosis. *Exp Cell Res* 163(1):87-94.

323. Chuang JY*, et al.* (2008) Phosphorylation by c-Jun NH2-terminal kinase 1 regulates the stability of transcription factor Sp1 during mitosis. *Mol Biol Cell* 19(3):1139-1151.

324. Dieker J*, et al.* (2008) Apoptosis-linked changes in the phosphorylation status and subcellular localization of the spliceosomal autoantigen U1-70K. *Cell Death Differ* 15(4):793-804.

325. Gui JF, Lane WS, & Fu XD (1994) A serine kinase regulates intracellular localization of splicing factors in the cell cycle. *Nature* 369(6482):678-682.

326. Tazi J*, et al.* (1993) Thiophosphorylation of U1-70K protein inhibits pre-mRNA splicing. *Nature* 363(6426):283-286.